BEST AVAILABLE IMAGES

Defective images within this document are accurate representations of the original documents submitted by the applicant.

Defects in the images may include (but are not limited to):

- BLACK BORDERS
- TEXT CUT OFF AT TOP, BOTTOM OR SIDES
- FADED TEXT
- ILLEGIBLE TEXT
- SKEWED/SLANTED IMAGES
- COLORED PHOTOS
- BLACK OR VERY BLACK AND WHITE DARK PHOTOS
- GRAY SCALE DOCUMENTS

IMAGES ARE BEST AVAILABLE COPY.

As rescanning documents *will not* correct images, please do not report the images to the Image Problem Mailbox.

REMARKS

Claims 47-54 were pending. Claims 47-48 and 51-52 are presently amended. New claim 55 is added to recite the method of claim 47 using specific compounds taught, e.g. in Section 5.2.2. at pages 19-21, in Section 5.3 at pages 22-26, etc., as inhibitors of activation of Src kinase induced by HBV or HBx. No new matter is added by any of the amendments.

Rejection Under Section 103

Claims 47-54 remain rejected under Section 103 as obvious in view of Moriya et al, 1996, Biochem. Biophys Res.Comm 218: 217-23 (Moriya). According to the Office Action, Moriya teaches "inhibition of HBx gene transcription and translation by administration of HBx antisense oligonucleotides" and that inhibition of activation of Src kinase would be "an inherent effect of the antisense oligonucleotide of Moriya." The Office Action concludes that "it would have been obvious to one of ordinary skill in the art to treat an HBV infected patient or cell with the antisense oligonucleotide of Moriya et al to inhibit HBV replication."

Attorneys for Applicants respectfully, but emphatically disagree. In order, however, to more clearly point out and distinctly claim certain of the embodiments of the present invention, the claims are presently amended to recite that "if the compound [to be used in the method] is an antisense molecule, it is an antisense molecule to a Src kinase family member." Support for this particular recitation is found in the specification, inter alia, at page 13, lines 16-27, in particular, at page 13, lines 23-27; in Section 5.2.2 at pages 19-22 and Section 5.3 at pages 22-30, in particular at page 19, lines 22-31. Further support for this particular recitation is found in Section 5.1 at page 17, lines 20-32. As clearly taught therein, Applicants' inventive discovery encompasses anti-HBV therapies targeted specifically at the HBx gene itself as well therapies targeted at genes of the Src family of kinases. Having taught use of antisense molecules targeted to the HBx gene and to the genes of Src kinase family members, the present claims directed, in part, to one of these specific embodiments are fully supported by the specification as originally filed. See, e.g., In re Johnson, 194 U.S.P.Q. 187, 196 (1977), where the court emphatically reversed the Board of Appeals and held that a specification having described the whole invention necessarily described the part remaining after the invention of another was excised.

In complete contrast to the present specification, which teaches, *inter alia*, use of anti-sense molecules targeted to a Src kinase family member to inhibit HBV infection or

replication, Moriya, at very most teaches that two specific anti-sense molecules to the HBx gene inhibit expression of a hepatitis B virus gene. Moriya does not suggest any means for inhibiting HBV other than the two specific anti-HBx antisense molecules. In no way does Moriya suggest inhibiting HBV infection or replication by targeting cellular Src kinase activation. Hence, it is clear that Moriya cannot and does not suggest or make obvious the subject matter of the present claims.

Accordingly, the rejection based on this reference has been obviated and must be withdrawn.

Rejection Under Section 112

Claims 47-54 remain rejected under Section 112, first paragraph, for alleged lack of written description. The Advisory Action asserts that the specification does not describe examples of inhibitors of Src kinase activation but rather describes only inhibitors of Src kinase enzymatic activity (use of which were claimed in the parent application).

Attorneys for Applicants respectfully disagree and submit that the specification clearly describes a genus of compounds, i.e. compounds that inhibit activation of Src kinase induced by HBV or HBx, within the scope of the present claims with sufficient clarity and specificity to enable those of skill to practice the claimed methods.

Attention is directed to the teaching of the specification, e.g. at page 12, lines 24-29, which indicates that the present invention encompasses methods and pharmaceutical compositions "designed to target HBx mediated activation of Src kinase, members of the Src tyrosine kinase family and components of the Src kinase family signal transduction pathway for the treatment of HBV infection." A number of different protocols to inhibit HBV infection and/or replication are described including, but not limited to inhibition of essential activities of Src kinase activation associated with HBV infections. In particular, at page 13, lines 16-27, the specification describes specific embodiments of the invention encompassing methods to inhibit HBV by inhibiting the Src family of kinases and to inhibit HBV by modulation of activation of the Src kinase signaling cascade. Specific compounds useful for either or both of these embodiments are taught, e.g. at page 13, lines 19-23 which teaches compounds including "specific Src kinase inhibitors, including but not limited to, tyrosine kinase inhibitors, drugs, organic compounds, peptides, polypeptides and nucleotides" for treating HBV. Further, at page 13, lines 23-27, the specification teaches additional useful compounds for inhibiting activation of Src kinase including "dominant-negative mutants,

SELEX RNAs, and antisense molecules targeted to Src kinase family members, Src-activated enzymes, downstream effectors of Src kinase and their signal transduction pathways." Attention is directed further to the detailed teaching of the specification in Section 5.2.2 at pages 19-21 and Section 5. In particular, at page 19, lines 23-31 the specification teaches that the methods use molecules, including antisense molecules which are known to inhibit members of the Src kinase, Ras, Raf and MAPK kinase, MAPK, c-Myc, cyclin-dependent kinases and/or other downstream effectors of the Src kinase signaling cascade. At page 20, line 35 through page 21, line 9, the specification teaches "further examples" including polypeptides such as Fyn dominant negative mutant proteins, as well as Ras, Raf, MAPK kinase, MAPK and Myc dominant negative mutants. In addition, specific references relating to each of the recited dominant negative mutant proteins in the Src kinase cascade are provided in the specification indicating that those skilled in the art at the time the application was filed would understand (and be able to make) the compounds enumerated in the specification. Moreover, attention is directed to the Examples, in particular, Example 6 at pages 46-56 which clearly demonstrate that HBx activates a variety of the Src kinase members. As indicated at page 16, lines 33-36, the results demonstrate that expression of the Src inhibitor Csk or domain at negative Src or Fyn proteins inhibited HBx induced activation of downstream Src kinase cascade. These data clearly support the teaching of the specification that the mentioned inhibitors of Src kinase family members, e.g. Fyn, Ras, etc., are useful to inhibit HBV infection and/or replication.

Attention is finally directed to the teaching of the specification at page 19, line 32 through page 20, line 20 which reads:

> In particular, compounds which may be used in accordance with the present invention to specifically target activation of Src kinase are binding proteins and competing ligands that prevent the intramolecular interaction between the carboxy-terminal phosphorylated tyrosine residue and the SH2 domain located in the amino-terminal half of the molecule and the immediately adjacent SH3 domain (Lin et al., 1993, Oncogene 8:1119-1126). In particular, compounds which may also be used in accordance with the present invention include tyrosine kinase inhibitors which block the activity the Src kinase signaling cascade and therefore would block HBV replication. Examples of such tyrosine kinase inhibitors include, but are not limited to, tyrphostin-derived inhibitors, which are derivatives of benzylidenemalonitrile, have been shown to have strong inhibitory activity of Src (Ramdas et al., 1995, Archives of Biochemistry and Biophysics 323:237-242), pyrazolopyrimidine PP1 (4-amino-5-(4-methylphenyl)-7-(t-

> butyl) pyrazolo [3,4-d] pyrimidine, a selective inhibitor of the Src family of kinases (Hanke et al., 1996, J. Biol. Chem. 271:695-791) and derivatives thereof. Other examples include microbial agents, such as angelmicin B, a specific inhibitor of Src tyrosine kinase activity, and derivatives thereof (Yokoyama et al., 1996, Leukemia Research 20:491-497), which may also be used to inhibit HBV replication.

Attention is also directed to Exhibits A-C submitted herewith. Each of these Exhibits teaches that representative members of the Src kinase activation inhibitors taught as useful in the specification indeed phosphorylate Src kinase. As known by those skilled in the art, when phosphorylated at a key tyrosine in the C-terminal tail, Src kinase activity is suppressed. Not only is Src kinase activity *per se* suppressed, but activities downstream in the Src kinase cascade are suppressed. Hence, the compounds described at pages 19-20 of the specification also fall within the scope of compounds useful for the presently claimed methods.[1]

In view of the above summarized detailed description, it is respectfully submitted that the written description requirement has been fully met with respect to the present claims. An applicant is not required to disclose every species encompassed by claims even in an unpredictable art. In re Angstadt, 537 F.2d 498 (CCPA 1976). As summarized above, the specification clearly provides a written description of representative examples of compounds which are inhibitors of Src activation induced by HBV or HBx. Accordingly, the rejection based on Section 112 cannot stand and must be withdrawn.

[1] With respect to specific inhibitors of the Src kinase mentioned at page 19, line 32 through page 20, line 20 of the specification, it is noted that the use of such compounds may fall within the scope of the claims of the parent application as well as the present claims, which are of a different scope and directed to a separate election group. If the Examiner deems it necessary, Applicants would be willing to submit a Terminal Disclaimer of the present claims (over the parent patent) in order to avoid any double patenting issues.

Conclusion

In view of the amendments herein, the remarks above and the evidence presented in the accompanying Exhibits, it is submitted that the claims are in form for allowance and early action to that end is respectfully requested. If any issues remain, it is requested that the undersigned be contacted at the telephone number below.

Respectfully submitted,

Date: July 14, 2004

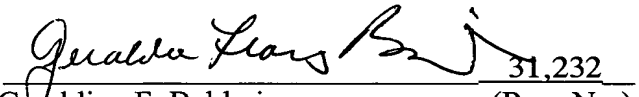

31,232

Geraldine F. Baldwin (Reg. No.)
JONES DAY
222 East 41st Street
New York, New York 10017-6702
(212) 326-3939

Integrin-dependent Translocation of Phosphoinositide 3-Kinase to the Cytoskeleton of Thrombin-Activated Platelets Involves Specific Interactions of p85α with Actin Filaments and Focal Adhesion Kinase

Christine Guinebault,* Bernard Payrastre,* Claire Racaud-Sultan,* Honoré Mazarguil,‡ Monique Breton,* Gérard Mauco,* Monique Plantavid,* and Hugues Chap*

*Institut National de la Santé et de la Recherche Médicale, Unité 326, Hôpital Purpan, 31059 Toulouse, France; and ‡LPTF du CNRS, 31077 Toulouse, France

Abstract. Thrombin-induced accumulation of phosphatidylinositol 3,4-bisphosphate (PtdIns(3,4)P_2) but not of PtdIns(3,4,5,)P_3 is strongly correlated with the relocation to the cytoskeleton of 29% of the p85α regulatory subunit of phosphoinositide 3-kinase (PtdIns 3-kinase) and is accompanied by a significant increase in PtdIns 3-kinase activity in this subcellular fraction. Actually, PtdIns(3,4)P_2 accumulation and PtdIns 3-kinase, pp60$^{c\text{-}src}$, and p125^{FAK} translocations as well as aggregation were concomitant events occurring with a distinct lag after actin polymerization. The accumulation of PtdIns(3,4)P_2 and the relocalization of PtdIns 3-kinase to the cytoskeleton were both dependent on tyrosine phosphorylation, integrin signaling, and aggregation. Furthermore, although p85α was detected in anti-phosphotyrosine immunoprecipitates obtained from the cytoskeleton of thrombin-activated platelets, we failed to demonstrate tyrosine phosphorylation of cytoskeletal p85α. Tyrphostin treatment clearly reduced its presence in this subcellular fraction, suggesting a physical interaction of p85α with a phosphotyrosyl protein. These data led us to investigate the proteins that are able to interact with PtdIns 3-kinase in the cytoskeleton. We found an association of this enzyme with actin filaments: this interaction was spontaneously restored after one cycle of actin depolymerization–repolymerization in vitro. This association with F-actin appeared to be at least partly indirect, since we demonstrated a thrombin-dependent interaction of p85α with a proline-rich sequence of the tyrosine-phosphorylated cytoskeletal focal adhesion kinase, p125^{FAK}. In addition, we show that PtdIns 3-kinase is significantly activated by the p125^{FAK} proline-rich sequence binding to the src homology 3 domain of p85α subunit. This interaction may represent a new mechanism for PtdIns 3-kinase activation at very specific areas of the cell and indicates that the focal contact-like areas linked to the actin filaments play a critical role in signaling events that occur upon ligand engagement of α_{IIb}/β_3 integrin and platelet aggregation evoked by thrombin.

THE accumulation of phosphatidylinositol 3,4-bisphosphate (PtdIns(3,4)P_2)[1] and PtdIns(3,4,5)P_3 in thrombin-stimulated human platelets is now well established (16, 24, 38, 41) and seems to be regulated differently (38). However, the exact mechanism of activation of phosphoinositide 3-kinase (PtdIns 3-kinase) in these cells is still obscure. The small G-protein rho (51), G-protein βγ subunit (44) protein kinase C (PKC) (26), Ca^{2+} (38), as well as tyrosine phosphorylation (19) may contribute to its activation. Possible ways of stimulation in other models also include physical association with specific proteins via the src homology 2 (SH2) domains or the proline-rich regions of the p85 subunit. This results in a conformational change of p85 that appears to be transmitted to the catalytic subunit (p110) as an activation signal (34, 37). Since PtdIns 3-kinase has been found to be associated with activated PDGF receptor (10) or pp60$^{v\text{-}src}$ (14), with a potentially very important role in mitogenesis (46) or oncogenic transformation (43), respectively, great interest has been elicited by its products (i.e., D3-phosphorylated phosphoinositides). Although their precise function is still unknown, these phospholipids have been suggested to play a role as second messengers activating downstream signaling enzymes like PKCζ isoform

Address all correspondence to B. Payrastre, INSERM U326, Hôpital Purpan, 31059 Toulouse, France. Tel.: (33) 61 49 1853. Fax: (33) 61 49 6749.

1. *Abbreviations used in this paper*: PtdIns, phosphatidylinositol; PKC, protein kinase C; SH3, src homology 3.

(29). Moreover, based on the homology of p110 with *Saccharomyces cerevisiae* protein Vps34p, PtdIns 3-kinase and/or its products have been recently suggested to play a role in intracellular sorting and down-regulating processes involving vesicle formation and targeting to the endosomal compartment (31). Another hypothesis is a possible role of PtdIns 3-kinase in regulating the polymerization and the organization of actin, as suggested by the simultaneous appearance of PtdIns(3,4,5)P_3 and actin polymerization of *N*-formyl peptide-stimulated human neutrophils (9).

In human platelets stimulated by thrombin, PtdIns(3,4,5)P_3 production occurs very rapidly (38), whereas the accumulation of PtdIns(3,4)P_2 is a late event dependent upon fibrinogen binding to the integrin receptor α_m/β_3 (38, 41, 42) and partly requires tyrosine phosphorylations (19, 48). Its production may be due to PtdIns(3,4,5)P_3 degradation by a 5-phosphatase (40), to the effect of a PtdIns(3)P 4-kinase (47), or to the direct action of PtdIns 3-kinase on PtdIns(4)P. Since accumulations of PtdIns(3,4)P_2 and PtdIns(3,4,5)P_3 display different sensitivities to Ca^{2+}, integrin mobilization (38), and tyrosine phosphorylation (48), it is more likely that PtdIns(3,4)P_2 synthesis in platelet is due to the action of a 4-kinase on PtdIns(3)P or to the action of PtdIns 3-kinase on PtdIns(4)P, both of which would involve PtdIns 3-kinase. However, we and others have previously observed a translocation of PtdIns 3-kinase to the cytoskeleton of thrombin-activated platelets (18, 50). It is noteworthy that an association of PtdIns 3-kinase with the cytoskeleton has also been reported in other cells (32). In human platelets, thrombin stimulation leads to a dramatic reorganization of the cytoskeleton (15), which is possibly triggered in part by interaction of intetrin receptors with their ligands (21). Interestingly, several proteins involved in signal transduction are found relocated to the cytoskeleton of thrombin-activated platelets; among these are various enzymes of phosphoinositide metabolism (18) and $pp60^{c\text{-}src}$ (7, 18). This cellular protooncogene tyrosine kinase has been described to interact with PtdIns 3-kinase in different cell types (34). $pp60^{c\text{-}src}$ is constitutively present in large amounts in platelets and may be responsible for the phosphorylation and the regulation of different enzymes (8). A potential role of this tyrosine kinase in the integrin-dependent part of PtdIns 3-kinase activation in platelets is thus conceivable. In this model, thrombine induces the activation of $pp60^{c\text{-}src}$, which is then translocated to the cytoskeleton after α_m/β_3 integrin receptor mobilization and aggregation (7). However, other non-receptor tyrosine kinases whose activation is related to integrin signaling and cytoskeleton reorganization, like focal adhesion kinase ($p125^{FAK}$), may also play crucial roles in platelet activation (27).

Taken together, these observations point to a potentially important and dynamic function of the cytoskeleton in various signal transduction pathways. Therefore, to determine its possible functional relationships, we decided to study in detail the translocation of PtdIns 3-kinase to the platelet cytoskeleton during thrombin activation. Interestingly, kinetic studies revealed a strong correlation between the relocation of PtdIns 3-kinase and the accumulation of PtdIns(3,4)P_2. Since these events were dependent on both aggregation and α_m/β_3 integrin receptor engagement, our approach was to ask whether PtdIns 3-kinase activation and translocation were related to tyrosine phosphorylation promoted by integrin signaling. The data obtained indicated an important role for the integrin-dependent tyrosine kinase activation; however, cytoskeletal p85α was not tyrosine phosphorylated. This observation led us to investigate the proteins that may interact with PtdIns 3-kinase in the cytoskeleton of activated platelets. We found that thrombin activation of platelets leads to the formation of multienzymatic complexes, including PtdIns 3-kinase and tyrosine-phosphorylated $p125^{FAK}$ in areas tightly associated with the actin filament system corresponding to focal contact-like domains. Their formation appears to be dependent upon aggregation and is related to integrin-dependent tyrosine kinase activation. In investigating these associations further, we found that a proline-rich sequence of human $p125^{FAK}$ (residues 706–711) directly bound to the SH3 domain of p85α. Interestingly, micromolar amounts of a peptide corresponding to the proline-rich region of $p125^{FAK}$ (706–711) increased the specific activity of PtdIns-3 kinase. We therefore propose that this interaction may represent a new mechanism for PtdIns 3-kinase activation at very specific areas (i.e., focal contact points). The strong correlation observed between the formation of these focal adhesion-like domains and the accumulation of PtdIns(3,4)P_2 in this model may help to elucidate its functional relationships and emphasize the dynamic role of the cytoskeleton in signal transduction.

Materials and Methods

Antibodies and Fusion Proteins

The mouse anti-actin antibody was obtained from Amersham International (Buckinghamshire, UK). Mouse anti-$p125^{FAK}$, mouse anti-phosphotyrosine 4G10, and rat anti-p85α antibodies came from Upstate Biotechnology Inc. (New York). A highly specific antibody against the p85α subunit was kindly provided by Dr. Waterfield (Ludwig Institute for Cancer Research, London). Sheep polyclonal antiserum against $pp60^{c\text{-}src}$ was from Cambridge Research Biochemicals Inc. (Cambridge, UK). The mouse anti-phosphotyrosine 4G10 coupled to agarose, the GST- p85α-SH2 (NH_2) immobilized or not on agarose, and the anti-GST antibody were from TEBU (Santa Cruz Biotechnology, Inc., Santa Cruz, CA). GST-p85α-SH3 was from PharMingen (San Diego, CA).

Preparation and Activation of Platelets

Platelet concentrates provided by the local blood bank (Centre Régional de Transfusion Sanguine de Toulouse) were used to prepare platelets as previously described (19) according to Ardlie et al. (2). For inositol lipid analysis, platelets were labeled with 0.3 mCi/ml ^{32}Pi (Amersham International) during 60 min in Ca^{2+}-free Tyrode's buffer (pH 6.5, 0.2 mM EGTA) at 37°C. After a washing step in the same buffer minus EGTA, platelets were resuspended in Tyrode's buffer containing 2.5 mM $CaCl_2$ (3×10^9 or 5×10^8 cells per ml when the tetrapeptide RGDS was used) (42). In some experiments, before the stimulation by human thrombin (Sigma Chemical Co., St. Louis, MO), platelets were preincubated for 5 min in the presence of 100 μM tyrphostin AG-213 (supplied by Dr. A. Levitzki, Hebrew University, Jerusalem, Israel) or for 15 s with 500 μM RGDS (Sigma Chemical Co.). Activation by thrombin was performed with shaking. Aggregation was followed in parallel by turbidimetry using an aggregometer (Chronolog, Havertown, PA) (3×10^9 or 5×10^8 cells per ml as indicated, 600 rpm.).

Lipid Extraction and Analysis

Reactions were stopped by addition of chloroform/methanol (vol/vol), and the lipids were extracted following a modified procedure of Bligh and Dyer (3). Lipids were immediately deacylated and analyzed using an HPLC technique on a Partisphere SAX column (Whatman International Ltd., UK) as previously described (41).

Cytoskeleton Extraction

Reactions were stopped, and cytoskeleton was immediately isolated by adding 1 vol of ice-cold CSK buffer containing 100 mM Tris-HCl, pH 7.4, 20 mM EGTA, 2 mM Na_3VO_4, 2 μg/ml aprotinin, 2 μg/ml leupeptin, 1 mM PMSF (Sigma Chemical Co.), and 2% (vol/vol) Triton X-100 to control or activated platelet suspensions (33). After a 10-min incubation at 4°C, the cytoskeletal and Triton X-100–soluble fractions were separated by centrifugation (12,000 *g*, 10 min, 4°C). For further use, cytoskeletons were washed as described by Grondin et al. (18) and subsequently resuspended in suitable buffers by sonication (20 kHz for 2 × 10 s) using an ultrasonic cell disruptor.

Isolation of Polymerized Actin and the Actin-Binding Protein–Rich Fraction

Actin filaments were isolated as previously described by Payrastre et al. (32). Briefly, cytoskeletons from resting or activated platelets were solubilized in 10 ml of buffer A containing 0.6 M KI, 100 mM Pipes, pH 6.5, 100 mM KCl, 10 μg/ml leupeptin, 1 mM PMSF, and 100 μM Na_3VO_4 for 20 min at 4°C with gentle shaking and centrifuged at 40,000 *g* for 20 min at 4°C. The supernatant, containing actin, was dialyzed at 4°C for 3 h against a buffer containing 10 mM Pipes, pH 6.8, 1 mM EGTA, 2 mM $MgCl_2$, 1 mM PMSF, 2 μg/ml aprotinin, and 100 μM Na_3VO_4. Actin was then repolymerized, and this suspension was centrifuged at 12,000 *g* for 10 min at 4°C. The pellet, corresponding to actin filaments and the actin-binding protein–rich fraction, was resuspended in 50 mM Tris-HCl (pH 7.3) and immediately used for the PtdIns 3-kinase assay or Western blotting.

PtdIns 3-Kinase Assay

PtdIns 3-kinase activity was measured in a final volume of 100 μl containing 50 mM Tris-HCl, pH 7.4, 1.5 mM DTT, 100 mM NaCl, 0.5 mM EDTA, 5 mM $MgCl_2$, 5 μM ATP, exogenous lipid vesicles (100 μM phosphatidylinositol plus 200 μM phosphatidylserine, prepared by sonication in 50 mM Tris-HCl, pH 7.4), and proteins from the different fractions. Reactions were started by adding 10 μCi of [γ-^{32}P]ATP (Amersham International) and were performed at 37°C with shaking for 10 min. Reactions were stopped by adding a mixture of chloroform/methanol (vol/vol), and lipids were extracted and analyzed as previously described (41).

Immunoprecipitation and Immunopurification

Cytoskeletons were resuspended in 1 ml of a lysis buffer containing 40 mM Tris-HCl, pH 7.4, 100 mM NaCl, 100 mM NaF, 10 mM EDTA, 40 mM $Na_4P_2O_7$, 2 mM Na_3VO_4, 2 μg/ml aprotinin, 2 μg/ml leupeptin, 1 mM PMSF, 0.2% SDS, and 1% (vol/vol) Triton X-100. After sonication (20 kHz for 2 × 10 s), shaking for 20 min, and centrifugation (12,000 *g* for 10 min at 4°C), the soluble fraction was collected and subsequently precleared for 30 min at 4°C with protein A–Sepharose CL-4B or protein G–Sepharose 4B fast flow, depending on the subclasses and the origin of the antibodies used (Sigma Immuno Chemicals). Precleared suspensions were then incubated for 120 min at 4°C with the different antibodies: anti-phosphotyrosine antibody 4G10 coupled to agarose, anti-p125^{FAK} antibody (dilution 1:200), or anti-p85α antibody (dilution 1:200). After the first 60 min, 50 μl of 10% (wt/vol) protein A– or protein G–Sepharose resuspended in lysis buffer was added. The immunoprecipitates were then washed three times as described (19). With anti-phosphotyrosine immunoprecipitates, the phosphotyrosyl proteins were eluted as previously described (19).

Gel Electrophoresis and Western Blotting

Proteins were solubilized in electrophoresis sample buffer (100 mM Tris-HCl, pH 6.8, 15% (vol/vol) glycerol, 25 mM DTT, 3% SDS), boiled for 5 min and separated on 7.5% SDS-PAGE. Proteins were then blotted onto nitrocellulose (Bio Rad Laboratories, Hercules, CA) as described previously (19). The nitrocellulose was blocked for 60 min at room temperature in 10 mM Tris-HCl, pH 8, 150 mM NaCl, 0.1% (vol/vol) Tween 20 (TBST) containing 5% milk powder or 2% BSA (Sigma Chemical Co.) when phosphotyrosyl proteins were analyzed. Immunodetection was performed with different antibodies as indicated in the figures. Antibody reaction was visualized using alkaline phosphatase– or peroxidase-conjugated secondary antibodies. Nitroblue tetrazolium salt and 5-bromo-4-chloro-3-indolylphosphate were used as reagents (Sigma Chemical Co.) for alkaline phosphatase; the ECL chemiluminescence system (Amersham International) was used for peroxidase. Quantification of the different bands was performed using a densitometric analyzer (CRIS, Ramonville, France), which determines the pixel volume in each area.

Overlay Assay

Total cytoskeletons isolated from thrombin-activated platelets (0.7 IU/ml for 5 min) or immunopurified p125^{FAK} were subjected to 5–15% gradient SDS-PAGE and blotted onto nitrocellulose. The nitrocellulose was incubated with 1% BSA, 1% milk powder in TBST (0.1% Tween 20) for 5 h and subsequently incubated overnight at 4°C in 50 mM Tris-HCl (pH 7.5) containing 12 mM 2-mercaptoethanol, 0.2 M NaCl, and 0.1% milk powder in the presence of GST-p85α–SH3, GST-p85α–SH2 (NH_2), or GST (at 15 μg/ml). Nitrocellulose was then washed in TBST (0.1% Tween 20) containing 1% milk powder for 1 h to remove unbound material and then probed with anti-GST mAb as previously described.

Peptide Synthesis

The peptides KPPRPG, KVVRVG, and KPPRPG were prepared by solid-phase synthesis on an automated peptide synthesizer (model 430A; Applied Biosystem Inc., Foster City, CA) according to *N-tert*butyloxycarbonyl (t-Boc)-amino acids and symmetric anhydride or hydroxybenzotriazole ester as activation chemistry. The products were removed from the resin and simultaneously deprotected by reaction with liquid anhydrous hydrofluoric acid in the presence of anisol and m-cresol as a cation scavenger at −5°C. The purity of the final products (97%) was assessed by analytical reverse-phase liquid chromatography (column Aquapore RP 300, L8, 220 mm, 4.6 mm) and fast atom bombardment mass spectrometry (MH+, 651.2) on a ZAP-HS double focusing spectrometer (VG Analytical, UK).

Affinity Column

The proline-rich peptide from p125^{FAK} was coupled to CNBr-activated Sepharose 4B beads at a ratio of 4 mg of peptide per ml of activated beads according to the instructions provided by the manufacturer (Pharmacia LKB Biotechnology Inc., Piscataway, NJ). Cytoskeletons were resuspended in 1 ml of lysis buffer as described for the immunoprecipitation method, precleared with Sepharose 4B, and incubated or not in the presence of a mixture of two different mAbs to the SH3 domain of p85α (obtained from Dr. Waterfield's Laboratory and Dr. Matsuda). 50 μl of 10% (wt/vol) beads coupled to the peptide were added during 120 min at 4°C. The beads were then washed three times as described for the immunoprecipitation method, resuspended in sample buffer, and separated by SDS-PAGE (7.5%). Proteins were transferred to nitrocellulose and probed with antibodies to p85α.

Assay of PtdIns 3-Kinase in the Presence of the Proline-rich Peptide from p125^{FAK}

PtdIns 3-kinase was immunopurified from the Triton X-100–soluble fraction of resting platelets and was assayed essentially as previously described except that the final concentration of ATP was 50 μM and the exogenous lipid vesicles used were 150 μM phosphatidylinositol 4-monophosphate/300 μM phosphatidylserine or 150 μM phosphatidylinositol/300 μM phosphatidylserine. After addition of the peptide (solubilized in 50 mM Tris-HCl, pH 7.4), samples were preincubated for 10 min at 4°C. The reaction was then started by adding 10 μCi of [γ-^{32}P]ATP and was performed at 37°C with shaking for 5 min. The lipids were immediately extracted, analyzed, and quantified by HPLC (41). Under these assay conditions, PtdIns(3)P or PtdIns(3,4)P_2 formation was linear with time for 10 min.

Results

PtdIns(3,4)P_2 but Not PtdIns(3,4,5)P_3 Synthesis Parallels Translocation of Activated PtdIns 3-Kinase to the Cytoskeleton

We and others have previously shown that upon thrombin stimulation, both p85α and PtdIns 3-kinase activity significantly relocate to the cytoskeleton of human platelets (18, 50). Quantitative immunoblotting (Fig. 1) showed that under resting conditions, p85α was hardly detectable in the

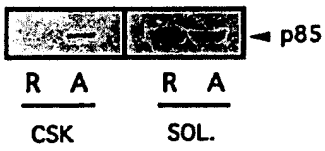

Figure 1. Quantitative immunodetection of p85α in the cytoskeleton. Cytoskeletons were extracted as indicated in Materials and Methods from resting (*R*) or thrombin-stimulated (0.7 IU/ml for 5 min) (*A*) platelets. Proteins from the cytoskeleton (*CSK*) and the corresponding Triton X-100–soluble (*SOL.*) fractions obtained from 1.6 × 10^8 platelets were separated by SDS-PAGE (7.5%) blotted onto nitrocellulose, and probed with the anti-p85α antibody.

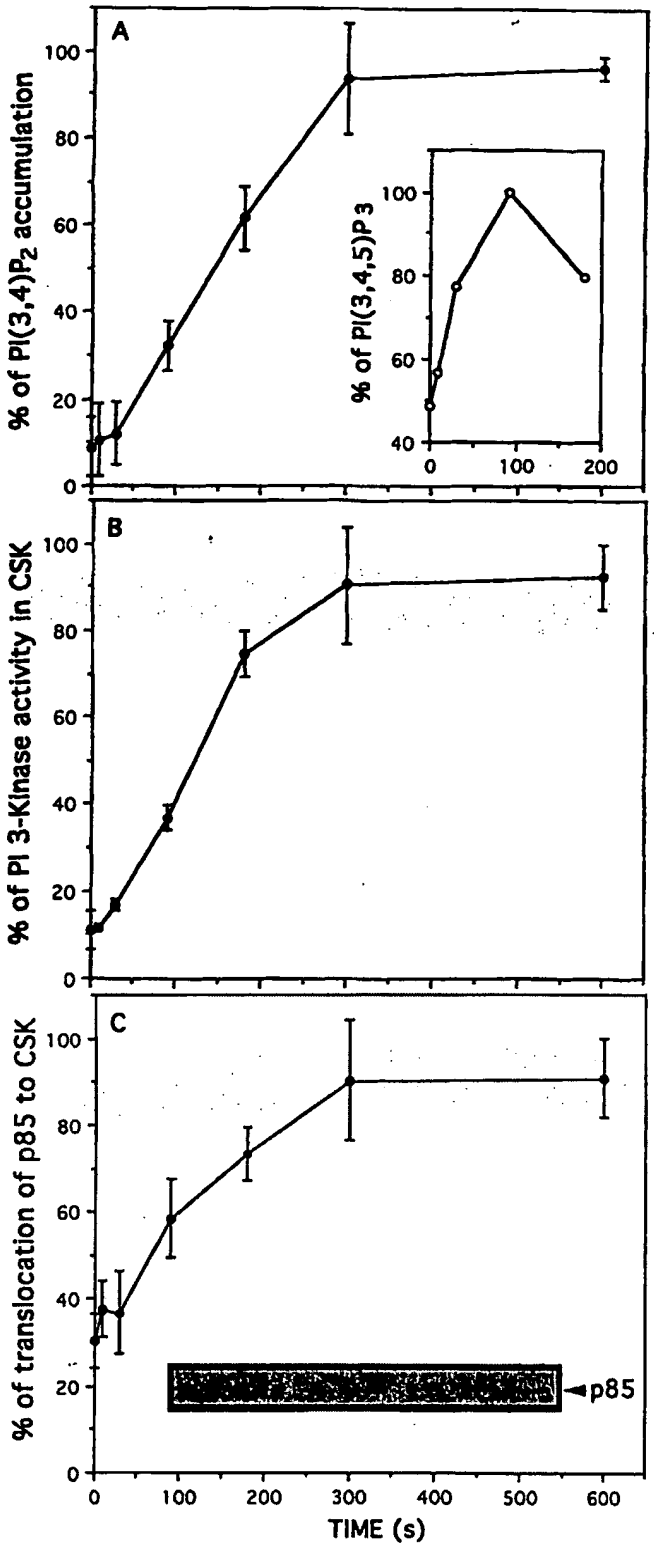

cytoskeleton, whereas up to 29 ± 9% was translocated to this compartment after 5 min of activation using 0.7 IU/ml thrombin. A parallel decrease in the Triton X-100–soluble fraction was observed. The use of a highly specific antibody from Dr. Waterfield's laboratory unambiguously identified platelet p85 as the α isoform (data not shown).

In agreement with Zhang et al. (50), when PtdIns 3-kinase was assayed in the homogenate and in the cytoskeleton obtained from thrombin-stimulated cells, its specific activity (picomoles per minute per p85α) was increased by eightfold in the cytoskeleton.

To investigate further a possible functional role for the relocation of PtdIns 3-kinase, we checked whether the kinetics of the production of D3-phosphorylated phosphoinositides were correlated with the redistribution of the enzyme. Interestingly, Fig. 2 shows a striking correlation between PtdIns-(3,4)P_2 accumulation in whole platelets, increasing PtdIns 3-kinase activity in the cytoskeleton, and translocation of p85α to the cytoskeleton (Fig. 2, *A*, *B*, and *C*, respectively). In contrast, the PtdIns(3,4,5)P_3 signal (Fig. 2 *A*, *inset*) appeared to be more rapid than PtdIns(3,4)P_2 synthesis, as previously reported (24, 38). Thus, the accumulation of PtdIns(3,4)P_2 but not of PtdIns(3,4,5)P_3 temporally correlated with the translocation of PtdIns 3-kinase to the cytoskeleton.

Tyrosine Phosphorylation, Integrin Engagement, and Aggregation Are Required for Association of PtdIns 3-Kinase with the Cytoskeleton and for PtdIns(3,4)P_2 Accumulation

Thrombin-induced platelet aggregation is accompanied by a number of biochemical events, among them pp60$^{c\text{-}src}$ translocation to the cytoskeleton, tyrosine phosphorylation of several cytoskeletal proteins, and actin polymerization. Fig. 3, *A* and *B* show that translocation of p85α, pp60$^{c\text{-}src}$, and p125^{FAK} correlated well and may be considered late events, since they were significantly detectable only after 30 s of stimulation. In addition, Fig. 3 *B* indicates that translocation of p85α, p125^{FAK}, and pp60$^{c\text{-}src}$ to the cytoskeleton was not due to an artifactual trapping of proteins during actin polymerization, which was very rapidly measurable. Indeed, the F-actin content increased about two times within 10 s of stimulation. Moreover, it is noteworthy that p85α, p125^{FAK}, and pp60$^{c\text{-}src}$ relocalization was significantly measurable only when 25% of aggregation (ΔT max%) was reached.

The tetrapeptide RGDS and tyrphostin AG-213 are commonly used to inhibit the binding of fibrinogen to integrin α_{IIb}/β_3 receptor and to inhibit tyrosine phosphorylation, respectively. Both compounds have been previously shown

Figure 2. Comparison of the time courses of PtdIns 3-kinase translocation and 3D-phosphorylated inositol lipids accumulation in whole cells upon thrombin stimulation. ^{32}P-labeled platelets (3 × 10^9 cells/ml) were activated with 0.7 IU/ml thrombin for increasing periods of time. Reactions were stopped by addition of chloroform/methanol (vol/vol). Lipids were immediately extracted and deacylated. [^{32}P]PI(3,4)P_2 (●) and [^{32}P]PI(3,4,5)P_3 (○) were subsequently separated and quantified using HPLC (*A*) as described in Materials and Methods. In parallel, platelets from the same preparation were incubated under similar conditions (1.6 × 10^8 cells per assay) and lysed by addition of CSK buffer. Cytoskeletons were immediately extracted and assayed for PtdIns 3-kinase activity (*B*) or analyzed for the presence of p85α by Western blotting (*C*). Results are expressed as percent control and are means ± SD of three to five independent experiments.

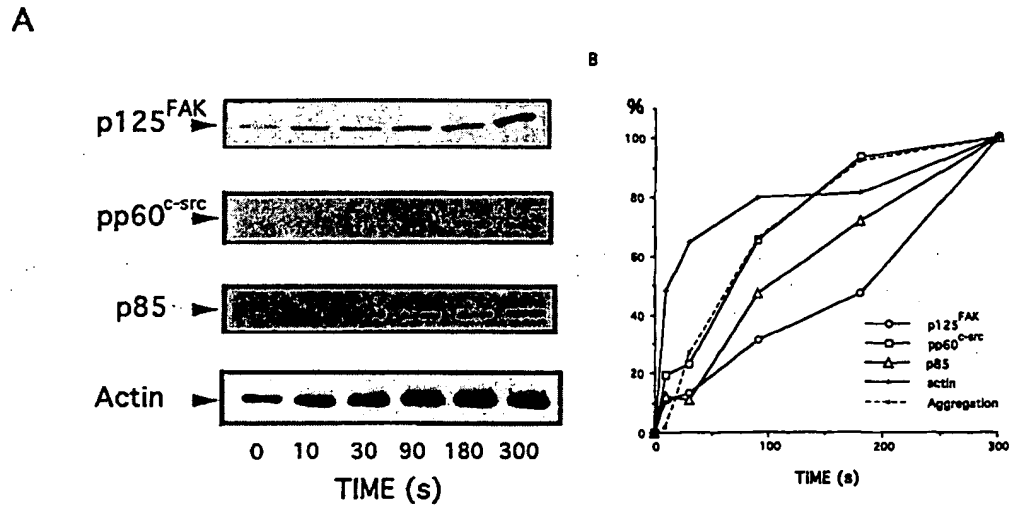

Figure 3. Analysis and comparison of different events occurring in cytoskeletons of thrombin-stimulated platelets. Platelets were stimulated with 0.7 IU/ml thrombin for increasing periods of time as indicated in the figure. The reactions were stopped by addition of CSK buffer, and cytoskeletons were immediately extracted. Cytoskeletal proteins (corresponding to 1.6×10^8 platelets) were separated by SDS-PAGE (7.5%), blotted onto nitrocellulose, and probed with different antibodies as indicated in the figure. Alkaline phosphatase detection was used for pp60$^{c\text{-}src}$ analysis, and the ECL system was used for p85α, p125^{FAK}, and actin detection (*A*). (*B*) Time course of quantitated Western blot by densitometric analysis; data are expressed as a percentage of maximal translocation for each protein and are representative of three different experiments.

to reduce significantly aggregation as well as PtdIns(3,4)P_2 accumulation induced by thrombin (19, 42). Here, we show that tyrphostin (Fig. 4 *A*) and RGDS (Fig. 4 *B*) were able to inhibit both the translocation of p85α to the cytoskeleton and PtdIns(3,4)P_2 synthesis (Table I), with RGDS being somewhat more potent. The translocation of pp60$^{c\text{-}src}$ has already been shown to depend on α_{IIb}/β_3 mobilization (22, 30); therefore, we used it as an internal control. Its relocalization was also clearly inhibited by RGDS (Fig. 4 *B*), whereas tyrphostin had a clear but weaker inhibitory effect. Table I indicates that the percentage of inhibition of aggregation (ΔT max %) induced by tyrphostin or RGDS varied in the same way as the percentage of inhibition of p85α translocation to the cytoskeleton, as well as the percentage of inhibition of PtdIns(3,4)P_2 accumulation. However, RGDS again had a more pronounced effect on aggregation. Moreover, EGTA (5 mM) was also able to inhibit thrombin-induced aggregation by 80 $\pm$ 3%, and interestingly, p85α relocalization and PtdIns(3,4)P_2 synthesis were both inhibited in the same range (85 $\pm$ 5%). Finally, the absence of shaking during thrombin stimulation abolished these events by about the same percentage as the inhibition observed with EGTA, clearly indicating that they are aggregation dependent. Therefore, integrin engagement, aggregation, and tyrosine phosphorylation are crucial for PtdIns(3,4)P_2 accumulation as well as p85α translocation to the cytoskeleton. To investigate these relationships further, we have immunopurified the phosphotyrosyl proteins from the cytoskeleton and probed them with anti-p85α and anti-pp60$^{c\text{-}src}$ antibodies. Interestingly, both proteins were absent in the pool of phosphotyrosyl proteins obtained from the cytoskeleton of resting cells, whereas they were clearly detected in the immunoprecipitates obtained from the cytoskeleton of thrombin-activated platelets (Fig. 5). Again, this was inhibited in the presence of tyrphostin. An interesting question then concerned the tyrosine phosphorylation state of cytoskeletal p85α.

Cytoskeletal Activated PtdIns 3-Kinase Is Not Tyrosine Phosphorylated on p85α

Anti-p85α immunoprecipitates were prepared from the cytoskeleton of resting or thrombin-activated platelets. The presence of p85α in such immunoprecipitates was analyzed by PtdIns 3-kinase assay and Western blotting (Fig. 6 *A*). Both PtdIns 3-kinase activity and p85α were clearly detected in the anti-p85 immunoprecipitate obtained from the cytoskeleton of activated platelets (Fig. 6 *A*), indicating the

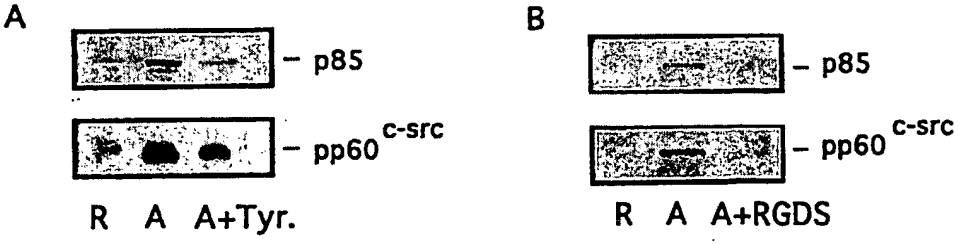

Figure 4. Effect of tyrphostin AG-213 and RGDS on p85α and pp60$^{c\text{-}src}$ relocalization. Cytoskeletons were prepared from resting (*R*) or thrombin-activated (0.7 IU/ml, 5 min) (*A*) platelets preincubated or not with tyrphostin (100 μM for 5 min) (panel *A*) or with RGDS (500 μM for 15 s) (panel *B*). Cytoskeletal proteins (corresponding to 1.6×10^8 platelets) were separated by SDS-PAGE (7.5%), blotted onto nitrocellulose, and probed with anti-p85α or anti-pp60$^{c\text{-}src}$ antibodies as indicated in the figure.

Table I. Effect of Tyrphostin and RGDS Treatment on Several Platelet Responses

Platelet responses	Percent of inhibition by tyrphostin (100 μM)	Percent of inhibition by RGDS (500 μM)
PtdIns(3,4)P_2 synthesis	53.0 ± 5.6	60.3 ± 6.9
p85 translocation to CSK	40.4 ± 12.0	54.2 ± 6.4
Aggregation ΔT max %	39.2 ± 10.5	81.5 ± 0.8

Platelets were preincubated or not with tyrphostin (100 μM) or RGDS (500 μM) and activated for 5 min by thrombin as indicated in Materials and Methods. PtdIns(3,4)P_2 synthesis was quantified using an h.p.l.c. technique. The translocation of p85α to the cytoskeleton (CSK) was detected by Western blotting experiments using anti-p85α antibody as a probe. Quantification was performed by densitometric analysis. Platelet aggregation was measured by turbidimetry using a Chronolog aggregometer (600 rev/min). Results are representative of three to five experiments, $P < 0.001$, unpaired t test.

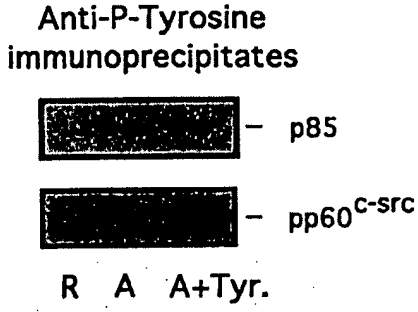

Figure 5. Detection of p85α and pp60$^{c\text{-}src}$ in anti-phosphotyrosine immunoprecipitates obtained from cytoskeleton of thrombin-stimulated platelets. Cytoskeletal proteins obtained from 1.5 × 10^9 resting (*R*) or thrombin-activated (0.7 IU/ml for 5 min) platelets, preincubated (*A+Tyr.*) or not (*A*) with 100 μM tyrphostin, were immunopurified using the agarose-coupled anti-phosphotyrosine antibody 4G10 and immunoblotted as indicated in each panel.

validity of the procedure. When these immunoprecipitated proteins were then probed with an anti-phosphotyrosine mAb (Fig. 6 *A*, *right panel*), we found that p85α present in the cytoskeleton of activated platelets was itself virtually not tyrosine phosphorylated. However, possibly only a small population of p85α is phosphorylated. Obviously, the best candidate would be p85α recovered in the anti-phosphotyrosine immunoprecipitate obtained from the cytoskeleton of thrombin-stimulated platelets. To check this possibility, we first estimated, using nonlimiting amounts of antibody, the p85α content recovered in the anti-phosphotyrosine immunoprecipitate from the cytoskeleton of activated platelets (Fig. 6 *B*, lane *2*) compared with the content of p85α recovered in the anti-p85α immunoprecipitate from a similar cytoskeleton (Fig. 6 *B*, lane *1*). The data indicate that only a subpopulation of p85α was recovered in the anti-phosphotyrosine immunoprecipitate. Finally, when the immunopurified phosphotyrosyl proteins were then probed with an anti-phosphotyrosine antibody (Fig. 6 *B*, lane *3*), no 85-kD band could be detected, indicating that, after a 5-min stimulation, the pool of p85α recovered in the anti-phosphotyrosine immunoprecipitate was virtually not tyrosine phosphorylated. These data raised the question of the identification of the proteins interacting with PtdIns 3-kinase in the cytoskeleton.

Translocation of PtdIns 3-Kinase Is Directed to the Actin Filament System

As a first attempt to localize PtdIns 3-kinase in the cytoskeleton, we performed a selective extraction procedure. By solubilizing cytoskeleton in potassium iodine followed by in vitro polymerization of actin as previously described (32), we selectively obtained the actin filament system consisting of actin and actin-binding proteins. As indicated in Fig. 7, actin was indeed present in these fractions, with a significant increase in F-actin content upon thrombin stimulation. As shown in Fig. 7, p85α was hardly detectable in the F-actin-rich fraction obtained from resting platelets, whereas in thrombin-activated platelets, p85α was clearly present in the F-actin fraction. Interestingly, p125^{FAK} and pp60$^{c\text{-}src}$ were also strongly present in this fraction (Fig. 7). Finally, a significant PtdIns 3-kinase activity was measured in the isolated actin filamental system of stimulated cells (Fig. 7), indicating that both p85α and the catalytic subunit p110 were associated with actin or with an actin-binding protein in stimu-

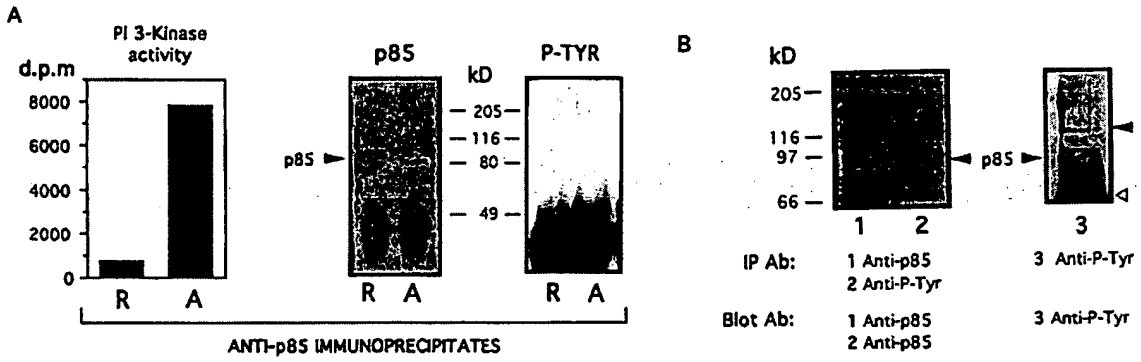

Figure 6. Analysis of the state of tyrosine phosphorylation of cytoskeletal p85α. (*A*) Cytoskeletal proteins obtained from 1.5 × 10^9 resting (*R*) or thrombin-activated (0.7 IU/ml for 5 min) (*A*) platelets were immunoprecipitated using the anti-p85α antibody. The immunoprecipitates were checked for the presence of PtdIns 3-kinase by measuring its lipid kinase activity and by Western blotting using anti-p85α antibody or the anti-phosphotyrosine antibody 4G10 as probes as indicated in the figure. (*B*) Cytoskeletons obtained from 1.5 × 10^9 thrombin-activated (0.7 IU/ml for 5 min) platelets were used for immunoprecipitations using the anti-p85α antibody (lane *1*) or the agarose-coupled anti-phosphotyrosine antibody 4G10 (lanes *2* and *3*). Immunoprecipitated proteins were then separated by SDS-PAGE (7.5%), blotted onto nitrocellulose, and probed with anti-p85α antibody (lanes *1* and *2*) or the anti-phosphotyrosine antibody 4G10 (lane *3*). The closed arrow on the upper right corresponds to 125 kD. The open arrowhead below shows the reactivity of immunoglobulin heavy chain.

lated platelets. Moreover, this result shows that PtdIns 3-kinase was still able to bind to the actin filament system after one cycle of depolymerization–repolymerization of actin in vitro. These data do not prove a direct association of PtdIns 3-kinase with actin, since several proteins may be candidates to link this enzyme to the actin filament system. Our previous data suggested an association of p85α with a cytoskeletal tyrosine-phosphorylated protein; pp60$^{c\text{-}src}$ is a possible candidate (20). A 125-kD protein is also strongly recognized by anti-phosphotyrosine antibodies in the cytoskeleton of activated platelets (Fig. 6 *B*, lane *3*). Since platelet aggregation induces focal contact-like areas, p125^{FAK} may thus be a good candidate as well (36). Therefore, we investigated the possible interactions between PtdIns 3-kinase and these two non-receptor tyrosine kinases.

Cytoskeletal PtdIns 3-Kinase Is Associated with Tyrosine-Phosphorylated p125^{FAK}

Despite the use of various antibodies and methodologies, we were unable to demonstrate the presence of pp60$^{c\text{-}src}$ in the anti-p85α immunoprecipitate (or the other way around) obtained from cytoskeleton (data not shown). Thus, we have no evidence for a direct interaction between PtdIns 3-kinase and pp60$^{c\text{-}src}$ in the cytoskeleton of activated platelets.

We then prepared anti-p125^{FAK} immunoprecipitates from the cytoskeleton of resting and thrombin-stimulated platelets. They were probed with anti-phosphotyrosine and anti-p85α antibodies. Fig. 8 shows that p125^{FAK} present in the cytoskeleton of resting platelets was weakly phosphorylated, whereas significant tyrosine phosphorylation was observed upon thrombin stimulation. It is noteworthy that a protein of ~190 kD was also recognized and may be a putative p125^{FAK}-binding phosphotyrosyl protein or a member of the focal adhesion complex. When anti-p85α antibody was used as a probe, no signal appeared in the anti-p125^{FAK} immunoprecipitate obtained from the cytoskeleton of resting platelets, whereas a clear and single 85-kD protein was detected upon thrombin stimulation. These data indicate a thrombin-dependent physical interaction between the regulatory subunit (p85α) of PtdIns 3-kinase and the tyrosine-phosphorylated p125^{FAK} in the cytoskeleton of activated platelets. This interaction appears specific, since under similar conditions, p85α was not recovered when nonimmune IgG1 from mouse was used instead of the anti-p125^{FAK} antibody (Fig. 8, lane *C*). Moreover, in agreement with our previous data (Fig. 6), the cytoskeletal p125^{FAK}-associated p85α was virtually not tyrosine phosphorylated, since no 85-kD protein was revealed in the anti-p125^{FAK} immunoprecipitate with the anti-phosphotyrosine antibody (Fig. 8, *left panel*).

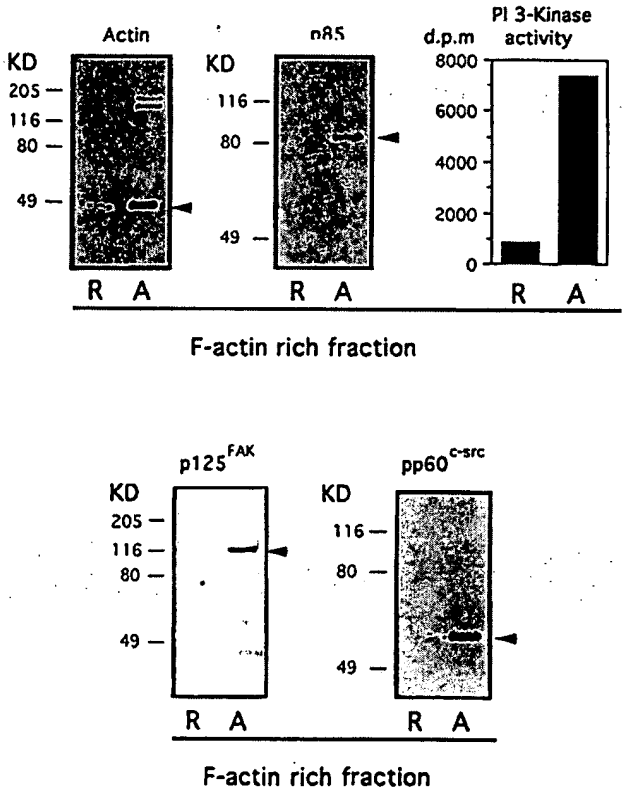

Figure 7. Association of p85α with the actin filament system. Proteins of the F-actin-rich fraction corresponding to 8 × 10^6 resting or activated-platelets were separated by SDS-PAGE (7.5%), and analyzed by Western blotting. The presence of actin, p85α, p125^{FAK}, and pp60$^{c\text{-}src}$ was checked using specific antibodies as indicated above each panel.

Interaction of a Proline-rich Sequence of p125^{FAK} (706–711) with the SH3 Domain of p85α as a New Mechanism of PtdIns 3-Kinase Activation

To determine the domain of interaction between p125^{FAK} and p85α, we first investigated the potential binding of the SH2 domain of p85α to the tyrosine-phosphorylated region of p125^{FAK}. Using the immobilized p85α–SH2 (NH_2) domain, we were unable to precipitate p125^{FAK} significantly. More-

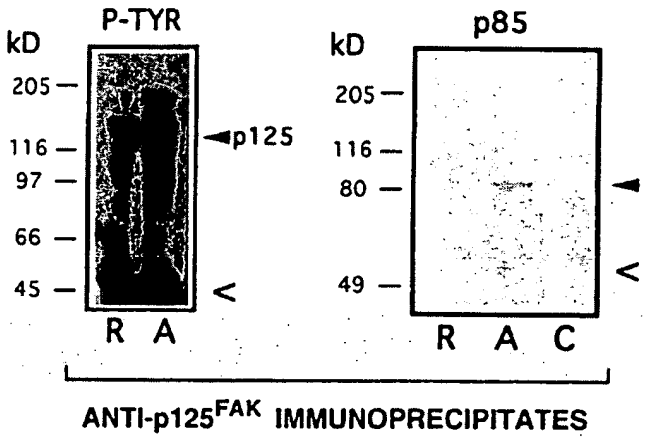

Figure 8. Presence of p85α in anti-p125^{FAK} immunoprecipitates from cytoskeletons of thrombin-stimulated platelets. Anti-p125^{FAK} immunoprecipitates were prepared from cytoskeletons of 1.5 × 10^9 resting (*R*) or thrombin-stimulated (0.7 IU/ml for 5 min) (A) platelets. After SDS-PAGE (7.5%), the proteins were analyzed by Western blotting with the anti-phosphotyrosine antibody 4G10 or the anti-p85α antibody as indicated above each panel. To evaluate the specificity of the association, a control in which nonimmune IgG1 from mouse was used instead of anti-p125^{FAK} antibodies is included (lane *C*). The open arrowhead shows the position of immunoglobulin heavy chain.

over, overlay technique did not indicate binding of GST-p85α-SH2 (NH_2) to the immunopurified tyrosine-phosphorylated p125^{FAK} on nitrocellulose (data not shown). These negative data are in agreement with the fact that p125^{FAK} does not possess the typical consensus p85-SH2 binding domain in the potential tyrosine phosphate-containing sequence found near its catalytic domain.

Another possibility was the binding of a proline-rich domain of p125^{FAK} to the SH3 domain of p85α. We therefore synthesized a peptide, KPPRPG, corresponding to a proline-rich sequence of human p125^{FAK} (residues 706–711). Once immobilized on Sepharose beads, this peptide could significantly bind cytoskeletal p85α (Fig. 9). This direct interaction seems to be specific, since PLCγ1, another SH3-containing enzyme of the phosphoinositide metabolism present in platelets, was not found to bind to this peptide (data not shown). In addition, preincubation of resuspended cytoskeleton, obtained from activated platelets, with specific antibodies directed to the SH3 domain of p85α significantly prevented this association (Fig. 9, *A* and *B*, lane *3*), strongly suggesting that the proline-rich sequence of p125^{FAK} (701–711) interacts with the SH3 domains of p85α. As a control, unrelated antibodies (nonimmune IgG1 from mouse or mAbs directed against the EGF receptor, which is not present in platelets) used instead of anti-p85α-SH3 antibodies were not able to reduce the association significantly (data not shown). Moreover, Fig. 9 *C* shows that the p85α-SH3 domain used as GST-p85α-SH3 was also able to bind directly to the peptide KPPRPG in vitro NH_2. Fig. 10 *A* indicates that p85α-SH3 but not p85α-SH2 (NH_2) was able to bind in vitro to the immunopurified p125^{FAK} obtained from cytoskeleton of activated platelets. Since weak interactions may be favored in these experiments, we have done overlay assay in which blots of immunopurified p125^{FAK} (Fig. 10 *B*, lane *1*) or total cytoskeletal proteins obtained from activated platelets (lanes *2* and *3*) were probed with GST-p85α-SH3 (lanes *1* and *3*) or with GST alone as a control (lane *2*) and then detected with an anti-GST antibody. Under these conditions, p85α-SH3 was able to bind to immunopurified p125^{FAK} (Fig. 10 *B*, lane *1*) and to a 125-kD protein of the cytoskeleton of activated platelets that matches p125^{FAK} (Fig. 10 *B*, lane *3*). In addition, p85α-SH3 was found to bind more weakly to three other proteins (Fig. 10 *B*, lane *3*) of ~93, 64, and 68 kD, which have yet to be identified.

Finally, we assessed the effect of the binding to p85α of the proline-rich sequence of p125^{FAK} on PtdIns 3-kinase activity. As shown in Fig. 11, the peptide KPPRPG significantly increased the PtdIns 3-kinase activity of immunopurified enzyme by 2.5-fold. Half-maximal activation was obtained in the presence of 10 μM peptide. Preincubation of the enzyme with antibodies directed to the SH3 domain of p85α before addition of the peptide reduced this activation by ~40% (data not shown). Finally, a control peptide, KVVRVG (Fig. 11) or KPPRVG (data not shown), was unable to activate PtdIns 3-kinase significantly under similar conditions.

To prove definitively that the direct binding of the peptide is responsible for the activation of PtdIns 3-kinase, we preincubated the immunopurified enzyme with or without 50 μM peptide for 120 min in lysis buffer lacking SDS, washed the immunocomplex twice to remove the unbound peptide, and finally assayed for PtdIns 3-kinase. Again, a twofold increase in activity was observed, indicating that the direct binding of the peptide is responsible for the activation of PtdIns 3-kinase.

Discussion

In agreement with Zhang et al. (50), we have demonstrated that ~30% of p85α is translocated to the cytoskeleton of thrombin-stimulated platelets. The translocation of p85α is

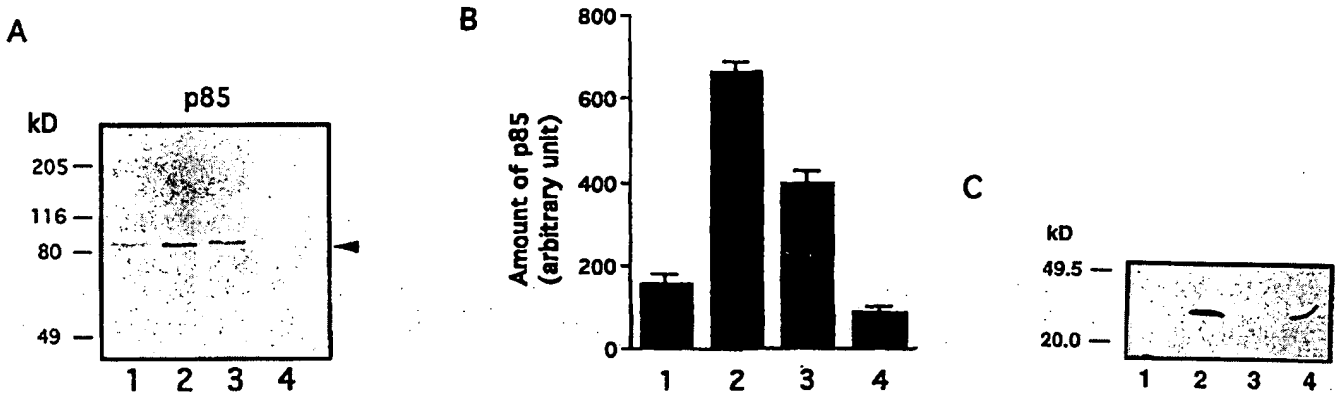

Figure 9. Association of the immobilized proline-rich sequence of p125^{FAK} (706–711) with the SH3 domain of p85α. Proteins from cytoskeleton of resting (lane *1*) or thrombin-activated (0.7 IU/ml for 5 min) (lane *2*) platelets were adsorbed onto Sepharose beads coupled to the p125^{FAK} proline-rich region (706–711) as described in Materials and Methods. Alternatively, proteins from cytoskeleton of activated platelets were preincubated for 30 min with antibodies directed to the SH3 domain of p85α and then adsorbed onto Sepharose beads coupled to the p125^{FAK} proline-rich region (706–711) (lane *3*). Finally, proteins from cytoskeleton of activated platelets were adsorbed to Sepharose beads alone as a control (lane *4*). After SDS-PAGE (7.5%), the proteins adsorbed were analyzed by Western blotting with the anti-p85α antibody (*A*). (*B*) Quantification by densitometric analysis of the Western blot. Data are expressed in arbitrary units (pixel points) and are means ± SEM of three different experiments. Finally, the direct binding of p85α-SH3 to the proline-rich region of p125^{FAK} (706–711) was analyzed in *C*. Purified GST-p85α-SH3 was diluted in lysis buffer to 5 μg/ml and incubated for 1.5 h with Sepharose beads alone (lane *1*) or with Sepharose beads coupled to the peptide (lane *2*). As a control, GST alone was incubated with the Sepharose beads coupled to the peptide (lane *3*). After extensive washing, the adsorbed proteins were analyzed by Western blotting with the anti-GST antibody. Lane *4* shows the position of GST-p85α-SH3 (37 kD) on the blot.

likely accompanied by a functional p110 catalytic subunit, since PtdIns 3-kinase activity was measured in the cytoskeleton of activated platelets and exhibited a higher specific activity than in the homogenate. Interestingly, PtdIns(3,4)P_2 but not PtdIns(3,4,5)P_3 synthesis paralleled the translocation of both p85α and PtdIns 3-kinase activity to the cytoskeleton, strongly suggesting a relationship between these two events. In thrombin-stimulated platelets, PtdIns(3,4,5)P_3 is produced very rapidly, whereas PtdIns(3,4)P_2 accumulates at a later stage (24, 38). Although PtdIns(3,4)P_2 has been shown to be a degradation product of PtdIns(3,4,5)P_3 in neutrophils, Sorisky et al. (38) have demonstrated that the production of these two phospholipids is regulated differently in thrombin-stimulated platelets. In this model, in contrast to the PtdIns(3,4)P_2 response, the accumulation of PtdIns(3,4,5)P_3 is unaffected by Ca^{2+} or the tetrapeptide RGDS (38, 42). Our results suggest that the redistribution of PtdIns 3-kinase to the cytoskeleton may be of importance for the accumulation of PtdIns(3,4)P_2. Detailed time course studies of PtdIns(3,4)P_2 accumulation and PtdIns 3-kinase, p125^{FAK}, and pp60$^{c\text{-}src}$ relocalization revealed that these events are in fact concomitant and significantly detectable only when 25–30% of aggregation (ΔT max %) is reached. Similar data have been obtained by Torti et al. (45) for the low molecular weight GTP-binding protein Rap2B. In contrast, actin polymerization is very rapidly detected, since double the amount of F-actin is observed within 10 s of stimulation. One may note that this time course of polymerization fits rather well with the PtdIns(3,4,5)P_3 signal as previously shown in fMLP-stimulated neutrophils (9). Moreover, it is noteworthy that the state of actin polymerization may in turn influence the phosphorylation state of several cytoskeletal proteins, including the focal adhesion kinase p125^{FAK} (23).

On the other hand, we have previously shown that PtdIns(3,4)P_2 accumulation is inhibited by RGDS (42). Here we demonstrate that the redistribution of p85α to the actin cytoskeleton and aggregation (ΔT max %) are inhibited in a similar manner by RGDS. In addition, EGTA (5 mM)

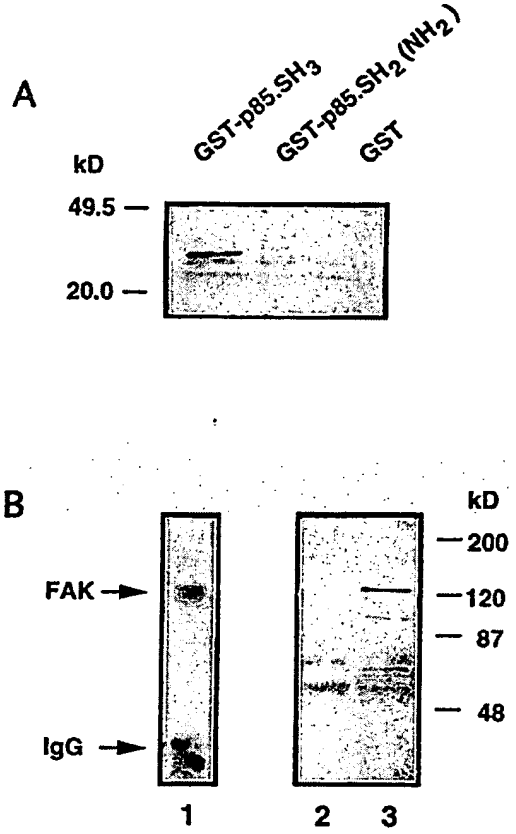

Figure 10. Direct binding of p85α–SH3 to cytoskeletal p125^{FAK}. p125^{FAK} was immunopurified from cytoskeleton of thrombin-activated platelets (0.7 IU/ml for 5 min) as described in Materials and Methods. The immunocomplex was then incubated in lysis buffer at 4°C for 1.5 h in the presence of 15 μg/ml GST-p85α–SH3, GST-p85α–SH2 (NH2), or GST alone, as indicated in the figure. After two washes in lysis buffer and three washes in 50 mM Tris-HCl, pH 7.35, 150 mM NaCl, the adsorbed proteins were analyzed by Western blotting using the anti-GST antibody as a probe (*A*). (*B*) Immunopurified p125^{FAK} (lane *1*) or total cytoskeletal proteins prepared from activated platelets (lanes *2* and *3*) were resolved by 7.5% or 5–15% SDS-PAGE, respectively, and blotted onto nitrocellulose for overlay assay as indicated in Materials and Methods. Proteins on nitrocellulose were then probed with GST-p85α–SH3 (lanes *1* and *3*) or with GST alone (lane *2*) and subsequently detected with anti-GST antibody using the ECL system. The nitrocellulose of lane *3* has then been stripped according to the procedure provided in the ECL kit and reprobed with the anti-p125^{FAK} antibody. The position of p125^{FAK} is indicated by the arrowhead.

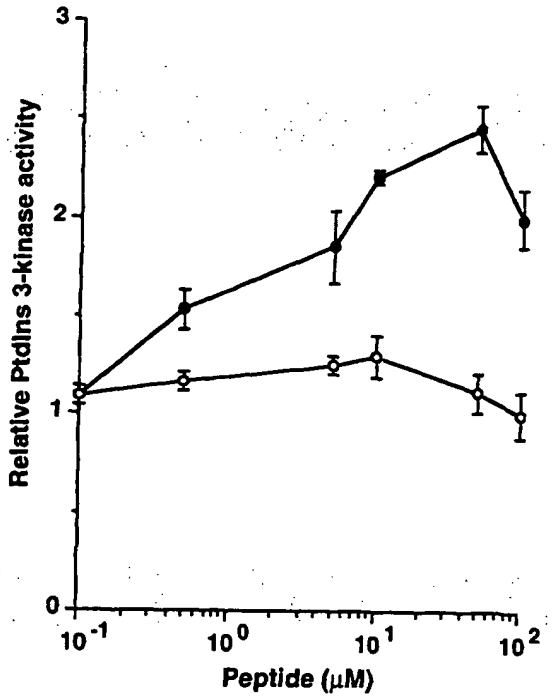

Figure 11. Activation of PtdIns 3-kinase by the peptide containing the proline-rich sequence of p125^{FAK} (706–711). Immunopurified PtdIns 3-kinase was assayed in the presence of increasing concentrations of the peptide corresponding to the proline-rich sequence of p125^{FAK} (KPPRPG) (●) or a control peptide with the same number of charges (KVVRVG) (○). Products of PtdIns 3-kinase were quantitated by HPLC as described in Materials and Methods. Results are expressed as PtdIns 3-kinase activity relative to that measured in the absence of peptide, which was taken as 1. The results shown are mean ± SD of three to five different experiments.

or the absence of shaking during activation significantly inhibited the association of p85α with the cytoskeletons as well as the accumulation of PtdIns(3,4)P_2. Therefore, aggregation via the binding of adhesive proteins to their receptors, especially fibrinogen binding to α_{IIb}/β_3, is required for both the production of PtdIns(3,4)P_2 and the translocation of PtdIns 3-kinase and pp60$^{c\text{-}src}$ to the actin cytoskeleton. The similarity both in the time course and in the sensitivity of tyrphostin and RGDS of PtdIns(3,4)P_2 synthesis and PtdIns 3-kinase translocation to the cytoskeleton suggests that these events might be tightly linked. This is not the case for PtdIns(3,4,5)P_3 production, which is not regulated in the same way (38, 48). Such a difference would be explained by the presence in human platelets of a PtdIns 3-kinase activated by G-protein βγ subunits (44), which was recently identified in other hematopoietic cells (39). Our present data and those previously obtained on Glanzmann's thrombastenic platelets (42) may suggest a role for the α_{IIb}/β_3-linked actin cytoskeleton in the compartmentalization of activated PtdIns 3-kinase. The inhibitory effect of tyrphostin that we observed is in agreement with the fact that when RGDS blocks the binding of fibrinogen and other ligands to α_{IIb}/β_3, thrombin-induced tyrosine phosphorylation of several substrates is also blocked (11, 17). The chronology of this cascade of events may also explain why RGDS has a more potent inhibitory effect than tyrphostin. Thus, both fibrinogen binding to α_{IIb}/β_3 and the subsequently induced tyrosine phosphorylations are crucial events for the translocation of PtdIns 3-kinase to the actin cytoskeleton and the production of PtdIns(3,4)P_2 in thrombin-stimulated platelets. The role of tyrosine kinases in this mechanism is confirmed by the presence of a fraction of p85α in anti-phosphotyrosine immunoprecipitates obtained from the cytoskeleton of thrombin-activated platelets. However, we have found that the pool of cytoskeletal p85α is virtually not tyrosine phosphorylated, even though only a subpopulation of p85α is recovered in the anti-phosphotyrosine immunoprecipitate. Furthermore, we were also unable to show the tyrosine phosphorylation of p85α in the Triton X-100–soluble fraction of activated platelets (data not shown). Therefore, its presence in the pool of phosphotyrosyl proteins is possible only if p85α is physically associated with another tyrosine-phosphorylated protein. This result stimulated us to investigate the proteins that may interact with PtdIns 3-kinase in the cytoskeleton of activated platelets. We found that the relocalization of PtdIns 3-kinase and pp60$^{c\text{-}src}$ is preferentially directed to the actin filament system consisting of F-actin and actin-binding proteins. Functional PtdIns 3-kinase is still able to bind to the actin filaments even after one cycle of depolymerization-repolymerization of actin in vitro. Our observations are consistent with the recent data obtained by Fox et al. (13). These authors have observed that the Triton X-100–insoluble membrane skeleton components sedimented at 100,000 *g*, such as spectrin, vinculin, or talin, as well as pp60$^{c\text{-}src}$, pp62$^{c\text{-}yes}$, and p21^{ras}-GAP, are redistributed to the Triton X-100–insoluble low speed fraction (15,000 *g*) during thrombin-induced aggregation. In this respect, it is noteworthy that a number of proteins that have been identified in the platelet membrane skeleton are actin-binding proteins (12, 13). Our data do not prove a direct association with actin, since actin-binding proteins may link PtdIns 3-kinase to F-actin and since we found a population of cytoskeletal p85α associated with a tyrosine-phosphorylated protein. The kinase pp60$^{c\text{-}src}$ is found in the actin-rich fraction and has been described to interact weakly with PtdIns 3-kinase in the Triton X-100–soluble fraction of thrombin-activated human platelets (20). Therefore, we have investigated such a possibility in the cytoskeleton. However, using both Western blot and enzymatic assays, we have failed to find a clear interaction between PtdIns 3-kinase and pp60$^{c\text{-}src}$ under our conditions (data not shown). The association between p85α and src-like kinases has been described in other models and seems to be due to SH3-mediated interactions (35); this mechanism might be minor in platelets (20).

However, another interesting candidate is p125^{FAK}, a protein tyrosine kinase involved with integrin signaling that is phosphorylated and activated upon thrombin stimulation of platelets (27). Moreover, actin-dependent cytoskeletal interactions seem to be necessary for these events (27). Interestingly, p125^{FAK} is not activated in platelets from Glanzmann's thrombasthenia (27), which also fail to produce PtdIns(3,4)P_2 (42). Our results show both the presence of a tyrosine-phosphorylated form of p125^{FAK} in the cytoskeleton of thrombin-activated platelets and an interaction between tyrosine-phosphorylated p125^{FAK} and non–tyrosine-phosphorylated p85α in this cytoskeleton. Furthermore, the amount of p85α found associated with p125^{FAK} is comparable to the amount of p85α recovered in the anti-phosphotyrosine immunoprecipitate. This association may therefore explain the presence of non–tyrosine-phosphorylated p85α in such immunoprecipitates and the increase in its ability to be precipitated with the anti-phosphotyrosine antibody after thrombin stimulation. It is noteworthy that the potential tyrosine phosphate–containing domain found near the catalytic domain of p125^{FAK} (1) does not exhibit the consensus motif known to bind the SH2 domain of p85α, and using different approaches, we were unable to demonstrate an association by this way. However, two proline-rich domains (564–576 and 694–714) containing the PPXP motif (6, 49) are found in the sequence of p125^{FAK} (1). Here we show that a peptide corresponding to residues 706–711 of human p125^{FAK} binds to the SH3 domain of non–tyrosine-phosphorylated p85α. This binding seems to be specific, since the p85α SH3 domain was also able to bind to immunopurified p125^{FAK} in vitro or to a 125-kD cytoskeletal protein that matches p125^{FAK} on nitrocellulose.

Moreover, this binding led to a significant activation of PtdIns 3-kinase. This activation possibly results from the induction of a conformational change leading to the activation of the p110 catalytic subunit, which is comparable to the activation described for PtdIns 3-kinase by the tyrosine-phosphorylated PDGF receptor (10), IRS-1 (28) and the *src* family kinase SH3 (34). Our data strongly suggest a new mode of PtdIns 3-kinase regulation in which binding of proline-rich sequence of p125^{FAK} (706–711) to the SH3 domain of p85α increased enzymatic activity of this lipid kinase. This mechanism is operative during thrombin-induced aggregation and may be important for enzyme access to its substrate at very specific areas of the cell (i.e., focal contacts). The role of 3D-phosphorylated phospholipids at these particular points has now to be investigated in detail. However, with respect to the data published recently, it is possible

to suggest that these lipids may play a role in the organization of actin polymerization, leading to the formation of actin filament bundles linked to focal contact points.

We propose that p125^{FAK} is responsible, at least in part, for the indirect binding of PtdIns 3-kinase to actin microfilaments and plays a critical role in activating and directing this lipid kinase to an appropriate location. Since we demonstrate here a role of aggregation, integrin receptor engagement and subsequent tyrosine phosphorylation in PtdIns 3-kinase translocation, and concomitant PtdIns(3,4)P_2 accumulation, it is tempting to suggest that p125^{FAK} may be a key enzyme in coupling integrin receptor signaling with these events. During the reviewing process of this manuscript, Chen and Guan (4, 5) described an interaction of p125^{FAK} with PtdIns 3-kinase in fibroblasts. Interestingly, this association was induced by cell adhesion to fibronectin-coated culture dishes (5) or by PDGF treatment (4). Our results also suggest that PtdIns 3-kinase likely displays different modes of interaction with cytoskeletal elements since only ~25% of cytoskeletal p85α is found associated with p125^{FAK}. This physical interaction may be transient, and PtdIns 3-kinase may then be compartmentalized in other cytoskeletal areas possibly to be down-regulated. The presence of the SH2 and SH3 domains as well as SH3-binding motifs in the p85 subunit (25) may explain the different targeting of these associations. Further work is necessary to identify all of the different cytoskeletal proteins with which PtdIns 3-kinase may be associated and their relevant biochemical and functional relationships.

In conclusion, focal contact–like areas induced upon thrombin stimulation of platelets, involving α_{IIb}/β_3, p125^{FAK}, as well as other phosphotyrosyl proteins and actin microfilaments, are very important for PtdIns 3-kinase relocation and PtdIns(3,4)P_2 accumulation. Whether this inositol lipid may in turn play a role in stabilizing the clot remains to be established.

We thank Dr. M. Waterfield and Dr. R. Dhand for kindly providing the highly specific anti-p85α antibody. We are grateful to Drs. P. M. P. Van Bergen en Henegouwen and L. Wolfraim for fruitful discussions and Miss C. Alary and Mr. J. Mathieu for technical assistance.

This work was supported in part by a grant from Association pour la Recherche contre le Cancer and from La Ligue Nationale Contre le Cancer.

Received for publication 18 October 1994 and in revised form 12 January 1995.

References

1. André, E., and M. Becher-André. 1993. Expression of an N-terminally truncated form of human focal adhesion kinase in brain. *Biochem. Biophys. Res. Commun.* 190:140–147.
2. Ardlie, N. G., M. A. Packham, and J. F. Mustard. 1970. Adenosine diphosphate-induced platelet aggregation in suspensions of washed rabbit platelets. *Br. J. Haematol.* 19:7–12.
3. Bligh, E. G., and W. J. Dyer. 1993. A rapid method of total lipid extraction and purification. *Can. J. Biochem. Physiol.* 37:911–917.
4. Chen, H.-C., and J.-L. Guan. 1994a. Stimulation of phosphatidylinositol 3′-kinase association with focal adhesion kinase by platelet-derived growth factor. *J. Biol. Chem.* 269: 31229–31233.
5. Chen, H.-C., and J.-L. Guan. 1994b. Association of focal adhesion kinase with its potential substrate phosphatidylinositol 3-kinase. *Proc. Natl. Acad. Sci. USA.* 91:10148–10152.
6. Chen, J. K., W. S. Lane, A. W. Brauer, A. Tanaka, and S. L. Schreiber. 1993. Biased combinatorial libraries: novel ligands for the SH3 domain of phosphatidylinositol 3-kinase. *J. Am. Chem. Soc.* 115:12591–12592.
7. Clark, E. A., and J. S. Brugge. 1993. Redistribution of activated pp60$^{c\text{-}src}$ to integrin-dependent cytoskeletal complexes in thrombin-stimulated platelets. *Mol. Cell. Biol.* 13:1863–1871.
8. Dhar, A., and S. D. Shukla. 1994. Electrotransjection of p60$^{v\text{-}src}$ monoclonal antibody inhibits activation of phospholipase C in platelets. A new mechanism for platelet-activating factor responses. *J. Biol. Chem.* 269: 9123–9127.
9. Eberle, M., A. E. Traymor-Kaplan, L. A. Sklar, and J. Novganer. 1990. Is there is relationship between phosphatidylinositol *tris*phosphate and F-actin polymerization in human neutrophils? *J. Biol. Chem.* 264: 16725–16728.
10. Escobedo, F. A., D. R. Kaplan, W. M. Kawanaugh, C. W. Turck, and C. T. Williams. 1991. A phosphatidylinositol 3-kinase binds to platelet-derived growth factor receptors through a specific receptor sequence containing phosphotyrosine. *Mol. Cell. Biol.* 11:1125–1132.
11. Ferrel, J. E., and G. S. Martin. 1989. Tyrosine-specific protein phosphorylation is regulated by glycoprotein IIb-IIIa in platelets. *Proc. Natl. Acad. Sci. USA.* 86:2234–2238.
12. Fox, J. E. B. 1993. The platelet cytoskeleton. *Thromb. Haemostasis.* 70: 884–893.
13. Fox, J. E. B., L. Lipfert, E. A. Clark, C. C. Reynolds, C. D. Austin, and J. S. Brugge. 1993. On the role of platelet membrane skeleton in mediating signal transduction. Association of α_{IIb}/β_3, pp60$^{c\text{-}src}$, pp62$^{c\text{-}src}$, and the p21^{ras} GTPase-activating protein with the membrane skeleton. *J. Biol. Chem.* 268:25973–25984.
14. Fukui, Y., and H. Hanafusa. 1989. Phosphatidylinositol kinase activity associates with viral p60src protein. *Mol. Cell. Biol.* 9:1651–1658.
15. Furman, M. I., T. M. Gardner, and P. J. Goldschmidt-Clermont. 1993. Mechanism of cytoskeletal reorganization during platelet activation. *Thromb. Haemostasis.* 70:229–232.
16. Gaudette, D. C., H. M. Aukemas, C. A. Jolly, R. S. Chapkin, and B. J. Holub. 1993. Mass and fatty acid composition of the 3-phosphorylated phosphatidylinositol bisphosphate isomer in stimulated human platelets. *J. Biol. Chem.* 268:13773–13776.
17. Golden, A., J. S. Brugge, and J. S. Shattil. 1990. Role of platelet membrane glycoprotein IIb-IIIa in agonist induced tyrosine phosphorylation of platelet proteins. *J. Cell Biol.* 11:3117–3127.
18. Grondin, P., M. Plantavid, C. Sultan, M. Breton, G. Mauco, and H. Chap. 1991. Interaction of pp60$^{c\text{-}src}$, phospholipase C, inositol-lipid and diacylglycerol-kinases with the cytoskeletons of thrombin stimulated platelets. *J. Biol. Chem.* 266:15705–15709.
19. Guinebault, C., B. Payrastre, C. Sultan, G. Mauco, B. Breton, S. Levy-Toledano, M. Plantavid, and H. Chap. 1993. Tyrosine kinases and phosphoinositide metabolism in thrombin stimulated human platelets. *Biochem. J.* 292:851–856.
20. Gutking, J. S., P. M. Lacal, and K. C. Robbins. 1990. Thrombin-dependent association of phosphatidylinositol 3-kinase with pp60$^{c\text{-}src}$ and p59^{fyn} in human platelets. *Mol. Cell. Biol.* 10:3806–3809.
21. Haimovich, B., L. Lipfert, J. S. Brugge, and S. J. Shattil. 1993. Tyrosine phosphorylation and cytoskeletal reorganization in platelets are triggered by interaction of integrin receptors with their immobilized ligands. *J. Biol. Chem.* 268:15868–15877.
22. Horwath, A. R., L. Muszbeck, and S. Kellie. 1992. Translocation of pp60$^{c\text{-}src}$ to the cytoskeleton during platelet aggregation. *EMBO (Eur. Mol. Biol. Org.) J.* 11:855–861.
23. Huang, M.-M., L. Lipfert, M. Cunningham, J. S. Brugge, M. H. Ginsberg, and S. J. Shattil. 1993. Adhesive ligand binding to integrin α_{IIb}/β_3 stimulates tyrosine phosphorylation of novel protein substrates before phosphorylation of pp125^{FAK}. *J. Cell Biol.* 122:473–483.
24. Huang, R. S., A. Sorisky, W. R. Church, E. R. Simons, and S. E. Rittenhouse. 1991. Thrombin receptor-directed ligand accounts for activation by thrombin platelet phospholipase C and accumulation of 3-phosphorylated phosphoinositide. *J. Biol. Chem.* 266:18435–18438.
25. Kapeller, R., K. V. S. Prasad, O. Janssen, W. Hou, B. S. Schaffhausen, C. E. Rudd, and L. C. Cantley. 1994. Identification of two SH3-binding motifs in the regulatory subunit of phosphatidylinositol 3-kinase. *J. Biol. Chem.* 269:1927–1933.
26. King, W. G., G. L. Kucera, A. Sorisky, J. Zhang, and S. E. Rittenhouse. 1991. Protein kinase C regulates the stimulated accumulation of 3-phosphorylated phosphoinositides in platelets. *Biochem. J.* 278:475–480.
27. Lipfert, L., B. Haimovich, M. D. Schaller, B. S. Cobb, J. T. Parsons, and J. S. Brugge. 1992. Integrin-dependent phosphorylation and activation of the protein tyrosine pp125^{FAK} in platelets. *J. Cell Biol.* 113:905–912.
28. Myers, M. G., J. M. Backer, X. J. Sun, S. Shoelson, P. Hu, J. Schlessinger, H. Yoakim, B. Schaffhausen, and M. F. White. 1992. IRS-1 activates phosphatidylinositol 3-kinase by associating with src homolgoy 2 domain of p85. *Proc. Natl. Acad. Sci. USA.* 89:10350–10354.
29. Nakanishi, H., K. A. Brewer, and J. H. Exton. 1993. Activation of the ζ izoenzyme of protein kinase C by phosphatidylinositol 3,4,5-trisphosphate. *J. Biol. Chem.* 268:13–16.
30. Oda, A., B. J. Druker, M. Smith, and E. W. Salzman. 1992. Association of pp60$^{c\text{-}src}$ with Triton X100 insoluble residue in human blood platelets requires platelet aggregation and actin polymerization. *J. Biol. Chem.* 267:20075–20081.
31. Panayotou, G., and M. D. Waterfield. 1992. Phosphatidylinositol 3-kinase: a key enzyme in diverse signaling processes. *Trends Cell Biol.* 2: 358–360.
32. Payrastre, B., P. M. P. Van Bergen en Henegouven, M. Breton, J. C. Den

Hartigh, M. Plantavid, A. J. Verkleij, and J. Boonstra. 1991. Phosphoinositide kinase, diacylglycerol kinase and phospholipase C activities associated to the cytoskeleton: effect of epidermal growth factor. *J. Cell Biol.* 115:121–128.

33. Pho, D. B., C. Vasseur, E. Desbruyères, and A. Olomuck. 1984. Evidence for the presence of tropomyosin in the cytoskeletons of ADP- and thrombin-stimulated blood platelets. *FEBS (Fed. Eur. Biochem. Soc.) Lett.* 173:164–168.
34. Pleiman, C. M., W. H. Hertz, and J. C. Cambien. 1994. Activation of phosphatidylinositol 3′ kinase by SRC-family kinase SH3 binding to the p85 subunit. *Science (Wash. DC).* 23:1609–1612.
35. Prasad, K. V. S., O. Janssen, R. C. C. L. Kappeller, and C. E. Rudd. 1993. Src-homology 3 domain of protein kinase p59fyn mediates binding to phosphatidylinositol 3-kinase in T cells. *Proc. Natl. Acad. Sci. USA.* 90:7366–7370.
36. Schaller, M. D., and J. T. Parsons. 1993. Focal adhesion kinase: an integrin-linked protein tyrosine kinase. *Trends Cell Biol.* 3:258–261.
37. Shoelson, S. E., M. Sivaraja, K. P. Williams, P. Hu, J. Schlessinger, and M. A. Weiss. 1993. Specific phosphopeptide binding regulates a conformational change in PI 3-kinase SH2 domain associated with enzyme activation. *EMBO (Eur. Mol. Biol. Org.) J.* 12:795–802.
38. Sorisky, A., W. G. King, and S. E. Rittenhouse. 1992. Accumulation of PtdIns(3,4)P_2 and PtdIns(3,4,5)P_3 in thrombin-stimulated platelets. Different sensitivities to Ca^{2+} or functional integrin. *Biochem. J.* 286: 581–584.
39. Stephens, L., A. Smrcka, F. T. Cooke, T. R. Jackson, P. C. Sternweis, and P. T. Hawkins. 1994. A novel phosphoinositide 3 kinase activity in myeloid-derived cells is activated by G protein $\beta\gamma$ subunits. *Cell.* 77:83–93.
40. Stephens, L. R., K. T. Hughes, and R. F. Irvine. 1991. Pathway of phosphatidylinositol(3,4,5)trisphosphate synthesis in activated neutrophils. *Nature (Lond.).* 351:33–39.
41. Sultan, C., M. Breton, G. Mauco, P. Grondin, M. Plantavid, and H. Chap. 1990. The novel inositol lipid phosphatidylinositol 3,4-bisphosphate is produced by human blood platelets upon thrombin stimulation. *Biochem. J.* 269:831–834.
42. Sultan, C., M. Plantavid, C. Bachelot, P. Grondin, M. Breton, G. Mauco, S. Levy-Toledano, J. P. Caen, and H. Chap. 1991. Involvement of platelet glycoprotein IIb-IIIa (αIIb-β3 integrin) in thrombin-induced synthesis of phosphatidylinositol 3′,4′-bisphosphate. *J. Biol. Chem.* 266:23554–23557.
43. Talmage, D. A., R. Freund, A. T. Young, J. Dahl, C. J. Dane, and T. L. Benjamin. 1989. Phosphorylation of middle T by pp60$^{c\text{-}src}$ a switch for binding of phosphatidylinositol 3-kinase and optimal tumorigenesis. *Cell.* 59:55–65.
44. Thomason, P. A., S. R. James, P. J. Casey, and C. P. Downes. 1994. A G-protein $\beta\gamma$-subunit-responsive phosphoinositide 3-kinase activity in human platelet cytosol. *J. Biol. Chem.* 269:16525–16528.
45. Torti, M., G. Ranaschi, F. Sinigaglia, E. G. Lapetina, and C. Balduini. 1993. Association of the low molecular weight GTP-binding protein rap2B with the cytoskeleton during platelet aggregation. *Proc. Natl. Acad. Sci. USA.* 90:7553–7557.
46. Valius, M., and A. Kazlauskas. 1993. Phospholipase C-γ1 and phosphatidylinositol 3-kinase are the downstream mediators of the PDGF receptor's mitogenic signal. *Cell.* 73:321–334.
47. Yamamoto, K., A. Graziani, C. Carpenter, L. C. Cantley, and E. G. Lapetina. 1990. A new pathway for the formation of phosphatidylinositol-3,4-bisphosphate. Phosphorylation of phosphatidylinositol-3-monophosphate by phosphatidylinositol-3-monophosphate 4-kinase. *J. Biol. Chem.* 265: 22086–22089.
48. Yatomi, Y., Y. Ozaki, and S. Kume. 1992. Synthesis of phosphatidylinositol 3,4-bisphosphate but not phosphatidylinositol 3,4,5-trisphosphate is closely correlated with protein-tyrosine phosphorylation in thrombin-activated platelets. *Biochem. Biophys. Res. Commun.* 186:1480–1486.
49. Yu, H., J. K. Chen, S. Feng, D. C. Dalgarno, A. W. Brauer, and S. L. Schreiber. 1994. Structural basis for the binding of proline-rich peptides to SH3 domains. *Cell.* 76:933–945.
50. Zhang, J., M. J. Fry, M. D. Waterfield, S. Jaken, L. Liao, J. E. B. Fox, and S. E. Rittenhouse. 1992. Activated phosphoinositide 3-kinase associates with membrane skeleton in thrombin-exposed platelets. *J. Biol. Chem.* 267:4686–4692.
51. Zhang, J., W. G. King, S. Dillon, A. Hall, L. Feig, and S. E. Rittenhouse. 1993. Activation of platelet phosphatidylinositide 3-kinase requires the small GTP-binding protein Rho. *J. Biol. Chem.* 268:22251–22254.

The EMBO Journal Vol.16 No.23 pp.7032–7044, 1997

Signal characteristics of G protein-transactivated EGF receptor

Henrik Daub, Christian Wallasch, Andreas Lankenau, Andreas Herrlich[1] and Axel Ullrich[2]

Department of Molecular Biology, Max-Planck-Institut für Biochemie, Am Klopferspitz 18A, 82152 Martinsried and [1]Institut für Pharmakologie, Freie Universität Berlin, Thielallee 67-73, 14195 Berlin, Germany

[2]Corresponding author

The epidermal growth factor receptor (EGFR) tyrosine kinase recently was identified as providing a link to mitogen-activated protein kinase (MAPK) in response to G protein-coupled receptor (GPCR) agonists in Rat-1 fibroblasts. This cross-talk pathway is also established in other cell types such as HaCaT keratinocytes, primary mouse astrocytes and COS-7 cells. Transient expression of either G_q- or G_i-coupled receptors in COS-7 cells allowed GPCR agonist-induced EGFR transactivation, and lysophosphatidic acid (LPA)-generated signals involved the docking protein Gab1. The increase in SHC tyrosine phosphorylation and MAPK stimulation through both G_q- and G_i-coupled receptors was reduced strongly upon selective inhibition of EGFR function. Inhibition of phosphoinositide 3-kinase did not affect GPCR-induced stimulation of EGFR tyrosine phosphorylation, but inhibited MAPK stimulation, upon treatment with both GPCR agonists and low doses of EGF. Furthermore, the Src tyrosine kinase inhibitor PP1 strongly interfered with LPA- and EGF-induced tyrosine phosphorylation and MAPK activation downstream of EGFR. Our results demonstrate an essential role for EGFR function in signaling through both G_q- and G_i-coupled receptors and provide novel insights into signal transmission downstream of EGFR for efficient activation of the Ras/MAPK pathway.

Keywords: EGF receptor/G protein-coupled receptors/MAP kinase/PI3-kinase/Src

Introduction

Definition of cellular responses such as proliferation or differentiation by a variety of external stimuli involves the regulation of transcriptional events in eukaryotic cells through intracellular signaling cascades, including signaling pathways that activate kinases of the mitogen-activated protein kinase (MAPK) family (Treisman, 1996). The extensively studied MAPKs of the ERK subfamily become activated in response to growth factors either through receptor tyrosine kinase (RTK)- or through G protein-coupled receptor (GPCR)-triggered signals (Pagès *et al.*, 1993; Faure *et al.*, 1994; Malarkey *et al.*, 1995; van Biesen *et al.*, 1996b). Transmission of these signals requires the formation of a complex between the Grb2 adaptor protein with the guanine nucleotide exchange factor Sos, which upon recruitment to the plasma membrane allows activation of the small G protein Ras, resulting in subsequent activation of the MAPK pathway (Egan *et al.*, 1993; van Biesen *et al.*, 1995; Dikic *et al.*, 1996). The critical function of Ras in MAPK signal transduction triggered by GPCRs which are coupled either to heterotrimeric G_i or G_q proteins (Crespo *et al.*, 1994) was shown to be sensitive to genistein, suggesting that a tyrosine kinase was involved in this process (van Corven *et al.*, 1993; Sadoshima and Izumo, 1996). Moreover, stimulation of various GPCRs, such as those for lysophosphatidic acid (LPA) (van Biesen *et al.*, 1995), thyrotropin-releasing hormone (Ohmichi *et al.*, 1994), endothelin-1 (ET-1) (Cazaubon *et al.*, 1994), bradykinin (Lev *et al.*, 1995) or thrombin (Chen *et al.*, 1996), rapidly induces tyrosine phosphorylation of the adaptor protein SHC and SHC–Grb2 complex formation, steps that couple both GPCRs and RTKs to Ras (Bonfini *et al.*, 1996; Chen *et al.*, 1996; van der Geer *et al.*, 1996). In addition, a recent report implicated an unidentified 100 kDa tyrosine-phosphorylated, Grb2-binding protein in LPA-induced MAPK activation (Kranenburg *et al.*, 1997).

Recently, we identified the epidermal growth factor receptor (EGFR) as an essential link in the GPCR-mediated MAPK activation pathway in Rat-1 fibroblasts treated with the GPCR agonists ET-1, LPA or thrombin (Daub *et al.*, 1996). Moreover, angiotensin II-induced platelet-derived growth factor receptor β (βPDGFR) and thrombin-stimulated insulin-like growth factor-1 receptor (IGF-1R) tyrosine phosphorylation were reported in primary rat smooth muscle cells (Linseman *et al.*, 1995; Rao *et al.*, 1995), suggesting that transactivation of distinct RTKs might contribute in a cell-type specific manner to GPCR-mediated mitogenic signaling. In addition to GPCR activation, a variety of stimuli including cellular stresses such as UV irradiation or calcium-dependent responses in PC12 cells result in ligand-independent RTK transactivation (Knebel *et al.*, 1996; Rosen and Greenberg, 1996; Weiss *et al.*, 1997). Interestingly, cytoplasmic kinases of the Src family were also implicated in signal generation by similar stimuli (Devary *et al.*, 1992; Rusanescu *et al.*, 1995). In particular, GPCR-mediated activation of the Ras/MAPK pathway was reported in some recent studies to involve Src function (Dikic *et al.*, 1996; Luttrell *et al.*, 1996; Sadoshima *et al.*, 1996; Schieffer *et al.*, 1996), which raised the possibility that concerted action of RTKs and Src family kinases might be required to initiate intracellular signaling cascades.

In the present study, we show that ligand-independent EGFR transactivation occurs in diverse cell types. Employing COS-7 cells, we demonstrate that G_q- and G_i-coupled receptors can mediate stimulation of EGFR

tyrosine phosphorylation and, moreover, that for both GPCR subfamilies this event is essential for the stimulation of SHC tyrosine phosphorylation and MAPK activation. In addition, we present evidence for phosphoinositide 3-kinase (PI3-K) function downstream of the EGFR and address the question of whether other tyrosine kinases might be involved in EGFR transactivation and signal transduction.

Results

EGFR transactivation in diverse cell types

We have shown previously that treatment of Rat-1 fibroblasts with the GPCR ligands ET-1, LPA and thrombin results in rapid induction of EGFR tyrosine phosphorylation. To substantiate these findings further, we investigated this mechanism in different cell lines. As shown in Figure 1A, stimulation of human HaCaT keratinocytes with thrombin or LPA resulted in enhanced tyrosine phosphorylation of endogenous EGFR. In addition, thrombin or extracellularly applied ATP triggered a comparable response in primary mouse astrocytes (Figure 1B). Although it is presently unclear whether ATP acts through GPCRs or ATP-gated ion channels (Barnard *et al.*, 1994; Salter and Hicks, 1995), EGFR transactivation might represent an important signaling element in ATP-evoked responses in astrocytes. Thrombin and LPA were also effective in COS-7 cells, where these GPCR ligands stimulated tyrosine phosphorylation of endogenous EGFR to a similar extent as 1–3 ng/ml EGF (Figure 1C). Thrombin receptor peptide (TRP) was able to mimic the thrombin response, confirming specific activation of the thrombin GPCR in COS-7 cells. The LPA vehicle bovine serum albumin (BSA), included as a negative control, showed no effect. For further characterization of the tyrosine-phosphorylated 170 kDa protein co-migrating with the EGFR, immunoprecipitations with different anti-EGFR antibodies were performed and the precipitates were treated with glycosidase. In all these control experiments, the 170 kDa band behaved exactly as the EGFR (data not shown). Moreover, time course experiments revealed that LPA rapidly induced EGFR tyrosine

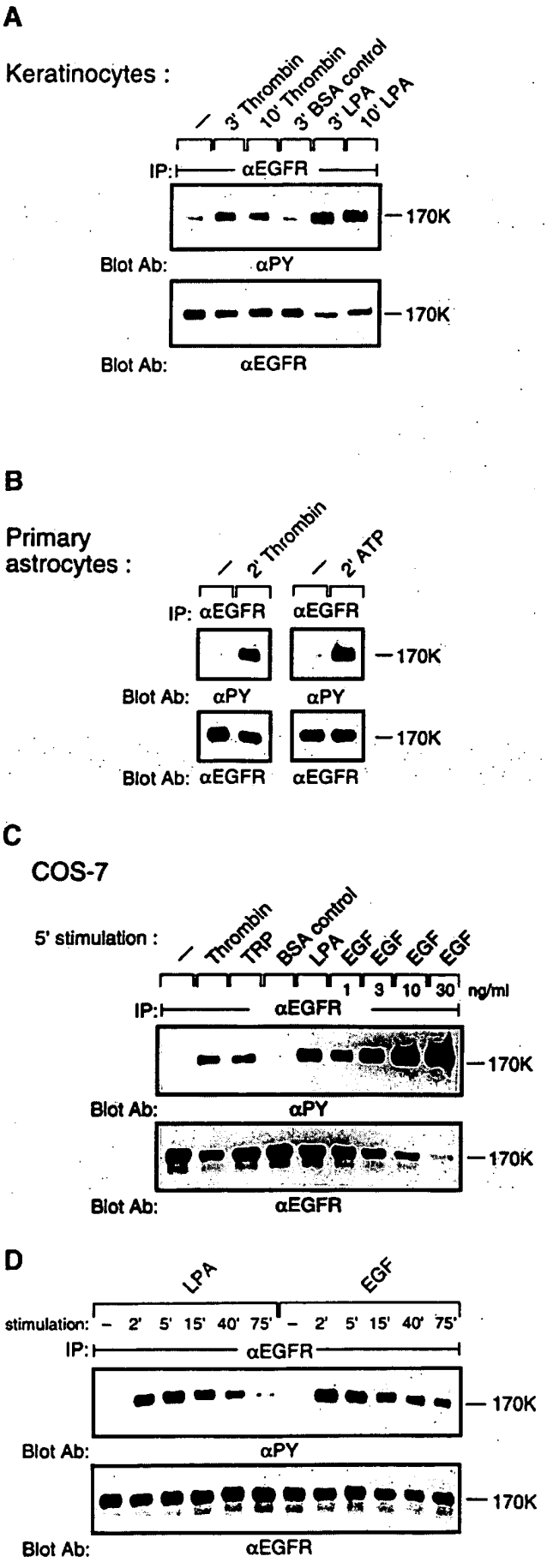

Fig. 1. EGFR transactivation in different cell lines. (**A**) Quiescent human HaCaT keratinocytes were treated for the indicated times with 2 U/ml thrombin, 10 μM LPA or LPA vehicle BSA. After lysis, EGFR was immunoprecipitated with anti-EGFR mAb 108.1. Following gel electrophoresis, tyrosine-phosphorylated EGFR was detected by immunoblotting with monoclonal anti-phosphotyrosine (αPY) antibody (upper panel). The amount of EGFR in immunoprecipitates was analyzed further by reprobing of the same filter with anti-EGFR antibody (lower panel). (**B**) Serum-starved primary mouse astrocytes were incubated for 2 min with 2 U/ml thrombin or 100 μM ATP, lysed and EGFR was immunoprecipitated using polyclonal anti-EGFR antibody. Immunoblotting was done with αPY mAb (upper panel), followed by reprobing with anti-EGFR antibody (lower panel). (**C**) Quiescent COS-7 cells were stimulated with 2 U/ml thrombin, 100 μM thrombin receptor peptide (TRP, peptide sequence: SFLLRNPNDKYEPF; van Corven *et al.*, 1993), LPA vehicle BSA, 10 μM LPA or the indicated concentrations of EGF for 5 min and lysed. (**D**) Quiescent COS-7 cells were treated for the indicated times with 10 μM LPA or 3 ng/ml EGF prior to lysis. The immunoprecipitations in (C) and (D) were performed with anti-EGFR mAb 108.1, followed by immunoblotting with monoclonal anti-phosphotyrosine antibody (upper panel) and subsequent reprobing with polyclonal anti-EGFR antibody (lower panel). Molecular size is indicated on the right.

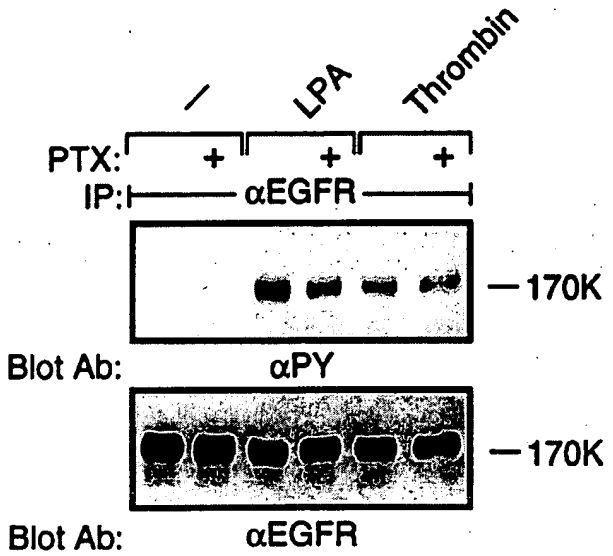

Fig. 2. Effect of PTX treatment on LPA- and thrombin-induced EGFR tyrosine phosphorylation in COS-7 cells. Serum-starved COS-7 cells were stimulated with 2 U/ml thrombin or 10 μM LPA for 5 min and lysed. Tyrosine phosphorylation of EGFR was assayed by immunoprecipitation with mAb 108.1 and immunoblotting with anti-phosphotyrosine antibody (upper panel), followed by reprobing with anti-EGFR antibodies (lower panel). Where indicated, cells were pre-treated with 100 ng/ml PTX for 18 h. Molecular weight is indicated on the right.

phosphorylation, only slightly lagging behind that induced by 3 ng/ml EGF. The EGF-induced EGFR tyrosine phosphorylation was more prolonged than that induced by LPA, possibly due to accelerated receptor down-regulation mediated by LPA-specific cellular responses (Figure 1D). Taken together, these experiments demonstrate that GPCR-mediated EGFR transactivation is not restricted to Rat-1 fibroblasts but occurs in various cell types from different species.

Stimulation of EGFR tyrosine phosphorylation by G_q- and G_i-coupled receptors in COS-7 cells

To examine the elements involved in EGFR transactivation further, we selected COS-7 cells, since this cell line has been used extensively to study GPCR signaling and, moreover, serves as a model system to investigate GPCR-mediated activation of the MAPK pathway (Crespo *et al.*, 1994; Hawes *et al.*, 1995; van Biesen *et al.*, 1995). First, we analyzed the effect of pertussis toxin (PTX) on EGFR transactivation. PTX catalyzes ADP ribosylation of α subunits in the G_i and G_o subfamilies of heterotrimeric G proteins, a covalent modification which leads to inactivation. Treatment of cells with PTX partially attenuated LPA-induced EGFR tyrosine phosphorylation, while the thrombin response was not significantly affected (Figure 2). Notably, PTX reduces the LPA-stimulated EGFR transactivation to a level similar to that observed after thrombin treatment. Since G_o proteins are not expressed in COS-7 cells (van Biesen *et al.*, 1996a), this indicates that LPA signals through G_i and through PTX-insensitive G proteins, while thrombin only utilizes PTX-insensitive pathways. To assess whether PTX-insensitive G proteins of the G_q subclass are able to mediate EGFR transactivation in COS-7 cells, we transiently expressed GPCRs known to be coupled predominantly to G_q proteins (Crespo *et al.*, 1994; Offermanns *et al.*, 1994). As shown in Figure 3A, exposure of cells transfected with bombesin receptor (BombR) or M1 muscarinic acetylcholine receptor (M1R) to the respective GPCR ligands resulted in increased EGFR tyrosine phosphorylation, which was not observed upon stimulation of control-transfected cells. In cells transfected with the G_i-coupled M2 muscarinic acetylcholine receptor (M2R), GPCR agonist-enhanced EGFR tyrosine phosphorylation was detectable, although this effect was weaker than that obtained upon G_q-coupled receptor stimulation (Figure 3B). Moreover, PTX did not affect bombesin-induced EGFR transactivation, while the carbachol-induced response mediated by M2R was blocked upon PTX pre-incubation (Figure 3C). These experiments show that EGFR transactivation may occur through the engagement of both PTX-insensitive and -sensitive pathways. The above experiment, which showed that, in the absence of PTX, LPA induces stronger EGFR tyrosine phosphorylation than thrombin while their responses become similar upon PTX pre-treatment, suggests that G_i-mediated and PTX-insensitive pathways might exert additive effects on EGFR transactivation in COS-7 cells. To address this question, we co-transfected G_i-coupled M2R and G_q-coupled BombR and stimulated either each receptor alone or both simultaneously. Co-stimulation with carbachol and bombesin resulted in a more pronounced induction of EGFR tyrosine phosphorylation than observed with either ligand alone, providing evidence for the cooperativity of G_i- and G_q-mediated pathways. Moreover, the combined effect on EGFR transactivation was similar to the response observed upon LPA treatment (Figure 3D).

Identification of Gab1 as Grb2-interacting protein potentially involved in GPCR-mediated signaling

We previously reported that several tyrosine-phosphorylated proteins including the EGFR, SHC and an unidentified 110 kDa protein associate with glutathione *S*-transferase (GST)–Grb2 fusion protein upon ET-1, LPA and thrombin stimulation in Rat-1 fibroblasts (Daub *et al.*, 1996). Specific association of a similar set of tyrosine-phosphorylated proteins was also detected when we stimulated COS-7 cells with LPA or 3 ng/ml EGF, which induces EGFR tyrosine phosphorylation comparable with the LPA response, and subsequently incubated lysates with GST–Grb2 fusion protein (Figure 4A). Pre-incubation with the EGFR-specific inhibitor AG1478 prevented LPA-induced association of tyrosine-phosphorylated proteins (Levizki and Gazit, 1995), indicating that, in addition to SHC, the 110 kDa protein represents an additional substrate for transactivated EGFR in COS-7 cells. Moreover, a Grb2-associating protein of similar molecular weight recently was implicated in LPA-induced signaling to the Ras/MAPK pathway, but was not identified (Kranenburg *et al.*, 1997). Utilizing an immunodepletion strategy, we were able to identify the 110 kDa protein as Gab1 (Holgado-Madruga *et al.*, 1996), since the tyrosine-phosphorylated 110 kDa protein upon LPA treatment was specifically and quantitatively removed when lysates were pre-cleared with polyclonal anti-Gab1 antiserum prior to *in vitro* association with GST–Grb2 (Figure 4B). When we performed immunoprecipitations with anti-Gab1 antiserum, LPA-induced stimulation of Gab1 tyrosine phosphorylation and

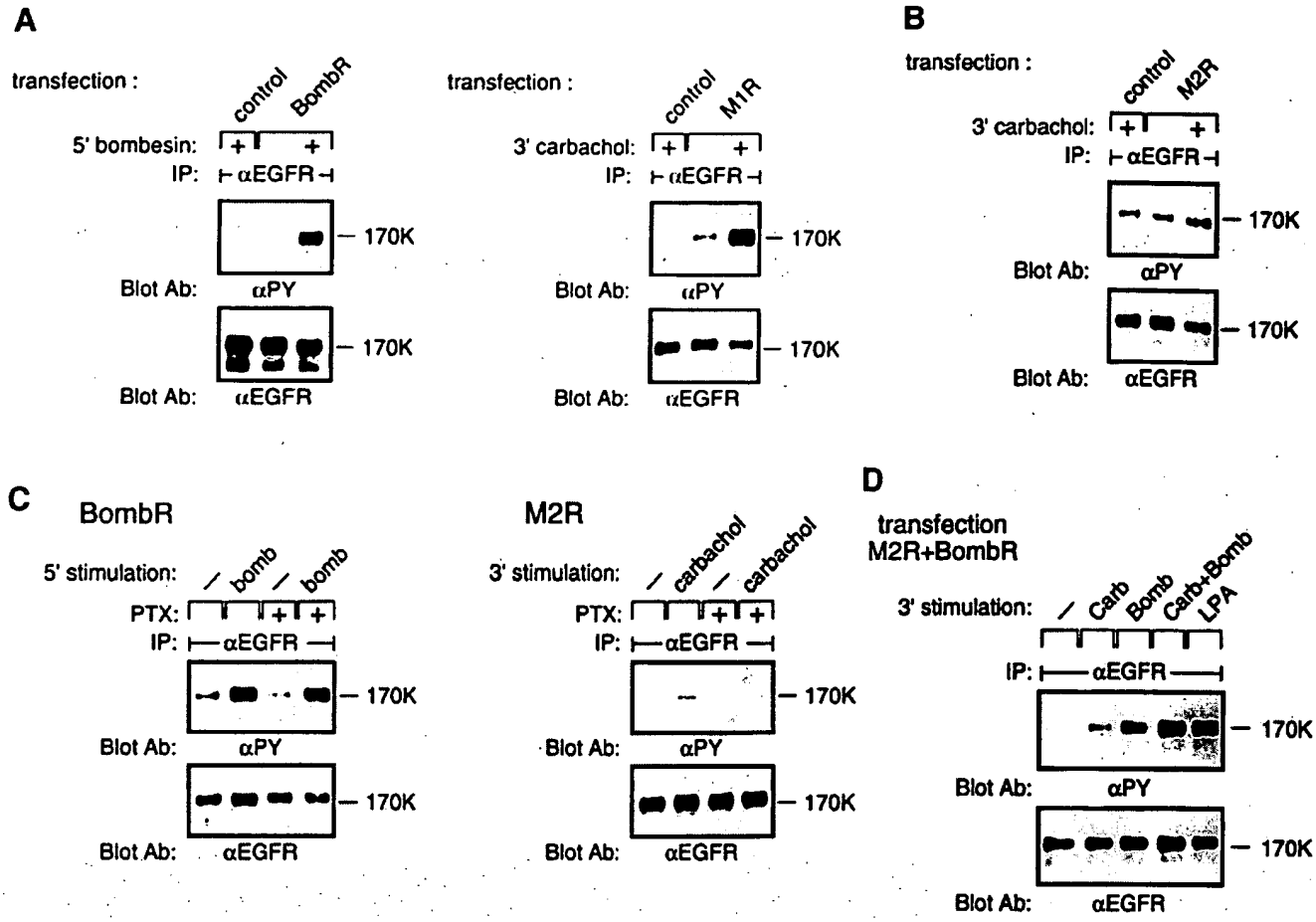

Fig. 3. Stimulation of endogenous EGFR tyrosine phosphorylation through transiently expressed G_q- and G_i-coupled receptors in COS-7 cells. COS-7 cells were transiently transfected in 6-well dishes with cDNA encoding BombR, M1R or M2R (0.5 μg each) or control-transfected as described in Materials and methods. Cells transfected with G_q-coupled receptors (**A**) were stimulated with 200 nM bombesin (BombR) or 1 mM carbachol (M1R) for the indicated times. Cell transiently expressing G_i-coupled M2 receptor (**B**) were treated with 1 mM carbachol as indicated. Control-transfected cells were subjected to the same agonist stimulation (A and B). BombR- or M2R-transfected cells were pre-treated for 18 h with 100 ng/ml PTX before agonist stimulation (**C**). Cells transiently co-expressing M2R and BombR were treated for 3 min with 1 mM carbachol and 200 nM bombesin, either alone or in combination, or 10 μM LPA for 3 min (**D**). After cell lysis, endogenous EGFR was immunoprecipitated with mAb 108.1 followed by immunoblotting with anti-phosphotyrosine antibody (upper panels). Filters were reprobed with anti-EGFR antibodies (lower panels). Molecular size is indicated on the right.

Gab1–Grb2 complex formation were clearly detectable in the absence but not in the presence of the GST–Gab1-N fusion protein used for antibody generation (Figure 4C). Moreover, both signaling events were abrogated when cells were pre-incubated with AG1478 in order to block EGFR function (Figure 4D), indicating that Gab1 functions downstream of EGFR in LPA signaling.

G_q- and G_i-coupled receptor-mediated SHC tyrosine phosphorylation requires functional EGFR

In order to establish that EGFR function represents a general prerequisite for GPCR-mediated tyrosine phosphorylation of proteins such as SHC, we transfected either the G_q-coupled BombR or the G_i-coupled M2R into COS-7 cells and determined SHC tyrosine phosphorylation and association of immunoprecipitated SHC with the adaptor protein Grb2 upon stimulation with the respective GPCR ligands. Bombesin, acting through its ectopically expressed receptor, stimulated SHC tyrosine phosphorylation as well as SHC–Grb2 complex formation. Both signaling events were blocked when the dominant-negative EGFR mutant HER-CD533 was co-transfected (Kashless *et al.*, 1991; Redemann *et al.*, 1992), while an analogous truncation mutant of the PDGFR (βPDGFR-CD504) had no inhibitory effect (Figure 5A), although both RTK mutants were expressed at comparable levels (data not shown). Furthermore, the EGFR-specific inhibitor AG1478 suppressed SHC tyrosine phosphorylation and complex formation with Grb2 upon stimulation of the G_i-coupled M2R (Figure 5B). Both approaches to inhibit EGFR function appeared to be specific, since SHC tyrosine phosphorylation and association with Grb2 induced by c-Src overexpression in COS-7 cells or upon nerve growth factor treatment of PC12 cells were unaffected (data not shown). Thus G_i- and G_q-mediated pathways depend on a functional EGFR to trigger SHC tyrosine phosphorylation, a signaling step considered to be critical for subsequent activation of Ras-dependent pathways.

EGFR inhibition interferes with MAPK activation by G_q- and G_i-coupled receptors

We previously demonstrated a functional role for EGFR in the GPCR-mediated activation of the MAPK pathway of Rat-1 cells upon stimulation with agonists such as

LPA. To establish the COS-7 cell system that allows the investigation of MAPK pathway control elements, we employed a transiently expressed hemagglutinin (HA) epitope-tagged form of the MAPK ERK2 (HA-ERK2) and measured phosphorylation of myelin basic protein (MBP). The system was calibrated with 2 ng/ml EGF, which induces EGFR tyrosine phosphorylation comparable with that obtained with LPA and resulted in MAPK activation which was, as expected, inhibited upon co-transfection of HER-CD533, while the dominant-negative βPDGFR-CD504 mutant had no effect (Figure 6A, left panel). Conversely, MAPK activation through βPDGFR was unaffected by HER-CD533 but abrogated by βPDGFR-CD504 co-expression (Figure 6A, middle panel). These controls confirmed the selective inhibition of EGFR and βPDGFR signaling by HER-CD533 and βPDGFR-CD504, respectively. Under these conditions, LPA-induced MAPK activation was reduced by nearly 80% upon HER-CD533 co-expression, while βPDGFR-CD504 showed no significant effect (Figure 6A, right panel). Co-transfection of either of the dominant-negatives RTK mutants, which were expressed at comparable levels as shown by [^{35}S]methionine labeling of cells transfected in parallel followed by nearly quantitative immunoprecipitation (Figure 6B), did not affect expression of HA-ERK2 (Figure 6A, lower panel). These data clearly confirm our previous Rat-1 cell experiments, which demonstrated that EGFR transactivation represents an essential step in the signaling cascade that mediates LPA-induced activation of the MAPK pathway. Using this tightly controlled transient transfection system, we investigated the role of EGFR in G_q- and G_i-mediated MAPK activation. As shown in Figure 6C, the dominant-negative EGFR mutant nearly abolished MAPK activity stimulated by the G_q-coupled BombR and inhibited MAPK activation through the G_i-coupled M2R by 50% (Figure 6C). Comparable results were obtained upon pre-treatment of cells with AG1478 to block specifically EGFR kinase function (Figure 6D), while pre-incubation with this tyrphostin did not significantly affect MAPK activation mediated either by co-transfected IGF-1R or induced by expression of v-Abl, an oncogenic variant of the tyrosine kinase c-Abl. The selectivity of AG1478 was demonstrated using EGFR$^{-/-}$ primary fibroblasts, in which even higher concentrations of the inhibitor did not affect GPCR-mediated MAPK activation (E.Zwick *et al.*, in preparation). Thus EGFR

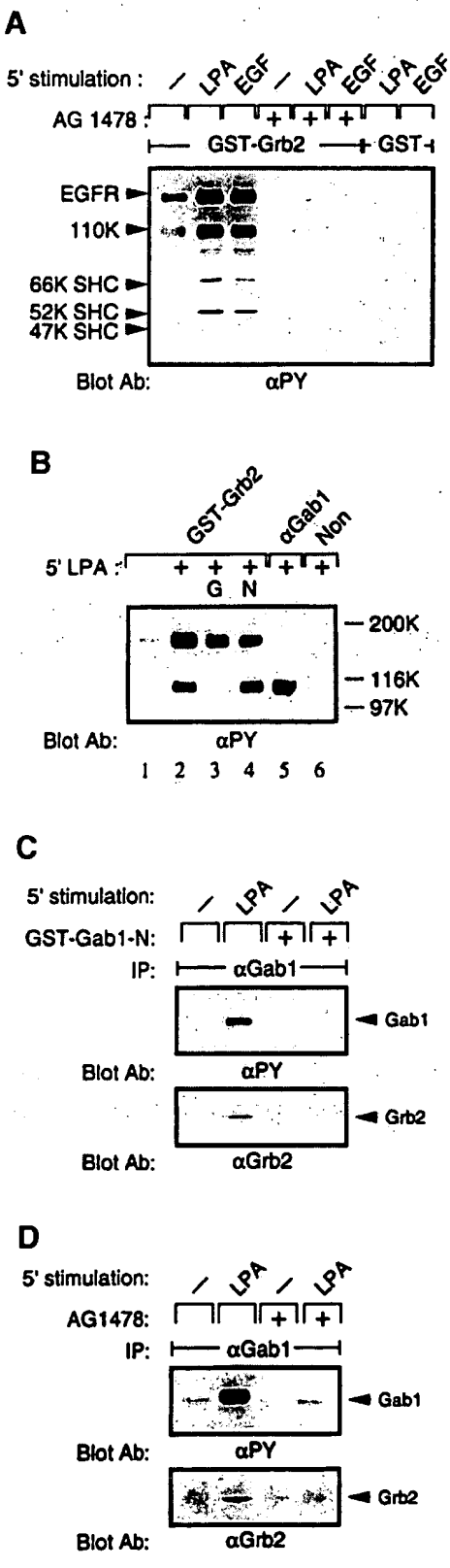

Fig. 4. Identification of Gab1 as Grb2-associated protein which becomes tyrosine phosphorylated upon LPA stimulation. (**A**) Following pre-incubation with or without 100 nM AG1478 for 10 min, quiescent COS-7 cells were stimulated for 5 min with 10 μM LPA or 3 ng/ml EGF. Lysates were subjected to *in vitro* association with GST–Grb2 fusion protein or GST alone, followed by immunoblotting with anti-phosphotyrosine antibody. The positions of tyrosine-phosphorylated EGFR, 110 kDa protein and SHC isoforms are indicated on the left. (**B**) Quiescent COS-7 cells were stimulated for 5 min with 10 μM LPA as indicated, and lysates were either control-incubated or immunoprecipitated with polyclonal anti-Gab1 antiserum (lane 5) or appropriate non-immune serum (lane 6) for 3 h at 4°C. Supernatants from these immunoprecipitations (G and N) and control-incubated lysates were then subjected to an *in vitro* association with GST–Grb2 fusion protein (lanes 1–4), followed by anti-phosphotyrosine immunoblotting. Molecular size is indicated on the right. (**C**) After stimulation with 10 μM LPA and lysis of COS-7 cells, anti-Gab1 immunoprecipitations were performed in the presence or absence of 10 μg of GST–Gab1-N fusion protein, followed by immunoblotting with anti-phosphotyrosine antibody (upper panel) or monoclonal anti-Grb2 antibody (lower panel). The positions of Gab1 and Grb2 are indicated on the right. (**D**) Following pre-incubation with or without 100 nM AG1478 for 10 min, quiescent COS-7 cells were stimulated for 5 min with 10 μM LPA. After lysis, Gab1 was immunoprecipitated using polyclonal anti-Gab1 antiserum and subsequently immunoblotted with anti-phosphotyrosine antibody (upper panel) or monoclonal anti-Grb2 antibody (lower panel). The positions of Gab1 and Grb2 are indicated on the right.

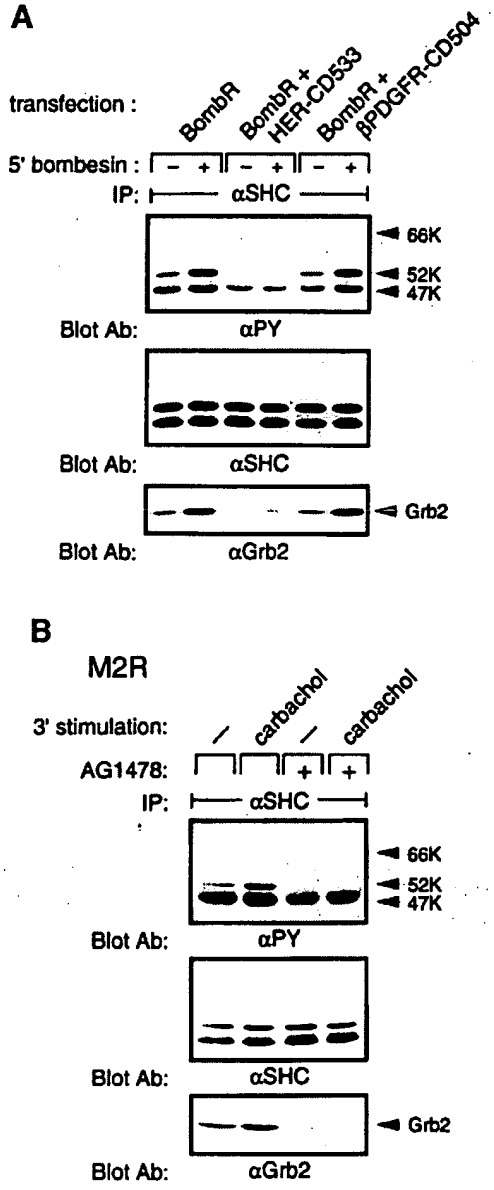

Fig. 5. Effect of EGFR inhibition on SHC tyrosine phosphorylation and SHC–Grb2 complex formation mediated through G_q- and G_i-coupled receptors. COS-7 cells were transiently transfected in 6-well dishes with cDNA encoding BombR plus either control vector or cDNA encoding HER-CD533 (0.3 μg/well) or βPDGFR-CD504 (0.5 μg/well) and stimulated with 200 nM bombesin for 5 min (A). Cells transfected with cDNA encoding M2R were pre-treated either with 100 nM AG1478 or an equal volume of DMSO for 10 min before stimulation with 1 mM carbachol (B). After lysis, SHC was immunoprecipitated using polyclonal anti-SHC antiserum and subsequently immunoblotted with anti-phosphotyrosine antibody (upper panels) or monoclonal anti-Grb2 antibody (lower panels). Filters were reprobed with polyclonal anti-SHC antibody (middle panels). The positions of SHC isoforms and Grb2 are indicated by arrowheads.

function is important for G_q- and G_i-mediated MAPK activation and, since in the case of the BombR (data not shown) and M2R (Crespo *et al.*, 1994) this event is suppressed by dominant-negative Ras, EGFR represents a pathway element upstream of Ras.

Interestingly, comparison of the time course of MAPK activation in COS-7 cells upon treatment of COS-7 cells with either LPA or 3 ng/ml EGF revealed that LPA induced MAPK activity more rapidly (Figure 6E). This suggests that during the initial phase of LPA-mediated MAPK activation, additional LPA-triggered signals synergize with EGFR-mediated signaling, leading to a more rapid MAPK activation than upon EGFR activation alone.

PI3-K is required for MAPK activation but not EGFR transactivation

To assess the role of PI3-K function in the GPCR-mediated transactivation signal leading to EGFR tyrosine phosphorylation, we pre-treated COS-7 cells with the PI3-K inhibitor wortmannin (100 nM) prior to LPA or EGF stimulation. As shown in Figure 7A, wortmannin did not affect EGFR tyrosine phosphorylation in response to either different LPA concentrations or 3 ng/ml EGF. Similar results were obtained for M2R- or BombR-mediated EGFR transactivation. and even up to 10 μM wortmannin had no effect on the LPA response (data not shown). Thus PI3-K is not involved in cross-talk between GPCRs and the EGFR in COS-7 cells. Next, we analyzed the effect of the PI3-K inhibitors wortmannin and LY294002 (Hawes *et al.*, 1996) on GPCR-mediated MAPK activation. Both inhibitors significantly reduced MAPK activity stimulated through M2R or in response to LPA, as reported previously (Hawes *et al.*, 1996; Lopez-Ilasaca *et al.*, 1997). Moreover, we found strong reduction of BombR-mediated MAPK stimulation. Surprisingly, PI3-K inactivation also markedly reduced MAPK activation induced by low doses of EGF (3 ng/ml), while the response to constitutively active Ras was not significantly affected (Figure 7B). Similar results were obtained when we examined tyrosine phosphorylation of endogenous ERK2 (data not shown). Our findings confirm that PI3-K function plays an essential role upstream of Ras in GPCR-mediated MAPK stimulation and, furthermore, indicate an important function downstream of the EGFR. In order to identify a potential site of PI3-K action downstream of EGFR, we tested whether PI3-K might interact with GST–Grb2 fusion protein. As shown in Figure 7C, the p85α subunit specifically interacted with GST–Grb2 in unstimulated cells, consistent with previous work (Wang *et al.*, 1995). Interestingly, however, stimulation with LPA or 3 ng/ml EGF enhanced this interaction. Moreover, this response was abrogated when cells were pre-treated with EGFR-specific inhibitor AG1478, although the basal level of Grb2-associated p85α was unaffected by EGFR inactivation. Furthermore, we detected an increase in PI3-K activity associating with GST–Grb2 upon LPA treatment, which was reversed upon AG1478 pre-treatment (Figure 7D). Control incubations indicated that most of the detected PI-K activity reflected PI3-K activity specifically associated with the GST–Grb2 fusion protein. Although we did not discriminate whether PI3-K interacts either directly with Grb2 or indirectly via a linker protein such as, for example, Gab1, EGFR-mediated recruitment of functionally active PI3-K into Grb2 complexes might represent the critical, PI3-K inhibitor-sensitive step necessary for subsequent activation of the MAPK cascade.

Effects of the Src tyrosine kinase inhibitor PP1

Since cytoplasmic tyrosine kinases of the Src family have been implicated recently in GPCR-mediated MAPK activation (Dikic *et al.*, 1996; Luttrell *et al.*, 1996;

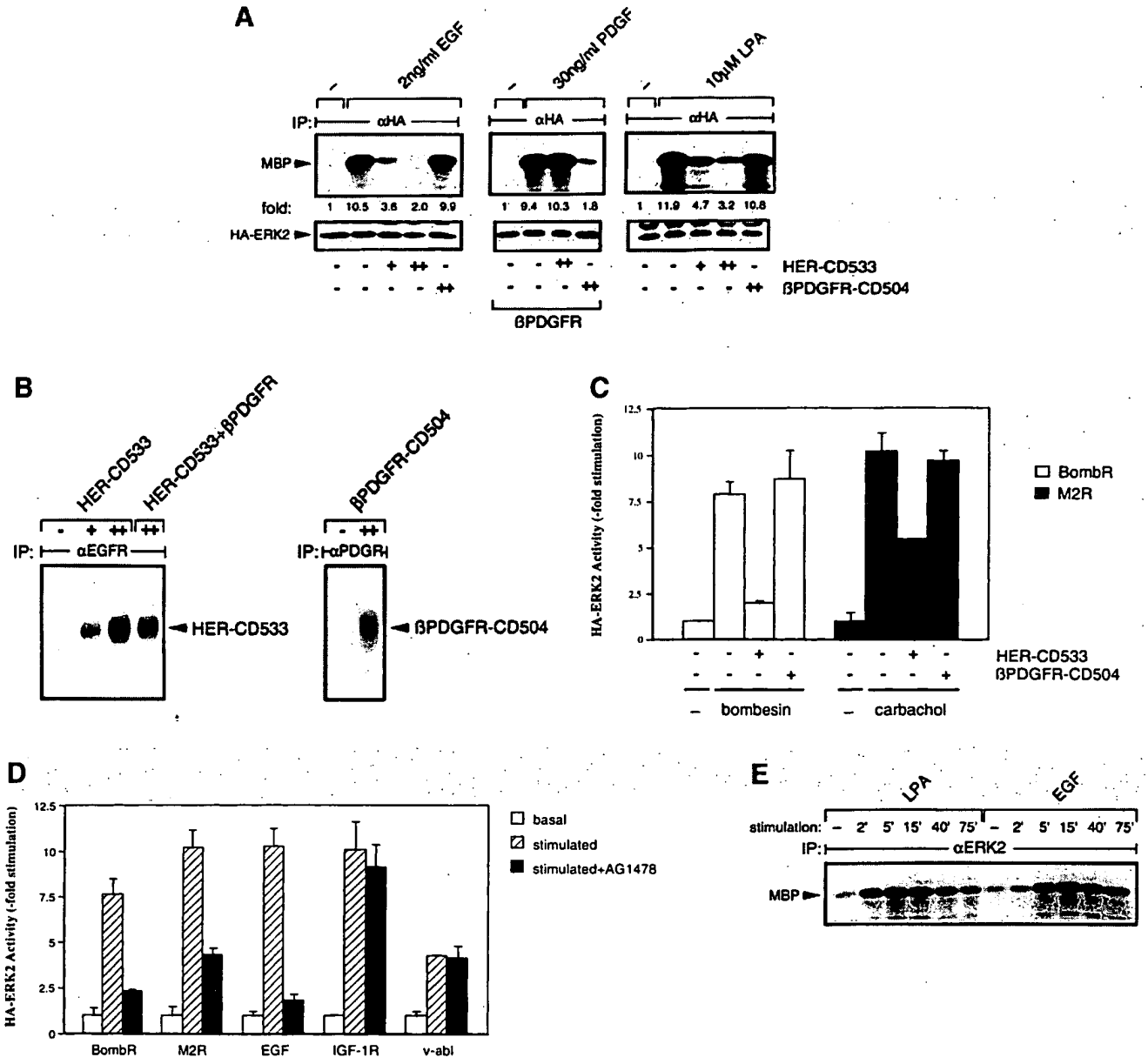

Fig. 6. Effect of EGFR inhibition on stimulation of MAPK activity. (A) COS-7 cells were transiently transfected with expression plasmid encoding HA-ERK2 (100 ng/well) plus either empty expression vector or plasmid encoding βPDGFR (25 ng/well). Where indicated, plasmids encoding HER-CD533 (+: 50 ng/well, ++: 150 ng/well) or βPDGFR-CD504 (++: 250 ng/well) were co-transfected. Following serum starvation for 24 h, cells were treated for 7 min with EGF (2 ng/ml), PDGF B/B (30 ng/ml) or LPA (10 μM), lysed and HA-ERK2 activity was determined using MBP as substrate as described in Materials and methods. Phosphorylated MBP was visualized by autoradiography after gel electrophoresis (upper panel) and HA-ERK2 was immunoblotted in parallel using polyclonal anti-ERK2 antibody (lower panel). For expression control, in parallel, transfected cells were labeled with [^{35}S]methionine and lysates were subjected to immunoprecipitation with monoclonal anti-EGFR antibody (B, left panel) or monoclonal anti-βPDGFR antibody (B, right panel). Mutant RTK expresion was visualized by autoradiography (18 h exposure). (C) COS-7 cells were transfected with expression plasmid encoding HA-ERK2 (100 ng/well) plus expression plasmids encoding either BombR or M2R (100 ng/well). Where indicated, plasmids encoding HER-CD533 (150 ng/well) or βPDGFR-CD504 (250 ng/well) were co-transfected. After 7 min stimulation with 200 nM bombesin or 1 mM carbachol, HA-ERK2 activity was determined. (D) COS-7 cells were transfected with expression plasmid encoding HA-ERK2 (100 ng/well) plus either empty expression vector or plasmids encoding BombR, M2R, IGF-1R (50 ng/well) or v-Abl (200 ng/well). Where indicated, cells were treated with 100 nM AG1478 10 min prior to stimulation with 200 nM bombesin, 1 mM carbachol, 3 ng/ml EGF or 10^{-7} M IGF-1 for 7 min and subsequent detemination of HA-ERK2 activity. (E) Serum-starved COS-7 cells were treated for the indicated times with 10 μM LPA or 3 ng/ml EGF prior to lysis. Immunoprecipitated endogenous ERK2 was subjected to an *in vitro* kinase assay, and phosphorylated MBP was visualized by autoradiography after gel electrophoresis. Data shown in (C) and (D) represent the mean ± SD for duplicate samples.

Sadoshima *et al.*, 1996; Schieffer *et al.*, 1996), we investigated a possible connection between Src and the EGFR. For this purpose, we utilized the tyrosine kinase inhibitor PP1, which was reported to be specific for Src-like kinases (Hanke *et al.*, 1996). Pre-treatment of cells with 10 μM PP1 attenuated tyrosine phosphorylation of endogenous Src. The residual Src tyrosine phosphorylation is most likely due to CSK-mediated phosphorylation at Tyr527, a non-autophosphorylation site with inhibitory functions (Luttrell *et al.*, 1997). Expression of a constitutively active Src mutant lacking this tyrosine resulted in increased Src tyrosine phosphorylation which was strongly inhibited

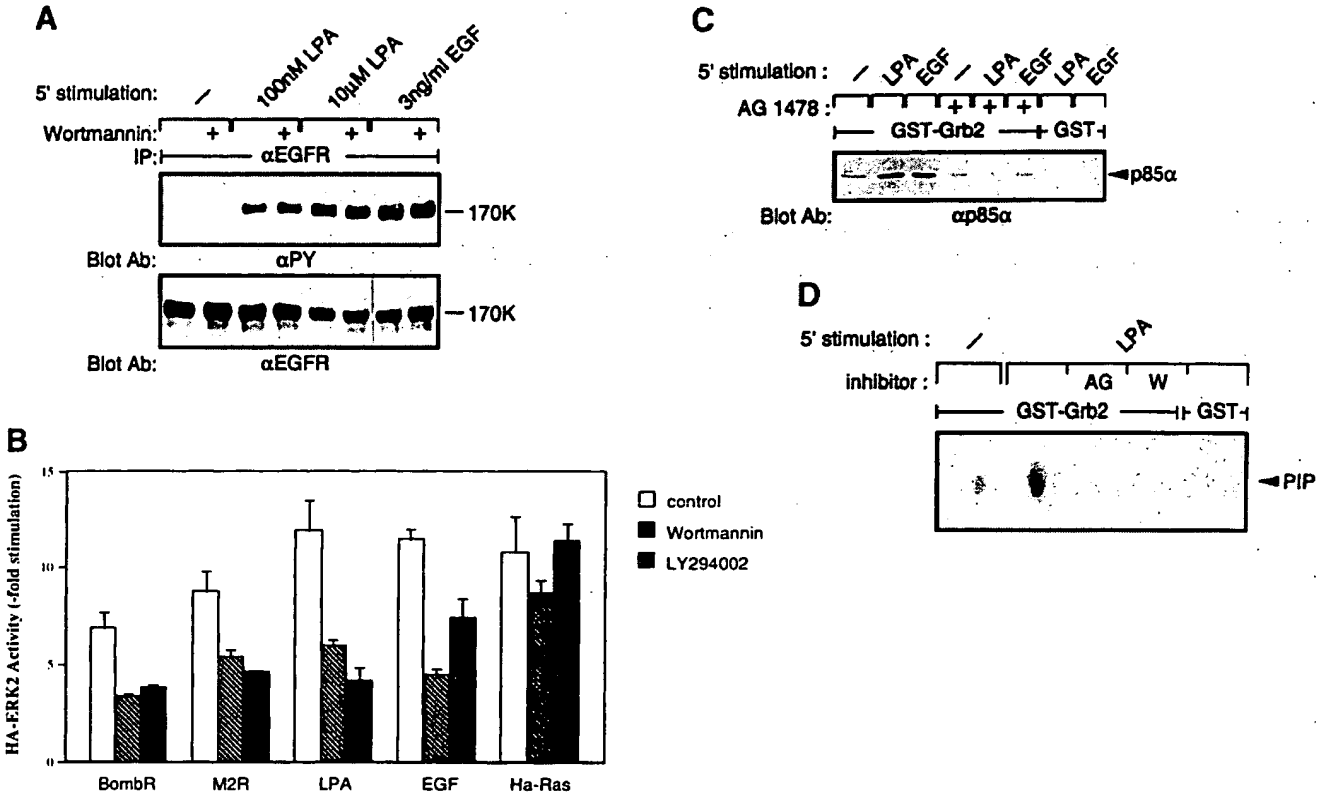

Fig. 7. Analysis of PI3-K function upon EGF or GPCR ligand stimulation in COS-7 cells. (A) Quiescent COS-7 cells were pre-treated either with vehicle or with 100 nM wortmannin for 10 min prior to stimulation with the indicated concentrations of LPA or EGF for 5 min. After cell lysis, endogenous EGFR was immunoprecipitated with mAb 108.1 followed by immunoblotting with anti-phosphotyrosine antibody (upper panel). Filters were reprobed with anti-EGFR antibodies (lower panel). Molecular size is indicated on the right. (B) COS-7 cells were transfected with expression plasmid encoding HA-ERK2 (100 ng/well) plus either empty expression vector or plasmids encoding BombR, M2R or Ha-Ras (200 ng/well). Cells were treated with vehicle, wortmannin (100 nM) or LY 294002 (25 μM) 10 min prior to stimulation with 200 nM bombesin, 1 mM carbachol, 10 μM LPA or 3 ng/ml EGF for 7 min and subsequent detemination of HA-ERK2 activity. Data shown represent the mean ± SD for duplicate samples. (C) Following pre-incubation with or without 100 nM AG1478 for 10 min, quiescent COS-7 cells were stimulated for 5 min with 10 μM LPA or 3 ng/ml EGF. Lysates were subjected to *in vitro* association with GST–Grb2 fusion protein or GST alone, followed by immunoblotting with anti-p85α antibody. The position of p85α is indicated on the right. (D) Similarly processed lysates from untreated or LPA-stimulated COS-7 cells were used for a PI3-K assay as described in Materials and methods. Where indicated, cells were pre-treated with 100 nM AG1478 (AG) or 100 nM wortmannin was included in immunoprecipitations (W). Phosphoinositide phosphate (PIP) was resolved by TLC and plates were then exposed to autoradiography.

upon PP1 pre-incubation. Furthermore, PP1 suppressed tyrosine phosphorylation of various Src substrates in COS-7 cells (Figure 8A) and led to moderately increased EGF-induced EGFR tyrosine phosphorylation, possibly due to an effect on EGFR down-regulation, while LPA-induced transactivation was somewhat inhibited (Figure 8B). This indicated that PP1 does not directly inhibit EGFR kinase and further suggests that Src-like kinases or another PP1-sensitive kinase partially contribute to EGFR transactivation upon LPA stimulation of COS-7 cells. Surprisingly, however, PP1 treatment strongly interfered with LPA- and EGF-stimulated SHC and Gab1 tyrosine phosphorylation, Gab1–Grb2 complex formation and MAPK activation (Figure 8C–E). Since PP1 did not affect MAPK activation in response to constitutively active Ras, we conclude that PP1 targets essential signaling elements upstream of Ras and downstream of the EGFR. Moreover, quantification of this data revealed that PP1-induced inhibition of Gab1 tyrosine phosphorylation was most similar to the effects observed at the level of MAPK, suggesting that this multisite docking protein represents the critical link to EGFR-dependent activation of the Ras/MAPK pathway in COS-7 cells. In general, our results establish PP1 as an excellent pharmacological reagent capable of dissociating EGFR tyrosine phosphorylation from immediate receptor-proximal signaling steps such as SHC and Gab1 tyrosine phosphorylation.

Discussion

We have demonstrated here that ectopic expression of G_q- and G_i-coupled receptors reconstitutes GPCR agonist-induced stimulation of EGFR tyrosine phosphorylation in COS-7 cells. LPA, acting through its endogenous receptor, utilizes both PTX-insensitive and -sensitive pathways leading to EGFR transactivation. While, as mentioned above, it is very likely that heterotrimeric G_i proteins account for the PTX-sensitive contribution to the LPA response (van Biesen *et al.*, 1996b), it remains to be established whether G_q signaling, although sufficient, indeed mediates the PTX-insensitive effects on EGFR tyrosine phosphorylation or, alternatively, whether other PTX-insensitive heterotrimeric G proteins may be involved in LPA signaling. Importantly, LPA treatment or stimulation with low doses of EGF, which activated EGFR to an extent similar to LPA, resulted in comparable tyrosine

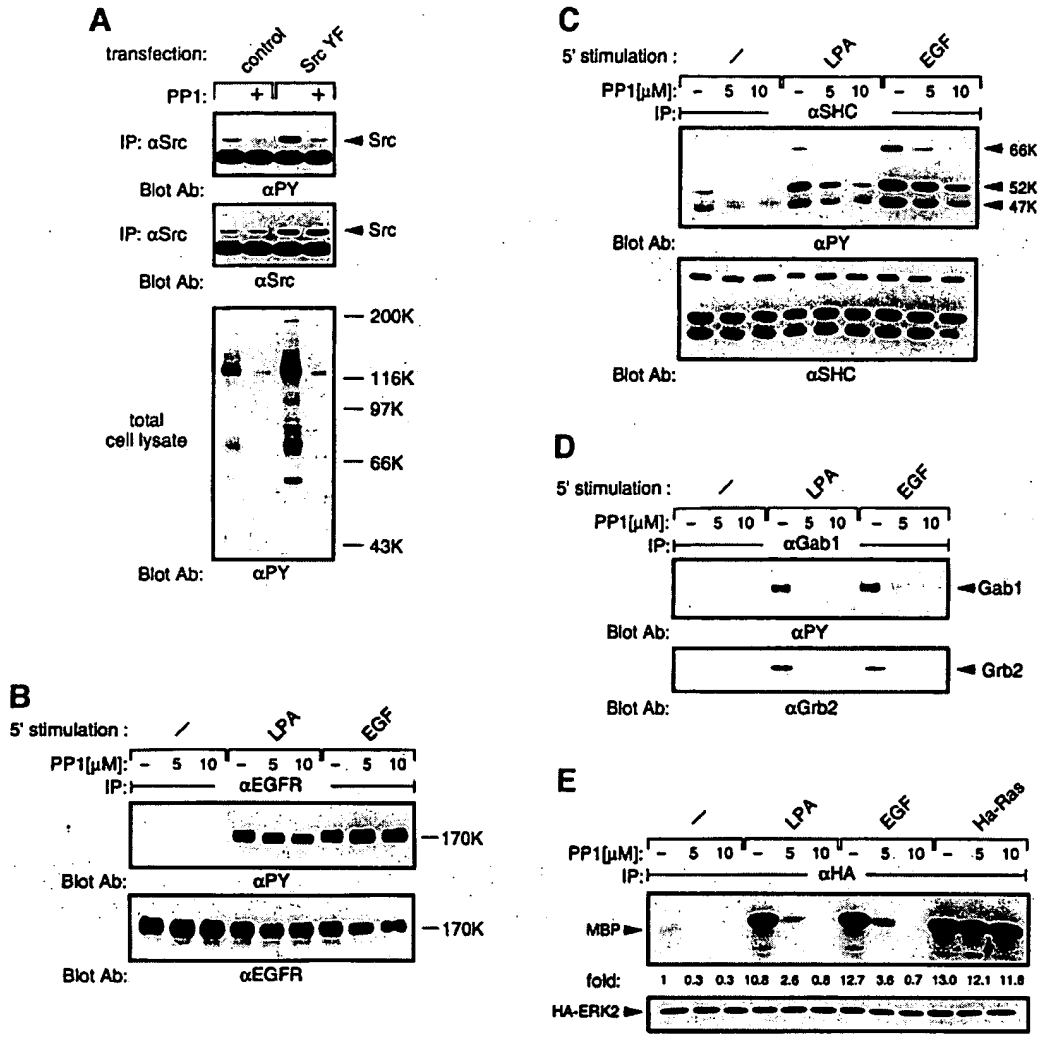

Fig. 8. Effects of PP1 on Src, LPA- and EGF-induced tyrosine phosphorylation of EGFR, SHC, Gab1 and activation of MAPK. (**A**) COS-7 cells were either control-transfected or transfected with plasmid DNA encoding Src Y527F, serum-starved and treated for 15 min with 10 μM PP1 where indicated. After lysis, Src was immunoprecipitated with monoclonal anti-Src antibody followed by immunoblotting with anti-phosphotyrosine antibody (upper panel) and reprobing with monoclonal anti-Src antibody (middle panel). Total cell lysates were immunoblotted with anti-phosphotyrosine antibody (lower panel). (B–D) Quiescent COS-7 cells were pre-treated either with vehicle or with the indicated concentrations of PP1 10 min prior to stimulation with 10 μM LPA or 3 ng/ml EGF for 5 min. Lysates were subjected to immunoprecipitation either with monoclonal anti-EGFR antibody (**B**), polyclonal anti-SHC antibody (**C**) or polyclonal anti-Gab1 antibody (**D**), followed by immunoblotting with anti-phosphotyrosine antibody (B–D, upper panel). Filters were reprobed with the respective antibodies (B and C, lower panel) or anti-Grb2 antibody (D, lower panel). Molecular weight or positions of SHC isoforms are indicated on the right. (**E**) COS-7 cells were transfected with expression plasmid encoding HA-ERK2 (100 ng/well) plus either empty expression vector or plasmid Ha-Ras (200 ng/well). Cells were treated with vehicle or the indicated concentrations of PP1 10 min prior to stimulation with 10 μM LPA or 3 ng/ml EGF for 7 min, lysed and HA-ERK2 activity was determined using MBP as substrate as described. Phosphorylated MBP was visualized by autoradiography after gel electrophoresis (upper panel) and HA-ERK2 was immunoblotted in parallel using polyclonal anti-ERK2 antidody (lower panel).

phosphorylation of Grb2-interacting proteins such as SHC, indicating a similar signaling capacity of either transactivated or EGF-activated EGFR in intact cells. Furthermore, LPA induced tyrosine phosphorylation of the docking protein Gab1, which quantitatively accounted for the tyrosine-phosphorylated 110 kDa protein previously described as associating with Grb2 (Holgado-Madruga *et al.*, 1996). Conversely, this result demonstrates that tyrosine-phosphorylated proteins of similar molecular weight, such as, for example, focal adhesion kinase or c-Cbl, are not present at detectable levels, although these tyrosine kinases can bind to Grb2 (Meisner *et al.*, 1995; Schlaepfer *et al.*, 1997). Moreover, since the docking protein Gab1 plays an important role in RTK-mediated definition of biological responses (Holgado-Madruga *et al.*, 1996; Weidner *et al.*, 1996), our identification of Gab1 as a substrate molecule for LPA-induced tyrosine phosphorylation suggests that this signaling molecule might also be critical for GPCR-initiated signal transmission.

Focusing on the tyrosine kinase substrate SHC for further analysis, we found induction of tyrosine phosphorylation mediated either through G_q-coupled BombR or through G_i-coupled M2R. These findings extend previous results from Lefkowitz and colleagues who attributed GPCR-mediated SHC tyrosine phoshorylation solely to G_i signaling in COS-7 cells (van Biesen *et al.*, 1995; Luttrell *et al.*, 1996). In fact, our experiments show that transiently transfected COS-7 cells are a useful model system to study SHC tyrosine phosphorylation, and our results are consistent with previous data that implicated

G_q-mediated pathways triggered by angiotensin II, bradykinin or thrombin (Cazaubon *et al.*, 1994; Ohmichi *et al.*, 1994; Lev *et al.*, 1995; Chen *et al.*, 1996; Sadoshima and Izumo, 1996) as well as activation of the G_i-coupled *N*-formyl chemoattractant receptor (Ptasznik *et al.*, 1995) in SHC tyrosine phosphorylation and SHC–Grb2 complex formation. Importantly, we found that both signaling events were completely abrogated upon BombR or M2R stimulation when EGFR function was blocked specifically. Thus, EGFR links signals emanating from G_q- and G_i-coupled receptors to the adaptor protein SHC. Although there are conflicting reports on the involvement of SHC in GPCR-mediated activation of the Ras/MAPK pathway (Chen *et al.*, 1996; Kranenburg *et al.*, 1997; Lopez-Ilasaca *et al.*, 1997), this adaptor and, perhaps even more importantly, Gab1 appear to play a significant role in the signal transmission pathway via Grb2 and Sos, resulting in activation of the Ras/MAPK signal (van Biesen *et al.*, 1995; Dikic *et al.*, 1996). Consistent with this role for the EGFR, we observed that BombR-mediated MAPK activation was nearly abolished and the M2R-mediated response was significantly reduced when we specifically inactivated endogenous EGFR either by expression of the dominant-negative EGFR truncation mutant HER-CD533 or by treatment of cells with nanomolar concentrations of the selective EGFR inhibitor AG1478. While there is a consensus that Ras is required for G_i-mediated MAPK activation, one must point out that previous studies have produced contradictory results, reporting either Ras-dependent or Ras-independent MAPK activation through G_q-coupled receptors in COS-7 cells (Crespo *et al.*, 1994; Hawes *et al.*, 1995; Pace *et al.*, 1995). In the case of BombR, expression of a dominant-negative Ras allele interferes with MAPK activation to a similar extent as EGFR inhibition, consistent with the notion that EGFR is positioned upstream of Ras. Moreover, G_q signaling is sufficient to activate Ras (Sadoshima and Izumo, 1996), and further evidence exists that signaling factors such as SHC, Grb2 and Sos, which act upstream of Ras, play essential roles in G_q-mediated MAPK activation (Chen *et al.*, 1996; Dikic *et al.*, 1996). With respect to the contradictory results about G_q signaling in COS-7 cells, one possible explanation could be that up to a certain receptor expression level Ras is required and, when expression exceeds this threshold, additional pathways are activated which allow MAPK activation via Ras-independent routes.

In experiments where we pre-treated cells with the PI3-K inhibitor wortmannin, no differences in GPCR-induced EGFR tyrosine phosphorylation were detected, thus PI3-K activation does not account for an intermediate step in this pathway. Interestingly, PI3-K inhibitors not only attenuated MAPK activation in response to GPCR stimulation, but also in response to low doses of EGF, that mimicked, for example, the LPA effect on EGFR tyrosine phosphorylation. Thus, under these conditions, PI3-K might be required downstream of the EGFR. This assumption is supported further by our finding that recruitment of endogenous, catalytically active p85α/p110 PI3-K into Grb2-containing complexes occurs downstream of the EGFR. In addition, the PI3-Kγ isoform, which is activated by βγ-subunits of heterotrimeric G proteins, was implicated recently in G_i-mediated MAPK activation in COS-7 cells (Lopez-Ilasaca *et al.*, 1997). However, the involvement of this enzyme in BombR-mediated or EGF-stimulated MAPK activation is unlikely since it occurs in a βγ-independent manner (Faure *et al.*, 1994). Although it is presently unclear how PI3-K activity might contribute to activation of the MAPK pathway, one potentially interesting clue comes from observations that the PI3-K product phosphatidylinositol-3,4,5-trisphosphate (PIP_3) can interact directly with SH2 domains and might thereby contribute to the recruitment of SH2 domain-containing proteins such as p85, Grb2 or SHC to the plasma membrane (Rameh *et al.*, 1995). Consistent with this hypothesis, partial reduction of SHC tyrosine phosphorylation following GPCR stimulation was detected upon wortmannin treatment (Touhara *et al.*, 1995; Lopez-Ilasaca *et al.*, 1997). In addition, physical interaction of p85α/p110 PI3-K with multiprotein complexes containing Grb2, SHC and Gab1 could lead to locally increased PIP_3 levels which stabilize membrane association and thereby support further signal transmission. Moreover, the PI3-K product phosphatidylinositol-3,4-bisphosphate (PIP_2) binds to the pleckstrin homology (PH) domain of the serine/threonine kinase Akt (Franke *et al.*, 1997). While it is presently unclear whether this finding can be extended to other PH domain-containing proteins such as Sos or Gab1, it is noteworthy that, in addition to the C-terminal proline-rich part of Sos which interacts with Grb2, the N-terminal region comprising the PH domain is essential for Sos function (McCollam *et al.*, 1995; Byrne *et al.*, 1996). Further, homing of Sos to the plasma membrane might also be supported by βγ-subunits of heterotrimeric G proteins, which can interact directly with PH domain-containing proteins such as β-adrenergic receptor kinase (Shaw, 1996).

Finally, employing the tyrosine kinase inhibitor PP1, which slightly increased EGF-induced and only moderately inhibited LPA-induced EGFR tyrosine phosphorylation, we provide evidence that additional signaling factors, most probably tyrosine kinases, act downstream of the EGFR and significantly contribute to activation of the Ras/MAPK pathway. Although PP1 has been reported to be selective for Src-like kinases, our data must be interpreted carefully since inhibitory effects on other tyrosine kinases such as PYK2 may be possible, which could account for the effects observed. Moreover, there are some discrepancies concerning the role of Src in GPCR-mediated activation of the Ras/MAPK pathway. This is especially true in view of rather diverging reports regarding the participation of Src in GPCR-mediated activation of the Ras/MAPK pathway (Dikic *et al.*, 1996; Luttrell *et al.*, 1996; Sadoshima *et al.*, 1996; Schieffer *et al.*, 1996; Kranenburg *et al.*, 1997). It can be anticipated, however, that the identification of PP1 target molecules will provide important insights into the Ras/MAPK activation mechanism not only in response to GPCR stimulation, but also upon direct RTK ligand treatment. It is tempting to speculate that an autophosphorylated EGFR recruits substrates such as SHC which are thereby brought into proximity with and phosphorylated by an additional, PP1-sensitive tyrosine kinase such as Src. Recently, Luttrell *et al.* (1977) reported that Src family kinases mediate PTX-sensitive or βγ-induced EGFR tyrosine phosphorylation in COS-7 cells, and suggested that this

response does not involve activation of intrinsic EGFR kinase activity because of differential use of receptor phosphorylation sites. In our study, however, both the EGFR inhibitor AG1478, which targets the EGFR kinase domain, and the EGFR truncation mutant HER-CD533, which selectively blocks endogenous EGFR through formation of inactive heterodimers, fully abrogate EGFR tyrosine phosphorylation without affecting Src-induced tyrosine phosphorylation (Daub *et al.*, 1996; and data not shown). Moreover, our findings support the conclusion that the signal generation by either transactivation of the EGFR or direct EGF binding are indistinguishable.

While the mechanistic details of GPCR-mediated EGFR transactivation remain elusive, data obtained in other ligand-independent RTK activation scenarios such as UV irradiation or oxidant-induced EGFR tyrosine phosphorylation (Knebel *et al.*, 1996) strongly support the involvement of EGFR-antagonizing phosphatases whose inhibition could account for the GPCR-mediated responses observed. Alternatively, interaction with and perhaps even covalent modification by intermediate signaling factors might lead to GPCR-induced EGFR transactivation. Although the signaling events that immediately precede EGFR transactivation await further investigation, the data presented here not only establish the general significance of EGFR function in signals of diverse GPCR subclasses in diverse cell types, but further identify additional elements of GPCR and RTK signals, thereby providing important and novel insights into the signaling network involving two major classes of cell surface receptors.

Materials and methods

Reagents, antibodies and plasmids

COS-7 cells were from Genentech Inc. Human HaCaT keratinocytes were a gift from N.E.Fusenig (Boukamp *et al.*, 1988). Primary mouse astrocytes were prepared essentially as described (Jehan *et al.*, 1995). Culture media and Lipofectamine were purchased from Gibco-BRL. Protein A–Sepharose was from Pharmacia Biotech Inc. PP1 and LY294002 were obtained from Calbiochem. PDGF B/B was from Boehringer Mannheim, and AG1478 (Levitzki and Gazit, 1995) was kindly provided by P.Hirth. All other reagents were obtained from Sigma.

Antibodies purchased were monoclonal anti-HA antibody (Boehringer Mannheim), rabbit polyclonal anti-EGFR antibody (Santa Cruz), sheep polyclonal anti-EGFR antibody (UBI), mouse monoclonal anti-Grb2 antibody (UBI), mouse monoclonal anti-PI3-K antibody (UBI), rabbit polyclonal anti-ERK2 antibody (Santa Cruz) and mouse monoclonal anti-Src antibody (Calbiochem). Endogenous EGFR from COS-7 cells was precipitated with mouse monoclonal antibody 108.1 (Seedorf *et al.*, 1994); mouse monoclonal anti-PDGFRβ antibody 128D4C10 was a gift from H.J.Bühring. Rabbit polyclonal anti-SHC antibody has been described (Seedorf *et al.*, 1994). For Gab1 antibody generation, Gab1 cDNA was cloned from a human placenta cDNA library, the amino acids 23–189 were expressed as pGEX fusion protein in *Escherichia coli* and, after purification, used as antigen in rabbits. Identity with the published sequence (Holgado-Madruga *et al.*, 1996) was verified by DNA sequencing. Respective secondary antibodies were obtained from Bio-Rad and Dianova. For immunoblot detection, the ECL system from Amersham was used. Stripping and reprobing of blots were performed according to the manufacturers' recommendations.

All cDNAs used except SrcY527F (Luttrell *et al.*, 1997), which was in a retroviral expression vector (Daub *et al.*, 1996), were in cytomegalovirus-based expression plasmids containing HER-CD533 (Redemann *et al.*, 1992), βPDGFR (Vogel *et al.*, 1993), βPDGFR-CD504 (Strawn *et al.*, 1994), IGF1-R (Schuhmacher *et al.*, 1993), Ha-Ras (Lengyel *et al.*, 1995), v-Abl (Gishinzky *et al.*, 1995), BombR (Lustig *et al.*, 1993), M1R (Crespo *et al.*, 1994) and M2R (Faure *et al.*, 1994). Mouse ERK2 (Her *et al.*, 1991) was fused to an N-terminal HA epitope as described (Meloche *et al.*, 1992).

Cell culture and transfections

HaCaT keratinocytes and COS-7 cells were cultured in Dulbecco's modified Eagle's medium (DMEM) supplemented with 10% fetal bovine serum. Primary astrocytes were maintained in DMEM F-12 containing 10% fetal bovine serum. COS-7 cells were transiently transfected using Lipofectamine essentially as described (Hawes *et al.*, 1995). For transfection in 12-well dishes, cells were incubated for 4 h in 0.4 ml of serum-free medium containing 4 μl of Lipofectamine and 0.8 μg of total plasmid DNA per well. For transfections in 6-well dishes, 1.0 ml of serum-free medium containing 10 μl of Lipofectamine and 2.0 μg of total plasmid DNA per well were used. The transfection mixture was then supplemented with an equal volume of medium containing 20% fetal bovine serum and, 20 h later, cells were washed and cultured for a further 24 h in serum-free medium until lysis. For [^{35}S]methionine labeling, cells were incubated in methionine-free DMEM during starvation, and 50 μCi/ml [^{35}S]methionine were added 16 h prior to lysis.

Cell lysis, immunoprecipitation, association with fusion proteins and immunoblotting

Prior to lysis, cells grown to 80–90% confluency were treated with inhibitors and agonists as indicated, washed once with phosphate-buffered saline and then lysed for 10 min on ice in buffer containing 50 mM HEPES pH 7.5, 150 mM NaCl, 1% Triton X-100, 1 mM EDTA, 10% glycerol, 10 mM sodium pyrophosphate, 2 mM sodium orthovanadate, 10 mM sodium fluoride, 1 mM phenylmethylsulfonyl fluoride and 10 μg/ml aprotinin. Lysates were pre-cleared by centrifugation at 13 000 r.p.m. for 10 min at 4°C. Supernatants were diluted with an equal volume of HNTG buffer (Seedorf *et al.*, 1994) and subsequently immunoprecipitated using the respective antibodies and 30 μl of protein A–Sepharose for 4 h at 4°C. Alternatively, lysates were subjected to *in vitro* associations with either 3 μg of GST–Grb2 or 2 μg of GST as control pre-bound to 30 μl of gluthathione–agarose beads. Precipitates were washed three times with 0.5 ml of HNTG buffer, suspended in SDS sample buffer, boiled for 3 min and subjected to gel electrophoresis on 7.5% gels or 6–12.5% gradient gels. Following SDS–PAGE, proteins were transferred to a nitrocellulose membrane and immunoblotted.

MAPK assay

Epitope-tagged HA-ERK2 was immunoprecipitated from lysates obtained from 12-well dishes using 2.5 μg of 12CA5 antibody; endogenous ERK2 was immunoprecipitated using 0.5 μg of polyclonal anti-ERK2 antibody. Immunoprecipitates were washed three times with 0.25 ml of HNTG buffer and once with 0.4 ml of kinase buffer (20 mM HEPES pH 7.5, 10 mM $MgCl_2$, 1 mM dithiothreitol, 200 μM sodium orthovanadate). Subsequently, kinase reactions were performed in 30 μl of kinase buffer supplemented with 0.5 mg/ml MBP, 50 μM ATP and 1 μCi of [γ-^{32}P]ATP for 10 min at room temperature. Reactions were stopped by addition of 30 μl of 2× SDS sample buffer and subjected to gel electrophoresis on 15% gels. The upper parts of the gels were transferred to nitrocellulose membrane and immunoblotted with anti-ERK2 antibody; labeled MBP on the lower part was quantified using a PhosphorImager (Fuji).

Phosphatidylinositol 3-kinase assay

PI3-K assays were performed essentially as described (Wallasch *et al.*, 1995), with some modifications. Briefly, GST–Grb2 *in vitro* associations were washed twice with HNTG and then three times with 1 ml of buffer containing 50 mM HEPES pH 7.5, 150 mM NaCl, 0.5 mM EGTA, 0.2 mM sodium orthovanadate and 10% glycerol. Then 30 μl of a master mix consisting of 10 μl of 5× buffer (100 mM Tris–HCl pH 7.5, 500 mM NaCl, 25 mM Mg acetate, 25 mM $MnCl_2$, 2.5 mM EGTA), 10 μl of sonicated phosphatidylinositol (0.5 mg/ml in 20 mM HEPES pH 7.5), 5 μl of 2 mM adenosine and 5 μl of H_2O were added to the beads followed by a pre-incubation step for 10 min at room temperature. The kinase reaction was started by addition of 10 μl of 0.1 mM ATP containing 2.5 μCi of [γ-^{32}P]ATP and performed for 30 min at 30°C. The reaction was stopped by addition of 100 μl of 1 M HCl, and lipids were extracted from supernatants with 200 μl of methanol:chloroform (1:1 v/v). The lipid-containing organic phase was resolved on oxalate-coated, thin-layer chromatography plates (Merck) developed in methanol:chloroform:water:glacial acetic acid:acetone (40:13:7:12:15 by vol.). The plates were then dried and exposed for PhosphorImager (Fuji) analysis.

Acknowledgements

We are grateful to C.J.Marshall, J.Schlessinger, H.R.Bourne, M.Faure, R.Wetzker, E.Lengyel, M.L.Gishizky, N.E.Fusenig, P.Hirth and H.J.

Bühring for kindly providing us with different plasmids and reagents. We thank Cordula Ebner-von Eschenbach for excellent technical assistance and our colleagues E.Zwick, B.Fernandez, F.U.Weiss, J.Schneckenburger and R.Lammers for various DNA constructs, reagents and stimulating discussions. This work was supported by a grant from Sugen, Inc.

References

Barnard,E.A., Burnstock,G. and Webb,T.E. (1994) G protein coupled receptors for ATP and other nucleotides: a new receptor family. *Trends Pharmacol. Sci.*, **15**, 67–70.

Bonfini,L., Migliaccio,E., Pelicci,G., Lanfrancone,L. and Pelicci,P.G. (1996) Not all Shc's roads lead to Ras. *Trends Biochem. Sci.*, **21**, 257–261.

Boukamp,P., Petrussevska,R.T., Breitkreutz,D., Hornung,J., Markham,A. and Fusenig,N.E. (1988) Normal keratinization in a spontaneously immortalized aneuploid human keratinocyte cell line. *J. Cell Biol.*, **106**, 761–771.

Byrne,J.L., Paterson,H.F. and Marshall,C.J. (1996) p21Ras activation by the guanine nucleotide exchange factor Sos requires the Sos/Grb2 interaction and a second ligand-dependent signal involving the Sos N-terminus. *Oncogene*, **13**, 2055–2065.

Cazaubon,S.M., Ramos-Morales,F., Fischer,S., Schweighoffer,F., Strosberg,A.D. and Couraud,P.-O. (1994) Endothelin induces tyrosine phosphorylation and Grb2 association of Shc in astrocytes. *J. Biol. Chem.*, **269**, 24805–24809.

Chen,Y., Grall,D., Salcini,A.E., Pelicci,P.G., Pousségur,J. and van Obberghen-Schilling,E. (1996) Shc adaptor proteins are key transducers of mitogenic signaling mediated by the G protein-coupled thrombin receptor. *EMBO J.*, **15**, 1037–1044.

Crespo,P., Xu,N., Simonds,W.F. and Gutkind,J.S. (1994) Ras-dependent activation of MAP kinase pathway mediated by G-protein βγ subunits. *Nature*, **369**, 418–420.

Daub,H., Weiss,F.U., Wallasch,C. and Ullrich,A. (1996) Role of transactivation of the EGF receptor in signalling by G-protein-coupled receptors. *Nature*, **379**, 557–560.

Devary,Y., Gottlieb,R.A., Smeal,T. and Karin,M. (1992) The mammalian ultraviolet response is triggered by activation of Src tyrosine kinases. *Cell*, **71**, 1081–1091.

Dikic,I., Tokiwa,G., Lev,S., Courtneidge,S.A. and Schlessinger,J. (1996) A role for Pyk2 and Src in linking G-protein-coupled receptors with MAP kinase activation. *Nature*, **383**, 547–550.

Egan,S.E., Giddings,B.W., Brooks,M.W., Buday,L., Sizeland,A.M. and Weinberg,R.A. (1993) Association of Sos Ras exchange protein with Grb2 is implicated in tyrosine kinase signal transduction and transformation. *Nature*, **363**, 45–51.

Faure,M., Voyno-Yasenetskaya,T.A. and Bourne,H. (1994) cAMP and βγ subunits of heterotrimeric G proteins stimulate the mitogen-activated protein kinase pathway in COS-7 cells. *J. Biol. Chem.*, **269**, 7851–7854.

Franke,T.F., Kaplan,D.R., Cantley,L.C. and Toker,A. (1997) Direct regulation of the Akt proto-oncogene product by phosphatidylinositol-3,4-bisphosphate. *Science*, **275**, 665–668.

Gishizky,M.L., Cortez,D. and Pendergast,A.M. (1995) Mutant forms of growth factor-binding protein-2 reverse BCR-ABL-induced transformation. *Proc. Natl Acad. Sci. USA*, **92**, 10889–10893.

Hanke,J.H., Gardner,J.P., Dow,R.L., Changelian,P.S., Brissette,W.H., Weringer,E.J., Pollok,B.A. and Conelly,P.A. (1996) Discovery of a novel, potent, and Src family-selective tyrosine kinase inhibitor. *J. Biol. Chem.*, **271**, 695–701.

Hawes,B.E., van Biesen,T., Koch,W.J., Luttrell,L.M. and Lefkowitz,R.J. (1995) Distinct pathways of G_i- and G_q-mediated mitogen-activated protein kinase activation. *J. Biol. Chem.*, **270**, 17148–17153.

Hawes,B.E., Luttrell,L.M., van Biesen,T. and Lefkowitz,R.J. (1996) Phosphatidylinositol 3-kinase is an early intermediate in the Gβγ-mediated mitogen-activated protein kinase signaling pathway. *J. Biol. Chem.*, **271**, 12133–12136.

Her,J.-H., Wu,J., Rall,T.B., Sturgill,T.W. and Weber,M.J. (1991) Sequence of pp42/MAP kinase, a serine/threonine kinase regulated by tyrosine phosphorylation. *Nucleic Acids Res.*, **19**, 3743.

Holgado-Madruga,M., Emlet,D.R., Moscatello,D.K., Godwin,A.K. and Wong,A.J. (1996) A Grb2-associated docking protein in EGF- and insulin-receptor signalling. *Nature*, **379**, 560–564.

Jehan,F., Neveu,I., Naheilhan,P., Wion,D. and Brachet,P. (1995) Interactions between second messenger pathways influence NGF synthesis in mouse primary astrocytes. *Brain Res.*, **672**, 128–136.

Kashles,O., Yarden,Y., Fischer,R., Ullrich,A. and Schlessinger,J. (1991) A dominant negative mutation suppresses the function of normal epidermal growth factor receptors by heterodimerization. *Mol. Cell. Biol.*, **11**, 1454–1463.

Knebel,A., Rahmsdorf,H.J., Ullrich,A. and Herrlich,P. (1996) Dephosphorylation of receptor tyrosine kinases as target of regulation by radiation, oxidants or alkylating agents. *EMBO J.*, **15**, 5314–5325.

Kranenburg,O., Verlaan,I., Hordijk,P.L. and Moolenaar,W.H. (1997) G_i-mediated activation of the ras/MAP kinase pathway involves a 100 kDa tyrosine-phosphorylated Grb2 SH3 binding protein, but not Src or Shc. *EMBO J.*, **16**, 3097–3105.

Lengyel,E., Stepp,E., Gum,R. and Boyd,D. (1995) Involvement of a mitogen-activated protein kinase signaling pathway in the regulation of urokinase promoter activity by c-Ha-ras. *J. Biol. Chem.*, **270**, 23007–23012.

Lev,S., Moreno,H., Martinez,R., Canoll,P., Peles,E., Musacchio,J.M., Plowman,G.D., Rudy,B. and Schlessinger,J. (1995) Protein tyrosine kinase PYK2 involved in Ca^{2+}-induced regulation of ion channel and MAP kinase functions. *Nature*, **376**, 737–745.

Levitzki,A. and Gazit,A. (1995) Tyrosine kinase inhibition: an approach to drug development. *Science*, **267**, 1782–1788.

Linseman,D.A., Benjamin,C.W. and Jones,D.A. (1995) Convergence of angiotensin II and platelet-derived growth factor receptor signaling cascades in vascular smooth muscle cells. *J. Biol. Chem.*, **270**, 12563–12568.

Lopez-Ilasaca,M., Crespo,P., Pellici,P.G., Gutkind,J.S. and Wetzker,R. (1997) Linkage of G protein-coupled receptors to the MAPK signaling pathway through PI3-kinase γ. *Science*, **275**, 394–397.

Lustig,K.D., Conklin,B.R., Herzmark,P., Taussig,R. and Bourne,H.R. (1993) Type II adenylylcyclase integrates coincident signals from G_s, G_i, and G_q. *J. Biol. Chem.*, **268**, 13900–13905.

Luttrell,L.M., Hawes,B.E., van Biesen,T., Luttrell,D.K. Lansing,T.J. and Lefkowitz,R.J. (1996) Role of c-Src tyrosine kinase in G protein-coupled receptor- and Gβγ subunit-mediated activation of mitogen-activated protein kinases. *J. Biol. Chem*, **271**, 19443–19450.

Luttrell,L.M., Della Rocca,G.J., van Biesen,T., Luttrell,D.K. and Lefkowitz,R.J. (1997) Gβγ subunits mediate Src-dependent phosphorylation of the epidemal growth factor receptor. *J. Biol. Chem.*, **272**, 4637–4644.

Malarkey,K., Belham,C.M., Paul,A., Graham,A., McLees,A., Scott,P.H. and Plevin,R. (1995) The regulation of tyrosine kinase signalling pathways by growth factor and G-protein-coupled receptors. *Biochem. J.*, **309**, 361–375.

McCollam,L., Bonfini,L., Karlovich,C.A., Conway,B.R., Kozma,L.M., Banerjee,U. and Czech,M.P. (1995) Functional roles for the pleckstrin and Dbl homology regions in the Ras exchange factor Son-of-sevenless. *J. Biol. Chem.*, **270**, 15954–15957.

Meisner,H., Conway,B.R., Hartley,D. and Czech,M.P. (1995) Interactions of Cbl with Grb2 and phosphatidylinositol 3′-kinase in activated Jurkat cells. *Mol. Cell. Biol.*, **15**, 3571–3578.

Meloche,S., Pagès,G. and Pousségur,J. (1992) Functional expression and growth factor activation of an epitope-tagged p44 mitogen-activated protein kinase, $p44^{mapk}$. *Mol. Biol. Cell*, **3**, 63–71.

Offermanns,S., Heiler,E., Spicher,K. and Schultz,G. (1994) G_q and G_{11} are concurrently activated by bombesin and vasopressin in Swiss 3T3 cells. *FEBS Lett.*, **349**, 201–204.

Ohmichi,M., Sawada,T., Kanda,Y., Koike,K., Hirota,K., Miyake,A. and Saltiel,A.R. (1994) Thyrotropin-releasing hormone stimulates MAP kinase activity in GH3 cells by divergent pathways. *J. Biol. Chem.*, **269**, 3783–3788.

Pace,A.M., Faure,M. and Bourne,H.R. (1995) G_{i2}-mediated activation of the MAP kinase cascade. *Mol. Biol. Cell*, **6**, 1685–1695.

Pagès,G., Lenormand,P., L'Allemain,G., Chambard,J.-C., Meloche,S. and Pouysségur,J. (1993) Mitogen-activated protein kinases $p42^{mapk}$ and $p44^{mapk}$ are required for fibroblast proliferation. *Proc. Natl Acad. Sci. USA*, **90**, 8319–8323.

Ptasznik,A., Traynor-Kaplan,A. and Bokoch,G.M. (1995) G protein-coupled chemoattractant receptors regulate Lyn tyrosine kinase–Shc adapter protein signaling complexes. *J. Biol. Chem.*, **270**, 19969–19973.

Rameh,L.E., Chen,C.-S. and Cantley,L.C. (1995) Phosphatidylinositol (3,4,5)P_3 interacts with SH2 domains and modulates PI 3-kinase association with tyrosine-phosphorylated proteins. *Cell*, **83**, 821–830.

Rao,G.N., Delafontaine,P. and Runge,M.S. (1995) Thrombin stimulates phosphorylation of insulin-like growth factor-1 receptor, insulin receptor substrate-1, and phospholipase Cγ1 in rat aortic smooth muscle cells. *J. Biol. Chem.*, **270**, 27871–27875.

Redemann,N., Holzmann,B., von Rüden,T., Wagner,E.F., Schlessinger,J. and Ullrich,A. (1992) Anti-oncogenic activity of signalling-defective epidermal growth factor receptor mutants. *Mol. Cell. Biol.*, **12**, 491–498.

Rosen,L.B. and Greenberg,M.E. (1996) Stimulation of growth factor receptor signal transduction by activation of voltage-sensitive calcium channels. *Proc. Natl Acad. Sci. USA*, **93**, 1113–1118.

Rusanesco,G., Qi,H., Thomas,S.M., Brugge,J.S. and Haleggoua,S. (1995) Calcium influx induces neurite outgrowth through a Src–Ras signaling casette. *Neuron*, **15**, 1415–1425.

Sadoshima,J. and Izumo,S. (1996) The heterotrimeric G_q protein-coupled angiotensin II receptor activates $p21^{ras}$ via the tyrosine kinase–Shc–Grb2–Sos pathway in cardiac myocytes. *EMBO J.*, **15**, 775–787.

Salter,M.W. and Hicks,J.L. (1995) ATP causes release of intracellular Ca^{2+} via the phospholipase $C\beta/IP_3$ pathway in astrocytes from the dorsal spinal cord. *J. Neurosci.*, **15**, 2961–2971.

Schieffer,B., Paxton,W.G., Chai,Q., Marrero,M.B. and Bernstein,K.E. (1996) Angiotensin II controls $p21^{ras}$ activity via $pp60^{c\text{-}src}$. *J. Biol. Chem*, **271**, 10329–10333.

Schlaepfer,D.D., Broome,M.A. and Hunter,T. (1997) Fibronectin-stimulated signaling from a focal adhesion kinase-c-Src complex: Involvement of the Grb2, $p130^{cas}$, and Nck adaptor proteins. *Mol. Cell. Biol.*, **17**, 1702–1713.

Schuhmacher,R., Soos,M.A., Schlessinger,J., Brandenburg,D., Siddle,K. and Ullrich,A. (1993) Signaling-competent receptor chimeras allow mapping of major insulin receptor binding domain determinants. *J. Biol. Chem.*, **268**, 1087–1094.

Seedorf,K., Kostka,G., Lammers,R., Bashkin,P., Daly,R., Burgess,W.H., van der Bliek,A.M., Schlessinger,J. and Ullrich,A. (1994) Dynamin binds to SH3 domains of phospholipase Cγ and GRB-2. *J. Biol. Chem.*, **269**, 16009–16014.

Shaw,G. (1996) The pleckstrin homology domain: an intriguing multifunctional protein module. *BioEssays*, **18**, 35–46.

Strawn,L.M., Mann,E., Elliger,S.S., Chu,L.M., Germain,L.L., Niederfellner,G., Ullrich,A. and Shawver,L.K. (1994) Inhibition of glioma cell growth by a truncated platelet-derived growth factor-β receptor. *J. Biol. Chem.*, **269**, 21215–21222.

Touhara,K., Hawes,B.E., van Biesen,T. and Lefkowitz,R.L. (1995) G protein βγ subunits stimulate phosphorylation of Shc adapter protein. *Proc. Natl Acad. Sci. USA*, **92**, 9284–9287.

Treisman,R. (1996) Regulation of transcription by MAP kinase cascades. *Curr. Opin. Cell Biol.*, **8**, 205–215.

van Biesen,T., Hawes,B.E., Luttrell,D.K., Krueger,K.M., Touhara,K., Porfiri,E., Sakaue,M., Luttrell,L.M. and Lefkowitz,R.J. (1995) Receptor-tyrosine-kinase- and Gβγ-mediated MAP kinase activation by a common signalling pathway. *Nature*, **376**, 781–784.

van Biesen,T., Hawes,B.E., Raymond,J.R., Luttrell,L.M., Koch,W.J. and Lefkowitz,R.J. (1996a) G_o-protein α subunits activate mitogen-activated protein kinase via a novel protein kinase C-dependent mechanism. *J. Biol. Chem.*, **271**, 1266–1269.

van Biesen,T., Luttrell,L.M., Hawes,B.E. and Lefkowitz,R.J. (1996b) Mitogenic signaling via G protein-coupled receptors. *Endocr. Rev.*, **17**, 698–714.

van Corven,E.J., Hordijk,P.L., Medema,R.H., Bos,J.L. and Moolenaar, W.H. (1993) Pertussis toxin-sensitive activation of $p21^{ras}$ by G protein-coupled receptor agonists in fibroblasts. *Proc. Natl Acad. Sci. USA*, **90**, 1257–1261.

van der Geer,P., Wiley,S., Gish,G.D. and Pawson,T. (1996) The Shc adaptor protein is highly phosphorylated at conserved, twin tyrosine residues (Y239/240) that mediate protein–protein interactions. *Curr. Biol.*, **6**, 1435–1444.

Vogel,W., Lammers,R., Huang,J. and Ullrich,A. (1993) Activation of a phosphotyrosine phosphatase by tyrosine phosphorylation. *Science*, **259**, 1611–1614.

Wallasch,C., Weiss,F.U., Niederfellner,G., Jallal,B., Issing,W. and Ullrich,A. (1995) Heregulin-dependent regulation of HER2/neu oncogenic signaling by heterodimerization with HER3. *EMBO J.*, **14**, 4267–4275.

Wang,J., Auger,K.R., Jarvis,L.,Shi,Y. and Roberts,T.M. (1995) Direct interaction of Grb2 with the p85 subunit of phosphatidylinositol 3-kinase. *J. Biol. Chem.*, **270**, 12774–12780.

Weidner,K.M., DiCesare,S., Sachs,M., Brinkmann,V., Behrens,J. and Birchmeier,W. (1996) Interaction between Gab1 and the c-Met receptor tyrosine kinase is responsible for epithelial morphogenesis. *Nature*, **384**, 173–176.

Weiss,F.U., Daub,H. and Ullrich,A. (1997) Novel mechanisms of RTK signal generation. *Curr. Opin. Genet. Dev.*, **7**, 80–86.

Received on June 16, 1997; revised on September 16, 1997

MOLECULAR AND CELLULAR BIOLOGY, Aug. 1994, p. 5402–5411
0270-7306/94/$04.00+0

Vol. 14, No. 8

Csk Suppression of Src Involves Movement of Csk to Sites of Src Activity

BRIAN W. HOWELL AND JONATHAN A. COOPER*

Fred Hutchinson Cancer Research Center, Seattle, Washington 98104

Received 14 March 1994/Returned for modification 11 April 1994/Accepted 23 May 1994

Csk phosphorylates Src family members at a key regulatory tyrosine in the C-terminal tail and suppresses their activities. It is not known whether Csk activity is regulated. To examine the features of Csk required for Src suppression, we expressed Csk mutants in a cell line with a disrupted *csk* gene. Expression of wild-type Csk suppressed Src, but Csk with mutations in the SH2, SH3, and catalytic domains did not suppress Src. An SH3 deletion mutant of Csk was fully active against in vitro substrates, but two SH2 domain mutants were essentially inactive. Whereas Src repressed by Csk was predominantly perinuclear, the activated Src in cells lacking Csk was localized to structures resembling podosomes. Activated mutant Src was also in podosomes, even in the presence of Csk. When Src was not active, Csk was diffusely located in the cytosol, but when Src was active, Csk colocalized with activated Src to podosomes. Csk also localizes to podosomes of cells transformed by an activated Src that lacks the major tyrosine autophosphorylation site, suggesting that the relocalization of Csk is not a consequence of the binding of the Csk SH2 domain to phosphorylated Src. A catalytically inactive Csk mutant also localized with Src to podosomes, but SH3 and SH2 domain mutants did not, suggesting that the SH3 and SH2 domains are both necessary to target Csk to places where Src is active. The failure of the catalytically active SH3 mutant of Csk to regulate Src may be due to its inability to colocalize with active Src.

The Src protein tyrosine kinases have been implicated in a plethora of cellular signaling pathways including growth factor signaling (38, 76), integrin-mediated signaling (10), T- and B-cell activation (50), the response to UV radiation (19), and cellular transformation (12). These kinases share a common overall structure and a general mode of regulation (reviewed in reference 13). In resting fibroblasts, Src is found in a repressed state, in which a tyrosine (Y) in the C terminus, Y-527, is phosphorylated to high stoichiometry. Blocking phosphorylation of Y-527 by replacement with phenylalanine (F) activates Src (8, 34, 61, 63). Other activated mutants of Src have been shown to either lack this tyrosine or be hypophosphorylated at this site (25, 27).

Csk was detected as a protein tyrosine kinase that can phosphorylate the C-terminal Y of the Src kinases and suppress kinase activity (4, 51, 56, 57). In cells which carry a targeted disruption in the *csk* locus, the Src family members, Src, Fyn, and Lyn, are more active than in wild-type cells (26, 52). Low levels of Src Y-527 phosphorylating activity were detected in these cells (26), suggesting that Csk-related kinases, such as Ctk and Matk, may also phosphorylate this site in vivo (3, 33).

Csk has been shown to negatively regulate T-cell receptor signaling (9). Elevated levels of Csk reduced the effects of T-cell receptor stimulation on tyrosine phosphorylation and subsequent lymphokine release. It was proposed that this block is a direct effect of suppressing Lck and/or FynT kinase activities. Overexpression of Csk has also been shown to mitigate transforming properties of the oncogenic SH2/SH3 protein v-Crk when this protein is coexpressed with c-Src but not when it is coexpressed with SrcF527 (67). Csk therefore can be viewed as a key negative regulator of the kinases of the Src family.

The Src kinases are directed to cellular membranes by an amino-terminal sequence that includes a myristoylation signal (12, 62). Mutations in the myristoylation signal or adjacent sequences block membrane localization and Src biological activity (1, 16, 28, 31). Some Src family members, excluding Src, are also palmitoylated (58, 70). In resting cells, Src is associated predominantly with endosomal membranes (17, 31, 32), but activated versions of Src have also been found in large adhesion plaques known as podosomes or rosettes (36, 37, 53, 64). Also in the podosomes are high concentrations of phosphotyrosine-containing proteins, including Src itself, which is phosphorylated at Y-416 when active, together with proteins that have been phosphorylated by Src and Src-activated kinases. A number of Src substrates are cytoskeletal or translocate to the podosomes after transformation by Src (79–81). The action of Src in this compartment may be to remodel the cytoskeleton, modifying the normal adhesion plaques and redistributing them into clusters at the cell periphery (5). These structures are highly dynamic and, unlike normal adhesion plaques, will form on naked glass in the absence of serum (reviewed in reference 6). In platelets, Src may be involved in cytoskeletal reorganization as well (10). The activation of platelets by thrombin results in dephosphorylation of 10 to 15% of the Src at Y-527, a transient increase in the specific kinase activity, and the redistribution of the kinase to a cytoskeleton-rich, detergent-insoluble fraction of the cell (10).

The extracatalytic SH2 and SH3 domains, found in the Src kinases, Csk, and a number of catalytic and noncatalytic signal transduction molecules, mediate protein-protein interactions (35, 60). In Src, these domains are involved in the intramolecular suppression of the kinase. Expression of certain SH2 or SH3 mutants of Src transforms avian cells (54, 59, 69). Paradoxically, some mutations in the SH2 or SH3 domains of activated forms of Src decrease transforming activity or modify the transformed phenotype (23, 59). This suggests that the SH2

* Corresponding author. Mailing address: A2-025 Fred Hutchinson Cancer Research Center, 1124 Columbia St., Seattle, WA 98104. Phone: (206) 667-4454. Fax: (206) 667-6522.

and SH3 domains are involved in mediating the transforming signal. Indeed, these domains are important both for interaction with substrates including phosphatidylinositol 3-kinase (PI3 kinase), AFAP-110, paxillin, and FAK (11, 20, 30, 41, 79) and for subcellular localization (2, 21, 45).

Little is known about the roles of the extracatalytic domains of Csk, their effect on kinase activity, or the proteins with which they interact. We investigated the requirement of the Csk SH2 and SH3 domains for the suppression of Src. Wild-type and mutant forms of Csk were expressed in cells obtained from $csk^{-/-}$ mice, and their abilities to repress Src and their subcellular distributions were compared. Under conditions in which Src was active, Csk localized with Src to podosomes, but when Src was not active, Csk was diffusely localized in the cytoplasm. The codistribution of Csk with active Src required both the SH2 and SH3 domains of Csk. A correlation between Csk colocalization with Src and its ability to suppress Src activity was demonstrated.

MATERIALS AND METHODS

Vectors and cell lines. Csk mutants with deletions in the SH3 (amino acid 29 to 66) or SH2 (amino acid 82 to 158) domain, Csk(ΔSH3) and Csk(ΔSH2), were generated by PCR with pSP64CSK (55) as a template. The oligonucleotide pairs used for the PCR were oriented away from each other and contained *Mlu*I sites in their 5′ ends. The pairs were as follows: 5′CTCACGCGTAAGGTCTTGCTCGGCAGTG3′ and 5′CTCACGCGTAAGCGTGAGGGTGTGAAGG3′ for the SH3 mutation and 5′CTCACGCGTGGGCATAAGGCTGAGCTTG3′ and 5′CTCACGCGTGATGCCGACGGACTCTGCA3′ to generate the SH2 mutant. The PCR products were gel purified, restricted with *Mlu*I, and ligated. The *Bgl*II-to-*Bam*HI restriction fragments of these mutant DNAs, which contain the entire Csk coding region (55), were cloned into the *Bam*HI site of the pLXSH retroviral vector (46) for expression analysis. The FLVRES mutant, Csk(FLVRES), in which the RES motif at positions 107 to 109 was changed to KSI, was generated in an analogous manner except that a *Cla*I site was introduced into the 5′ ends of the oligonucleotides, which were as follows: 5′CGCCATCGATTTCACCAGGAAGAGGCCTGTCT3′ and 5′CGCCATCGATCACCAACTACCCTGGGGACTAC3′. The K-to-R mutation at position 222 (K-222-to-R mutation) of CSK (kinase-defective mutant) was generated by site-directed mutagenesis; this mutant [Csk(R-222)] was the kind gift of M. Okada. Wild-type Src [Src(wt)], the Y-527-to-F mutant, and the Y-419- and Y-527-to-phenylalanine double mutant previously described (15, 42) were shuttled into pLXSHD, which confers L-histidinol resistance (72).

Simian virus 40 T-antigen-transformed embryonic cell lines T29E ($csk^{-/-}$) and T24E ($csk^{+/+}$) were gifts of Akira Imamoto and Philippe Soriano, and their isolation has been described elsewhere (26). High-titer virus from the various Csk and Src mutants was collected as described previously (48) and used to infect the $csk^{-/-}$ cells. These cells were grown in Dulbecco's minimal essential medium plus 10% fetal bovine serum and selected in either hygromycin (50 μg/ml; Calbiochem) or L-histidinol (2 mM; Sigma) for at least 10 days until uninfected controls were dead. Immunofluorescence showed that >90% of the drug-resistant cells expressed detectable levels of Csk (data not shown; see Fig. 7).

Immunoprecipitations and kinase assays. Equal numbers of cells (6×10^6) were lysed on ice, in 1 ml of Nonidet P-40 IPB (0.1 M NaCl, 1% Nonidet P-40, 10 mM HEPES [*N*-2-hydroxyethylpiperazine-*N*′-2-ethanesulfonic acid; pH 7.4], 2 mM EDTA, 0.1% 2-mercaptoethanol, 20 μg of aprotinin per ml, 50 mM NaF, 0.2 mM Na_3VO_4) for Csk assays or in RIPA buffer (0.15 M NaCl, 1% Nonidet P-40, 1% sodium deoxycholate, 0.1% sodium dodecyl sulfate [SDS], 10 mM sodium phosphate [pH 7.0], 2 mM EDTA, 14 mM 2-mercaptoethanol, 20 μg of aprotinin per ml, 50 mM NaF, 2 mM Na_3VO_4) for Src assays. The lysates were clarified by centrifugation at 20,000 × *g* for 30 min at 4°C. The supernatant was collected, either 1 μg of affinity-purified Csk C-terminal peptide antibody (αCsk) (55) or 1 μg of mAb327 Src antibody (a gift from Joan Brugge, Ariad Pharmaceuticals) was added to the lysate, and the mixture was incubated on ice for 1 h. A goat anti-mouse secondary antibody was added to the Src immunoprecipitation mixtures for 30 min. A 30-μl portion of a 10% slurry of formaldehyde-fixed *Staphylococcus aureus* was added to each immunoprecipitation mixture. After 30 min on ice with occasional mixing, samples were loaded onto 1 M sucrose cushions of the same buffer and centrifuged for 20 min at 1,500 × *g*. Pellets were washed three times with lysis buffer and twice with PAN (100 mM NaCl, 10 mM PIPES [piperazine-*N*,*N*′-bis(2-ethanesulfonic acid); pH 7.0], 20 μg of aprotinin per ml). A total of 20% of each immunoprecipitate was assayed for kinase activity, and 20% was used for Western blotting (immunoblotting). Csk kinase assays were done in a solution containing 10 mM PIPES (pH 7.0), 10 mM $MnCl_2$, 0.75 μM [γ-^{32}P]ATP (3,000 Ci/mmol), and 300 μg of poly(Glu,Tyr) 4:1 (Sigma) for 10 min at 30°C. Reactions were stopped by the addition of doubly concentrated gel loading buffer (4% SDS, 40% glycerol, 0.2 M Tris-HCl [pH 6.8], 5.6 M 2-mercaptoethanol, 5 mM EDTA, 0.02% bromophenol blue) and analyzed by SDS-polyacrylamide gel electrophoresis. Incorporation of ^{32}P into the substrate poly(Glu,Tyr) was determined with a PhosphorImager (Molecular Dynamics). The specific activity was determined by comparing these values with Western blot signals. Src immunocomplex kinase assays were performed as described previously (14) in the presence of exogenously added enolase. Reactions were terminated with doubly concentrated gel loading buffer after 15 min at 30°C, and products were resolved on 10% polyacrylamide gels. The phosphorylation of enolase was quantified with a PhosphorImager. SDS-polyacrylamide gel electrophoresis for Csk Western blots was done by using 8% acrylamide and 0.21% bisacrylamide to increase separation between Csk and the heavy-chain immunoglobulin, and samples were not boiled in order to circumvent reduction of the heavy-light immunoglobulin complexes. Csk immunoblots were analyzed with affinity-purified αCsk antibodies and then with anti-rabbit immunoglobulin conjugated with horseradish peroxidase (Jackson Immunoresearch Labs), and Src immunoblots were analyzed with the biotinylated antibody mAb327 (a gift of Joan Brugge) and streptavidin-horseradish peroxidase (Amersham). For the antiphosphotyrosine blot (see Fig. 4), monoclonal antibody 4G10 (Upstate Biotechnology Incorporated [UBI]) and anti-mouse immunoglobulin conjugated with horseradish peroxidase (Jackson Immunoresearch Labs) were used. Blots were developed by enhanced chemiluminescence (Amersham).

Immunofluorescence. Cells were plated on glass coverslips treated with poly-L-lysine (Sigma) 24 to 36 h before analysis. In some experiments, cells were serum starved by plating them in serum for 8 h and then incubating them for 18 h in serum-free media. After being washed once with phosphate-buffered saline (PBS), cells were fixed in 3.7% formaldehyde in PBS for 10 min at 22°C and treated with TBP (0.5% Triton X-100, 1% bovine serum albumin in PBS) for 1 h at 4°C. The primary antibodies mAb327 (1 mg/ml; 1:100), affinity-purified αCsk (1:100), and antiphosphotyrosine antibody 4G10 (UBI) (1 mg/ml; 1:500) were incubated with coverslips in TBP for 2 h at

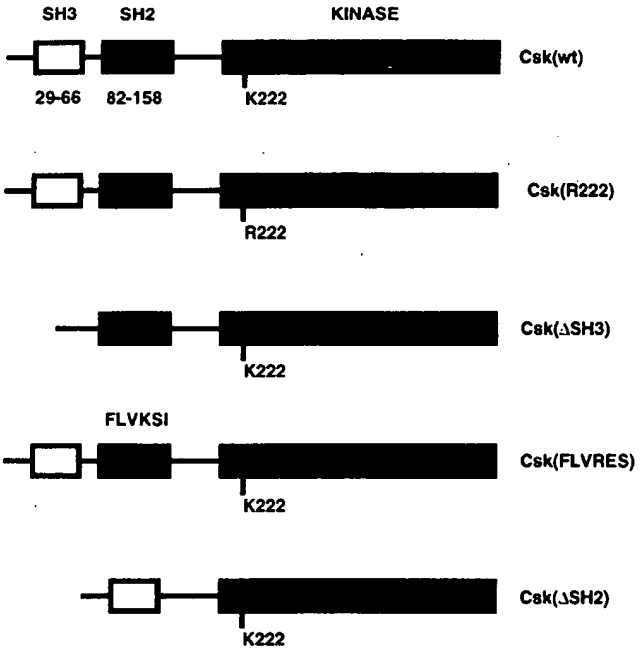

FIG. 1. Schematic representation of wild-type Csk and mutants generated. Shaded boxes represent the SH3, SH2, and catalytic domains. Numbers indicate amino acid residues. Lysine 222 (K222) in kinase subdomain II was mutated to arginine (R222) to inactivate the kinase. The invariant arginine in the FLVRES motif of the SH2 domain that has been shown to be crucial for phosphotyrosine binding (44) was mutated to lysine, and two downstream amino acids were changed to serine and isoleucine to generate the FLVRES mutant. The *csk* cDNAs used in this study were expressed in the retroviral vector pLXSH, which confers hygromycin resistance to infectants.

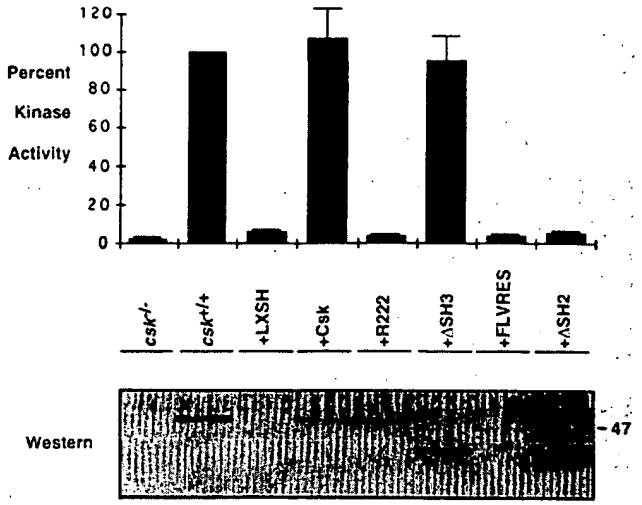

FIG. 2. In vitro kinase assays of anti-Csk immunocomplexes from wild-type and recombinant cell lines. (Upper panel) The bar graph represents the quantification of total phosphate incorporation into poly(Glu,Tyr) after kinase assays of immunocomplexes. The activity from $csk^{+/+}$ cells was arbitrarily set at 100%, and all numbers represent averages from three experiments. (Lower panel) The anti-Csk immunoblot shows the relative amounts of Csk used in the kinase assays whose results are shown in the upper panel and the differences in molecular weight between the mutants. Values obtained from similar blots were used to determine the relative specific activities of the various Csk mutants (Table 1). The abbreviations $csk^{-/-}$, $csk^{+/+}$, +LXSH, +Csk, +R222, +ΔSH3, +FLVRES, and +ΔSH2 denote the cell lines $csk^{-/-}$ and $csk^{+/+}$ and $csk^{-/-}$ cells infected with pLXSH vector, Csk(wt), Csk(R222), Csk(ΔSH3), Csk(FLVRES), and Csk (ΔSH2), respectively.

37°C in a humidified chamber. After being washed three times with PBS containing 0.5% Triton X-100, the secondary antibodies, fluorescein-conjugated donkey anti-mouse and Texas red-conjugated donkey anti-rabbit (Jackson Immunoresearch Labs), were diluted 1:400 in TBP and applied for 2 h at 37°C. Coverslips were washed and affixed to glass slides. Images were collected with a Bio-Rad MRC600 scanning laser confocal microscope. Controls performed with both secondary antibodies and only one primary antibody showed negligible cross-reactivity bleed-through into the opposite channel. All figures show optical sections of the cells closest to the substratum.

RESULTS

Expression of wild-type and mutant Csk. In order to identify the Csk domains required for Src suppression, wild-type and mutant forms of Csk were constructed and inserted into the retroviral vector pLXSH (47) and expressed in mouse embryo fibroblasts containing a targeted disruption of the *csk* gene (26). The $csk^{-/-}$ cell line allowed us to study the activities of mutant Csk molecules in the absence of endogenous Csk. As a control, cells isolated from a wild-type littermate were used. Four mutants were constructed (Fig. 1), a mutant with a lysine-to-arginine mutation at position 222 in the catalytic domain that is predicted to abolish kinase activity, mutants with deletions in either the SH3 or SH2 domain, and a mutant with a mutation in the SH2 domain FLVRES sequence (Fig. 1). The arginine (R) in this sequence has been shown to be required for phosphotyrosine binding by other SH2 domains (44, 60).

All constructs produced proteins of the predicted sizes in immunoprecipitation and Western blot analysis, although the FLVRES mutant had slightly increased electrophoretic mobility (Fig. 2). However, expression levels varied among mutants. In all cases but one the levels were comparable to or greater than those in $csk^{+/+}$ cells. The FLVRES mutant was underexpressed, which may represent an instability of the protein. Since the Csk antibody was directed against the C-terminal 13 residues, it should recognize all of the Csk mutants used in this study equally well. The relative amounts of Csk which immunoprecipitated from the various mutant lines were the same as those observed with the whole-cell lysates (data not shown).

The effects of the Csk mutations on kinase activity were assessed by immunoprecipitating Csk from the cell lines and assaying activity of the immune complexes against the exogenous substrate poly(Glu,Tyr) (Fig. 2). The relative specific activities of the Csk mutants were determined by normalizing the Csk kinase activity for the various levels of Csk observed in immunoblots of the same immunoprecipitates (Fig. 2). As expected, the expression of the empty vector pLXSH or Csk(R-222) did not produce significant amounts of kinase activity. The levels of specific and total kinase activities isolated from cells expressing Csk(wt) or Csk(ΔSH3) were comparable to levels in control $csk^{+/+}$ cells (Fig. 2 and Table 1). However, neither of the SH2 domain mutants, Csk(ΔSH2) and Csk (FLVRES), had detectable kinase activity. To ensure that mutations were not inadvertently introduced into the catalytic domain, the catalytic domain of the Csk(ΔSH2) construct was substituted with that of Csk(wt). The resulting construct also lacked kinase activity. When c-Src purified from a baculovirus

TABLE 1.

Cells[a]	Csk sp act[b,c]	Src sp act[c,d]	Total phosphotyrosine activity[d,e]	Csk total activity[b,c]	Inhibition of Src activity[f]	Inhibition of tyrosine phosphorylation[g]
csk$^{-/-}$	ND[h]	1.00	1.00	0.03 ± 0.01	0	0
csk$^{+/+}$	1.00	0.17 ± 0.05	0.09 ± 0.01	1.00	1.00	1.00
+LXSH	ND[h]	0.85 ± 0.17	0.95 ± 0.10	0.08 ± 0.01	0.18	0.05
+Csk	1.25 ± 0.15	0.18 ± 0.07	0.12 ± 0.01	1.08 ± 0.15	0.99	0.97
+R222	0.05 ± 0.02	0.86 ± 0.17	1.00 ± 0.10	0.05 ± 0.01	0.17	0.00
+ΔSH3	0.75 ± 0.10	0.73 ± 0.15	0.63 ± 0.06	0.95 ± 0.10	0.33	0.41
+FLVRES	ND	1.01 ± 0.15	0.76 ± 0.08	0.05 ± 0.01	−0.01	0.26
+ΔSH2	0.02 ± 0.02	1.09 ± 0.15	0.98 ± 0.10	0.07 ± 0.01	−0.11	0.02

[a] *csk*$^{-/-}$, *csk*$^{+/+}$, +LXSH, +Csk, +R-222, +ΔSH3, +FLVRES, and +ΔSH2 denote the cell lines *csk*$^{-/-}$ and *csk*$^{+/+}$ and *csk*$^{-/-}$ cells infected with pLXSH vector, Csk(wt), Csk(R-222), Csk(ΔSH3), Csk(FLVRES), and Csk(ΔSH2), respectively.
[b] Normalized to *csk*$^{+/+}$ cells at 1.00.
[c] Mean and range of four experimental results.
[d] Normalized to *csk*$^{-/-}$ cells at 1.00.
[e] Mean and range of two experimental results.
[f] Calculated by setting Src activity in *csk*$^{-/-}$ cells at 1.00 and activity in *csk*$^{+/+}$ cells at 0.00.
[g] Calculated by setting total protein phosphotyrosine immunoreactivity in *csk*$^{-/-}$ cells at 1.00 and immunoreactivity in *csk*$^{+/+}$ cells at 0.00.
[h] ND, not determined.

expression system (55) was used as the exogenous substrate for Csk, similar results were obtained (data not shown).

Src kinase activity and tyrosine phosphorylation of cellular proteins in cells expressing mutant forms of Csk. The Src protein from *csk*$^{-/-}$ cells was previously observed to have a higher specific activity than Src isolated from wild-type cells (26, 52). Csk and its mutants introduced into the *csk*$^{-/-}$ cell line were assayed for their effects on the specific kinase activity of the endogenous Src (Fig. 3). The kinase activities of Src immunocomplexes against the exogenous substrate enolase were measured. The various cell lines expressed similar levels of Src as determined by immunoblotting the Src immunoprecipitates with a biotinylated monoclonal antibody, mAb327 (Fig. 3). Slight variations in the amounts of Src in the immunoprecipitates were taken into account to determine the specific activities of Src (Table 1). The specific kinase activity of Src isolated from *csk*$^{-/-}$ cells expressing exogenous Csk(wt) was comparable to that of Src from the *csk*$^{+/+}$ cell line; in both cases the level of activity was about 5- to 6-fold lower than that of Src from *csk*$^{-/-}$ cells (Fig. 3 and Table 1). The inhibition of Src by Csk(wt) approximated *csk*$^{+/+}$ levels (Table 1), consistent with the similar levels of Csk expression. Expression of kinase-defective Csk(R-222) in *csk*$^{-/-}$ cells had no effect on Src activity. Likewise, the Csk SH2 domain mutants that had reduced kinase activity also did not repress Src. Interestingly, the expression of Csk(ΔSH3) inhibited Src kinase activity by 33%, compared with 99% for Csk(wt) (Table 1), even though the total Csk kinase activity from Csk(ΔSH3) cells was 95% of that from *csk*$^{+/+}$ cells (Fig. 3 and Table 1).

Total phosphotyrosine levels of the cell lines were compared by immunoblotting whole-cell lysates with an antiphosphotyrosine antibody (Fig. 4). The total phosphotyrosine immunoreactivity directly correlated with the activity of Src in each cell line (Table 1). The profile of antiphosphotyrosine reactive bands in the *csk*$^{-/-}$ cells was similar to that found with v-Src-transformed cells (Fig. 4) (29, 67, 69), suggesting that these proteins may be Src substrates. Immunoprecipitates of putative Src substrates AFAP-110, cortactin, paxillin, tensin, and FAK were found to be hyperphosphorylated on tyrosine (75). Phosphoproteins specific to the Csk-expressing lines were not observed, suggesting that Csk substrates such as Src are of low abundance or are phosphorylated to low stoichiometries.

Subcellular distribution of Csk and Src. In resting fibroblasts, c-Src is associated predominantly with endosomal membranes, whereas activated versions of Src are also found in association with specific adhesion structures termed podosomes (32, 36, 53, 73). In order to compare the subcellular distribution of Csk directly with that of Src, cells were fixed, permeabilized, and probed with αCsk and αSrc antibodies and then with Texas red-conjugated and fluorescein-conjugated secondary antibodies. Fluorescence from both wavelengths was collected with a confocal microscope. For detection of proteins in adhesion plaques, thin slices of the cells, close to the coverslip and below the nucleus, were examined. Endogenous Csk and c-Src exhibited weak cytoplasmic fluorescence in Rat2 fibroblasts (data not shown), and so both Src(wt) and Csk(wt) were overexpressed to aid detection (Fig. 5, upper panel). Csk and Src were both detected in the cytoplasm, with Src concen-

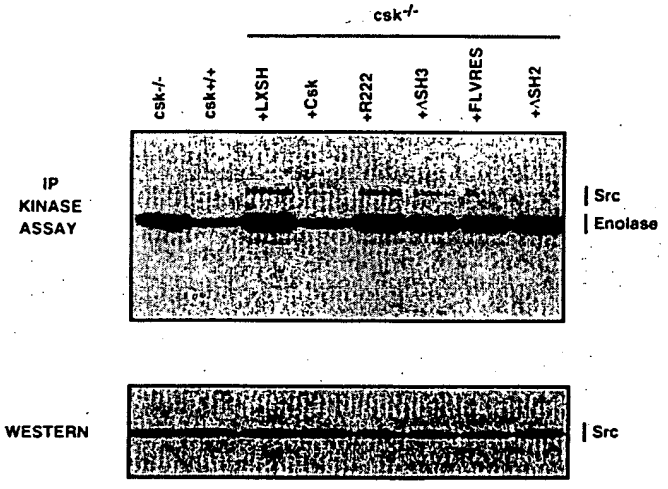

FIG. 3. In vitro kinase activities of Src immune complexes from wild-type and recombinant cell lines. (Upper panel) Kinase assays of mAb327 immunocomplexes are shown. Autophosphorylation and phosphorylation of exogenously added enolase are indicated to the right. (Lower panel) Biotinylated mAb327 was used to compare the relative amounts of Src in the immunocomplexes used for the kinase assays whose results are shown in the upper panel. Slight variations were accounted for when relative specific activities of Src were calculated (Table 1).

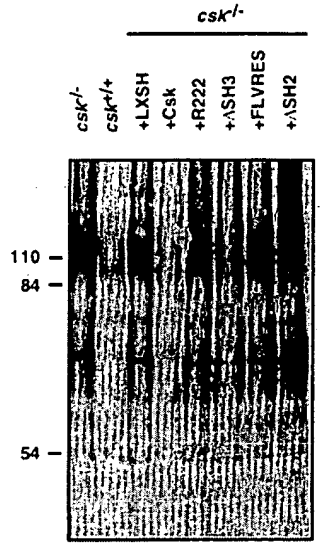

FIG. 4. Antiphosphotyrosine immunoblot of cell lysates. A Western blot of cell lysates with the antiphosphotyrosine antibody 4G10 for the indicated cell lines is shown.

trated to one side of the nucleus, as previously reported (17, 32). The localizations of Csk and Src overlapped, but while Src fluorescence appeared more intense in a perinuclear region, Csk fluorescence was more widely distributed throughout the cytoplasm. When Rat2 cells overexpressing activated Src(F-527) were examined, it was found that the majority of the Src was concentrated in adhesion structures (Fig. 5, middle panel) previously identified as podosomes (reviewed in reference 6) as well as in a perinuclear fluorescence. In these cells, both endogenous Csk (data not shown) and overexpressed Csk(wt) (Fig. 5, middle panel) were also concentrated in the podosomes. It has recently been suggested that the Csk SH2 domain may bind to the phosphorylated Y-416 in activated Src (71). To determine if Src Y-416 was required for the altered subcellular distribution of Csk in cells expressing activated Src, we coexpressed Csk with a double mutant of Src with phenylalanine substitutions for tyrosine at both Y-416 and Y-527. It has previously been shown that the double mutant does transform cells, albeit less well than the F-527 single mutant (34). The F-416 F-527 double-mutant Src was found in adhesion structures which are less prominent than those seen in the F-527-expressing Rat-2 fibroblasts (Fig. 5, lower panel). Like the structures in F-527 Src-expressing cells, these adhesion plaques reacted with antiphosphotyrosine and antivinculin antibodies (data not shown). Csk was found to colocalize with Src in these adhesion structures (Fig. 5, lower panel). These results suggested that Csk might be localized to places of Src activity rather than binding to Src phosphorylated at Y-416.

To determine if the active version and the repressed version of wild-type Src were differentially localized and to investigate the influence of Src activity on the subcellular distribution of Csk, wild-type Src was coexpressed with Csk(wt) or Csk(R-222) in $csk^{-/-}$ cells (Fig. 6). Tyrosine phosphorylation is suppressed by the expression of Csk(wt) but not by the expression of Csk(R-222) (Fig. 4). Accordingly, antiphosphotyrosine fluorescence from Csk(wt) cells was faint in comparison with that from Csk(R-222) cells (Fig. 6, right side). A minor subpopulation of cells expressing lower-than-average levels of Csk(wt) had stronger antiphosphotyrosine fluorescence (Fig. 6, arrows, and data not shown). Src immunofluo-

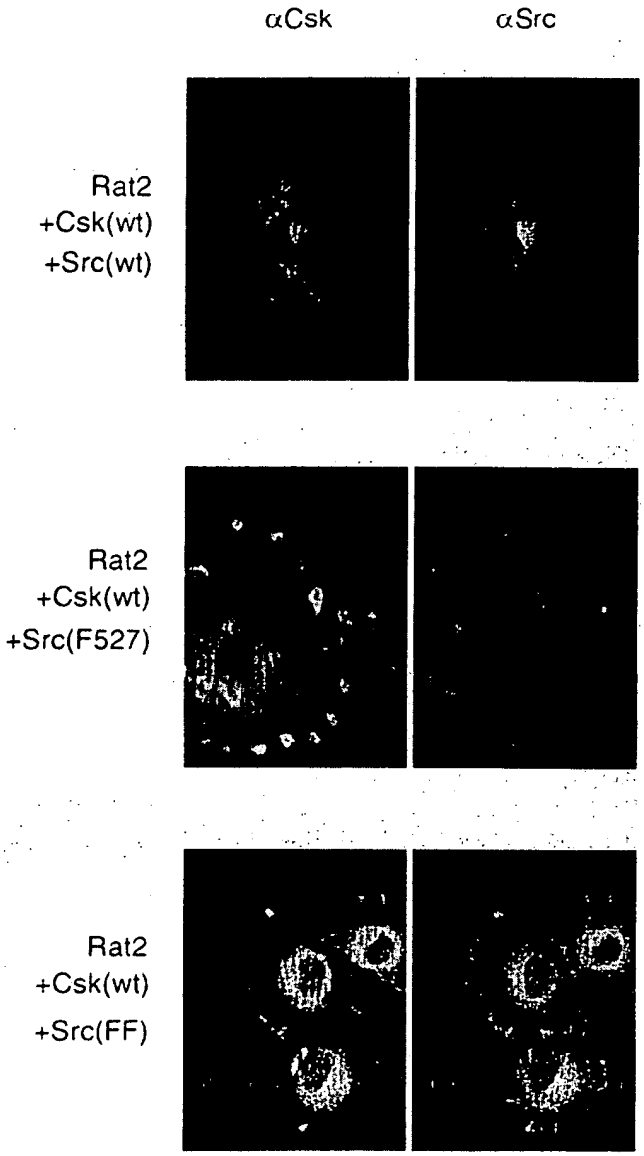

FIG. 5. Csk and Src subcellular distributions in Rat2 cells are dependent on Src activity. (Upper panel) Rat2 cells were infected with viruses encoding Csk(wt) and Src(wt). (Middle panel) Cells were infected with Src(F-527) in place of the wild-type kinase. (Lower panel) Cells were expressing the Src(F-416 F-527) mutant [Src(FF)] and Csk(wt). The left halves of the images represent Texas red immunofluorescence (αCsk), and the right halves represent fluorescein (αSrc) immunofluorescence.

rescence was absent from the periphery and concentrated in a perinuclear location in cells expressing Csk(wt) and Src(wt) (Fig. 6, upper left), as in Rat2 cells. When $csk^{-/-}$ cells expressing Src(wt) and Csk(R-222) were examined, the distributions of both Csk and Src were found to be dramatically different (Fig. 6, lower left). Src staining was predominantly associated with structures resembling adhesion plaques at the cell periphery, although some staining remained perinuclear. Csk was observed in the adhesion plaques at the cell periphery. Antiphosphotyrosine reactivity in these cells was intense and coincident with the presence of Csk(R-222) and Src in the adhesion plaques (Fig. 6, lower right). Interestingly, the antiphosphotyrosine fluorescence was seen almost exclusively at

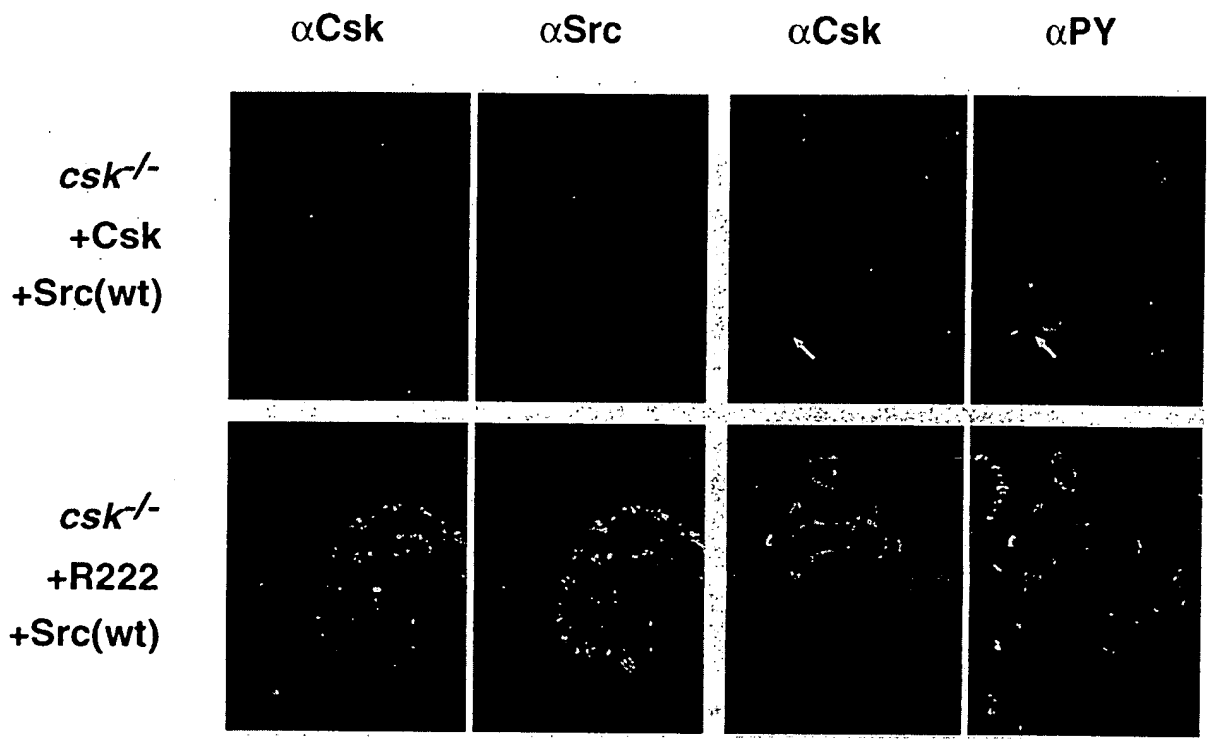

FIG. 6. Indirect immunofluorescence imaging of $csk^{-/-}$ cells overexpressing Src(wt) and infected with either Csk(wt) or Csk(R-222). The left halves of the split images depict Texas red (anti-rabbit) fluorescence patterns, and the right halves depict fluorescein (anti-mouse) fluorescence patterns. (Upper half) $csk^{-/-}$ cells infected with Src(wt) and Csk(wt) viruses were used. (Lower half) $csk^{-/-}$ cells were infected with Src(wt) and Csk(R-222). The pairs of slides on the left were incubated with anti-Csk (rabbit) and anti-Src (mouse) antibodies. The pairs of slides on the right were incubated with anti-Csk (rabbit) and antiphosphotyrosine (mouse) antibodies. Cells were serum starved for 18 h before fixation.

the adhesion structures in the cell and was not observed in other regions where Src was located. The redistribution of Csk is therefore consistent with a model in which Csk(R-222) localizes to regions of the cell where Src is active.

To determine whether Csk(wt) would localize with active Src in $csk^{-/-}$ cells, Csk(wt) and Src(F-527) were coexpressed. As in Rat2 cells, Src(F-527), Csk(wt), phosphotyrosine, and vinculin colocalized in podosome-like structures (Fig. 7 and data not shown). Together, these results suggest that the movement of Csk to adhesion structures depends on the kinase activity of Src. Movement of Csk is dependent on the catalytic activity of Csk only insofar as active Csk can repress Src activity and release Src and Csk from the adhesion plaques.

None of the SH2 or SH3 mutants of Csk could repress Src kinase activity (Fig. 3; Table 1). Examination of cells expressing these mutants together with Src(F-527) showed that the ability of Csk to colocalize with Src(F-527) to podosomes required that both the SH3 and SH2 domains be intact. Csk(ΔSH3), Csk(ΔSH2), and Csk(FLVRES) were not found in podosomes of any of the cells examined (Fig. 7). The failure of the enzymatically active Csk(ΔSH3) to repress Src activity in the cell (Fig. 3) could be related to its failure to colocalize with active Src in the cell.

DISCUSSION

Csk suppresses kinases of the Src family both in vitro and in vivo by phosphorylating key regulatory tyrosines in their C termini (4, 26, 51, 52, 56, 57). Deletion of the SH2 domain of Src, as well as the introduction of numerous point mutations in the C-terminal tail, renders Src a poor substrate for Csk, suggesting that a number of factors are involved in the kinase-substrate interaction (43, 55). In this report, we establish that the SH3, SH2, and kinase domains of Csk are all required for repression of Src activity in cells. Expression of wild-type Csk in $csk^{-/-}$ cells is sufficient to suppress Src kinase activity. The enzymatic activity of Csk is required for this suppression, since mutation of K-222 to R inactivates the kinase and prevents suppression. Both wild-type and kinase-inactive mutants of Csk redistribute to adhesion plaques in the presence of activated mutant Src. Deletion or mutation of key residues in the SH2 domain of Csk renders Csk inactive, and such mutants do not suppress Src activity. Such mutants also do not redistribute to adhesion structures in the presence of activated Src. Removal of the SH3 domain from Csk does not affect the ability of Csk to phosphorylate Src in vitro, but the resulting mutant fails to colocalize with Src to adhesion structures and does not suppress Src kinase activity effectively in vivo.

Src localization. We have observed that, in the absence of suppression by Csk, a fraction of Src molecules move from their normal perinuclear location to the adhesion plaques and tyrosine phosphorylation of adhesion plaque proteins is increased. The localization of derepressed wild-type Src in the absence of Csk resembles the localization of activated mutant and viral Src described by others (36, 37, 53, 64). It has become apparent that many Src substrates are localized in adhesion structures, and the redistribution of Src upon activation is arguably critical for Src action (39). The change in subcellular distribution of Src could result from the induction by Src of Src binding sites in the adhesion structures. Alternatively, or in addition, activation of Src may expose binding sites in Src that

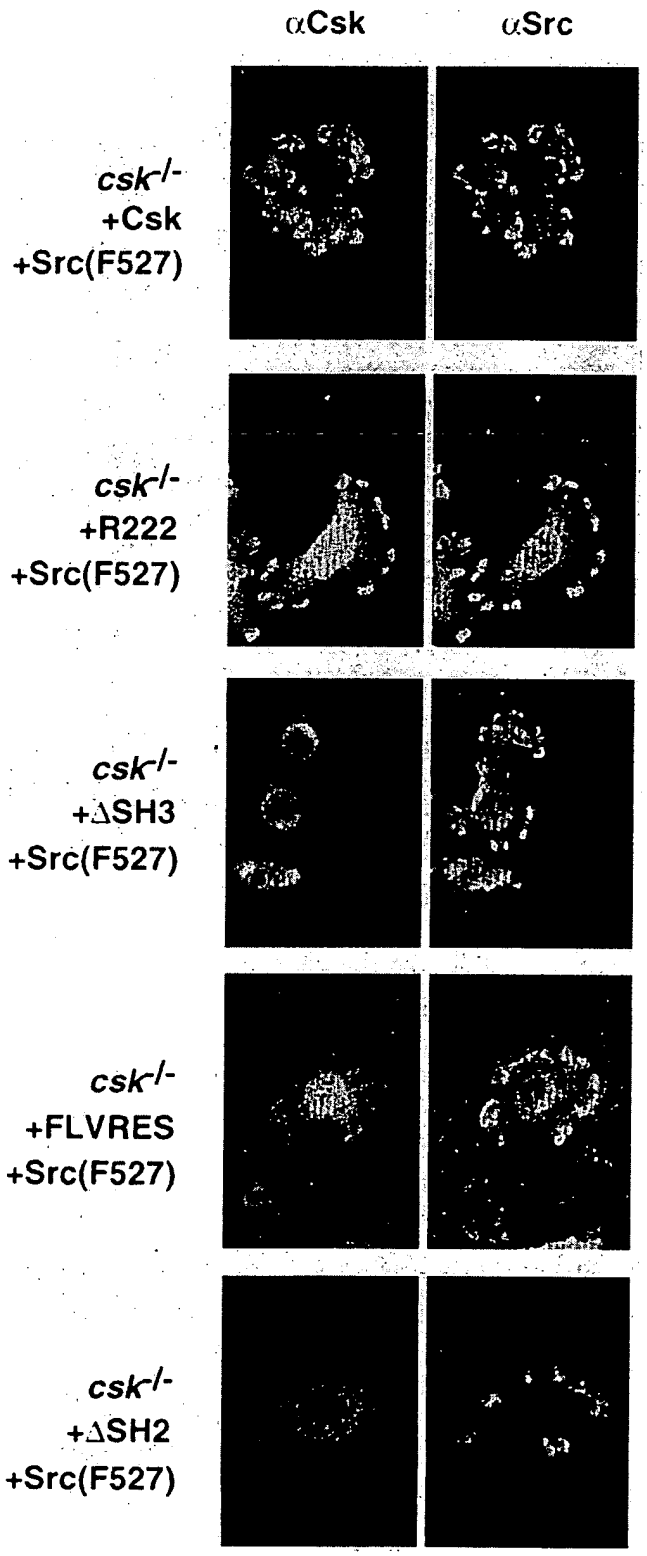

FIG. 7. Subcellular distributions of Csk and Src in $csk^{-/-}$ cells expressing activated Src and Csk variants. The left halves of the split images depict Texas red (anti-rabbit) fluorescence patterns, and the right halves depict fluorescein (anti-mouse) fluorescence patterns. The cell lines were infected with Src(F-527) and the versions of Csk indicated to the left of the images.

can interact with adhesion plaque proteins. It has been postulated that Src repression involves folding such that the SH2 domain and the phosphorylated tail are interacting (7, 12, 40, 65). The SH3 domain is also involved in maintaining this closed state (49, 55, 73). In such a folded state, domains involved in binding to adhesion plaques may be buried. On the other hand, in the active state, Src is phosphorylated at Y-416, not Y-527, and the SH2 and SH3 domains appear to be available for binding to phosphotyrosyl proteins and proline-rich motifs, respectively. The availability of these sites could promote movement to adhesion plaques. The Src SH3 domain can bind to the cytoskeletal proteins AFAP-110 and paxillin (30, 79). The SH2 domain binds to various phosphoproteins, including the PDGF receptor, AFAP110, and FAK, the focal adhesion kinase (11, 30, 38). Mutations in the SH2 and SH3 domains of activated Src interfere with cytoskeletal association or cytoskeletal architecture (21, 59, 77, 78).

Domains of Csk required for Csk activity and localization and for Src regulation. The functions of the SH2 and SH3 domains of Csk were investigated by mutagenesis. Mutations were introduced into these domains, and the mutant proteins were assayed for kinase activity and ability to suppress Src activity in vitro and in vivo. Deletion of the SH2 domain or mutation within the FLVRES motif of Csk greatly reduced Csk kinase activity in vitro and in vivo. This reduction contrasts with results with Src, whose SH2 domain can be mutated without loss of kinase activity, but resembles results with v-Fps, in which mutations in the SH2 domain significantly reduced kinase activity (18, 68). Perhaps the SH2 domain is required for the correct folding of Csk. Removal of the SH3 domain from Csk does not greatly affect the in vitro kinase activity against the exogenous substrates poly(Glu,Tyr) and baculovirus Src, indicating that the SH3 domain of Csk is not needed for correct folding of the kinase domain.

Both the SH2 and SH3 domains of Csk were needed for Csk relocalization to podosomes. The requirement of both domains suggests that binding through either domain alone is not of high enough affinity to anchor Csk to the adhesion structures.

The requirement of the Csk SH2 domain for localization suggests binding to tyrosine-phosphorylated proteins in the adhesion plaques. If so, the proteins are probably phosphorylated as a result of Src kinase activity, rather than Csk kinase activity, because Csk(R-222) localizes similarly to the podosome-like structures. On the other hand, the SH2 requirement may not indicate binding to phosphotyrosine. In the case of Src, certain mutations in the C-terminal part of the SH2 domain do not interfere with cytoskeletal localization, although they would be expected to reduce binding to phosphotyrosine (21). On the other hand, deletion of the first 20 amino acids of the Src SH2 domain prevents its association with the Triton X-100-insoluble fraction. The amino-terminal 20 amino acids of the Src and Csk SH2 domains are similar. Both of our Csk SH2 domain mutants affect this region, and therefore the N-terminal part of the SH2 domain may be interacting with the same adhesion structure component as Src.

The SH3 domain of Csk might be involved in an interaction with a protein that redistributes to adhesion plaques in Src-transformed cells, such as the Src substrates AFAP110 and cortactin (30, 81). Alternatively, Src may act on a protein normally found in adhesion structures to open up a binding site for the Csk SH3 domain. It is interesting that the Csk SH3 domain is divergent in sequence from that of Src and is poorly conserved in the Csk relatives Ctk and Matk. The Csk SH3 domain has been tested in vitro for binding to a number of proteins that bind to SH3 domains of Src and other proteins

(22). To date, binding of the Csk SH3 domain to other proteins or peptides has not been detected.

Does Csk bind to Src? One of the adhesion plaque proteins to which Csk may bind is Src itself. In principle, the Csk SH2 domain could bind to the phosphorylated Y-416 of activated Src (71). This hypothetical interaction alone does not explain the redistribution of Csk, since Csk is redistributed in cells transformed by the doubly mutant F-416 F-527 Src. The binding specificity of the Csk SH3 domain has yet to be determined. It could bind to proline-rich regions in Src (73). Although Src and Csk do not coimmunoprecipitate (66), interactions between Csk and the Src-related kinase Fyn have been observed (74). We have unsuccessfully assayed for Csk-Src complexes by coimmunoprecipitation, in vitro binding with bacterial fusion proteins, and the yeast two-hybrid system (24). If such complexes exist, they may be of low affinity or low stoichiometry.

While this study was under review, the binding of Csk to two tyrosine-phosphorylated cytoskeletal proteins was reported (65a). Csk was found to coimmunoprecipitate with FAK and paxillin from rat 3Y1 cells in which Csk was overexpressed. Because these cells did not contain an activated tyrosine kinase, some Csk may have been constitutively complexed with these proteins. On the other hand, a fusion protein containing the Csk SH2 and SH3 domains bound to tyrosine-phosphorylated FAK and paxillin in vitro (65a). Because a fusion protein containing only the SH3 domain did not bind, the SH2 domain may be required for correct function of the SH3 domain or may mediate binding to phosphotyrosine residues in paxillin and FAK. These results are consistent with our data indicating that Csk localization is directed by cytoskeletal proteins that have been modified by Src.

A model for Src regulation. The following model is consistent with the localization and activity of different Csk mutants. When Src is activated by biological stimuli, such as integrin-mediated adhesion, Src redistributes to adhesion plaques and there phosphorylates its substrates. Changes in the adhesion structures create binding sites for the SH3 and SH2 domains of Csk. Csk is then recruited to these structures, which brings it close to Src and allows phosphorylation and inhibition of Src. Both proteins are then released from the adhesion plaques. The Csk(ΔSH3) mutant supports this hypothesis. This mutant is active in vitro as a kinase yet fails to repress Src. This fact may be explained by the failure of this mutant to enter adhesion plaques, thus denying access to activated Src. The window of time during which Csk is absent from regions of activated Src may influence the signals transduced by Src. Studies with activated Src molecules with altered subcellular distributions have indicated that only those which localize to adhesion structures are transforming (39). Substrates critical for transmitting the Src signal may reside in this cellular compartment.

ACKNOWLEDGMENTS

We thank Akira Imamoto and Philippe Soriano for the *csk*$^{-/-}$ and *csk*$^{+/+}$ cells, Joan Brugge for the mAb327 antibodies, Larry Rohrschneider for the antivinculin antibody, Alasdair MacAuley for the Src mutants, and Masato Okada for the Csk(R-222) mutant. We would also like to thank Paul Goodwin and Tim Knight for assistance with confocal microscopy and graphics, Jenny Torgerson for preparing the manuscript, and Carol Laherty, Paul Stein, and members of our laboratory for reading it.

This work was supported by U.S. Public Health Service grant CA41072 and a fellowship from the Medical Research Council of Canada (B.W.H.).

REFERENCES

1. **Bagrodia, S., S. J. Taylor, and D. Shalloway.** 1993. Myristylation is required for Tyr-527 dephosphorylation and activation of pp60$^{c\text{-}src}$ in mitosis. Mol. Cell. Biol. 13:1464–1470.
2. **Barsagi, D., D. Rotin, A. Batzer, V. Mandiyan, and J. Schlessinger.** 1993. SH3 domains direct cellular localization of signaling molecules. Cell 74:83–91.
3. **Bennett, B. D., S. Cowley, S. X. Jiang, R. London, B. J. Deng, J. Grabarek, J. E. Groopman, D. V. Goeddel, and H. Avraham.** 1994. Identification and characterization of a novel tyrosine kinase from megakaryocytes. J. Biol. Chem. 269:1068–1074.
4. **Bergman, M., T. Mustelin, C. Oetken, J. Partanen, N. A. Flint, K. E. Amrein, M. Autero, P. Burn, and K. Alitalo.** 1992. The human p50^{csk} tyrosine kinase phosphorylates p56^{lck} at Tyr-505 and down regulates its catalytic activity. EMBO J. 11:2919–2924.
5. **Burridge, K., and K. Fath.** 1989. Focal contacts: transmembrane links between the extracellular matrix and the cytoskeleton. Bioessays 10:104–108.
6. **Burridge, K., K. Fath, T. Kelly, G. Nuckolls, and C. Turner.** 1988. Focal adhesions: transmembrane junctions between the extracellular matrix and cytoskeleton. Annu. Rev. Cell Biol. 4:487–525.
7. **Cantley, L., K. Auger, C. Carpenter, B. Duckworth, A. Graziani, R. Kapeller, and S. Soltoff.** 1991. Oncogenes and signal transduction. Cell 64:281–302.
8. **Cartwright, C. A., W. Eckhart, S. Simon, and P. L. Kaplan.** 1987. Cell transformation by pp60$^{c\text{-}src}$ mutated in the carboxy-terminal regulatory domain. Cell 49:83–91.
9. **Chow, L. M., M. Fournel, D. Davidson, and A. Veillette.** 1993. Negative regulation of T-cell receptor signalling by tyrosine protein kinase p50^{csk}. Nature (London) 365:156–160.
10. **Clark, E. A., and J. S. Brugge.** 1993. Redistribution of activated pp60$^{c\text{-}src}$ to integrin-dependent cytoskeletal complexes in thrombin-stimulated platelets. Mol. Cell. Biol. 13:1863–1871.
11. **Cobb, B. S., M. D. Schaller, T.-H. Leu, and J. T. Parsons.** 1994. Stable association of pp60^{src} and pp59^{fyn} with the focal adhesion-associated protein tyrosine kinase, pp125^{FAK}. Mol. Cell. Biol. 14:147–155.
12. **Cooper, J. A.** 1990. The *src*-family of protein tyrosine kinases, p. 85–113. *In* B. Kemp (ed.), Peptides and protein phosphorylation. CRC Press, Boca Raton, Fla.
13. **Cooper, J. A., and B. Howell.** 1993. The when and how of Src regulation. Cell 73:1051–1054.
14. **Cooper, J. A., and C. S. King.** 1986. Dephosphorylation or antibody binding to the carboxy terminus stimulates pp60$^{c\text{-}src}$. Mol. Cell. Biol. 6:4467–4477.
15. **Cooper, J. A., and A. MacAuley.** 1988. Potential positive and negative autoregulation of p60$^{c\text{-}src}$ by intermolecular autophosphorylation. Proc. Natl. Acad. Sci. USA 85:4232–4236.
16. **Cross, F. R., E. A. Garber, D. Pellman, and H. Hanafusa.** 1984. A short sequence in the p60^{src} N terminus is required for p60^{src} myristylation and membrane association and for cell transformation. Mol. Cell. Biol. 4:1834–1842.
17. **David-Pfeuty, T., and Y. Nouvian-Dooghe.** 1990. Immunolocalization of the cellular src protein in interphase and mitotic NIH c-src overexpresser cells. J. Cell Biol. 111:3097–3116.
18. **DeClue, J. E., I. Sadowski, G. S. Martin, and T. Pawson.** 1987. A conserved domain regulates interactions of the v-fps protein-tyrosine kinase with the host cell. Proc. Natl. Acad. Sci. USA 84:9064–9068.
19. **Devary, Y., R. A. Gottlieb, T. Smeal, and M. Karin.** 1992. The mammalian ultraviolet response is triggered by activation of Src tyrosine kinases. Cell 71:1081–1091.
20. **Flynn, D. C., T.-H. Leu, A. B. Reynolds, and J. T. Parsons.** 1993. Identification and sequence analysis of cDNAs encoding a 110-kilodalton actin filament-associated pp60^{src} substrate. Mol. Cell. Biol. 13:7892–7900.
21. **Fukui, Y., M. C. O'Brien, and H. Hanafusa.** 1991. Deletions in the SH2 domain of p60$^{v\text{-}src}$ prevent association with the detergent-insoluble cellular matrix. Mol. Cell. Biol. 11:1207–1213.
22. **Gout, I., R. Dhand, I. D. Hiles, M. J. Fry, G. Panayotou, P. Das, O. Truong, N. F. Totty, J. Hsuan, G. W. Booker, I. D. Campbell, and M. D. Waterfield.** 1993. The GTPase dynamin binds to and is activated by a subset of SH3 domains. Cell 75:25–36.

23. **Hirai, H., and H. E. Varmus.** 1990. Mutations in *src* homology regions 2 and 3 of activated chicken c-*src* that result in preferential transformation of mouse or chicken cells. Proc. Natl. Acad. Sci. USA **87**:8592–8596.
24. **Howell, B. W., and J. A. Cooper.** 1993. Unpublished results.
25. **Iba, H., F. R. Cross, E. A. Garber, and H. Hanafusa.** 1985. Low level of cellular protein phosphorylation by nontransforming overproduced pp60$^{c\text{-}src}$. Mol. Cell. Biol. **5**:1058–1066.
26. **Imamoto, A., and P. Soriano.** 1993. Disruption of the csk gene, encoding a negative regulator of src family tyrosine kinases, leads to neural tube defects and embryonic lethality in mice. Cell **73**:1117–1124.
27. **Jove, R., and H. Hanafusa.** 1987. Cell transformation by the viral *src* oncogene. Annu. Rev. Cell Biol. **3**:31–56.
28. **Kamps, M. P., J. E. Buss, and B. M. Sefton.** 1986. Rous sarcoma virus transforming protein lacking myristic acid phosphorylates known polypeptide substrates without inducing transformation. Cell **45**:105–112.
29. **Kamps, M. P., and B. M. Sefton.** 1988. Most of the substrates of oncogenic viral tyrosine protein kinases can be phosphorylated by cellular tyrosine protein kinases in normal cells. Oncogene Res. **3**:105–115.
30. **Kanner, S. B., A. B. Reynolds, H. C. Wang, R. R. Vines, and J. T. Parsons.** 1991. The SH2 and SH3 domains of p60^{src} direct stable association with tyrosine phosphorylated proteins p130 and p110. EMBO J. **10**:1689–1698.
31. **Kaplan, J. M., H. E. Varmus, and J. M. Bishop.** 1990. The *src* protein contains multiple domains for specific attachment to membranes. Mol. Cell. Biol. **10**:1000–1009.
32. **Kaplan, K. B., J. R. Swedlow, H. E. Varmus, and D. O. Morgan.** 1992. Association of p60$^{c\text{-}src}$ with endosomal membranes in mammalian fibroblasts. J. Cell Biol. **118**:321–333.
33. **Klages, S., D. Adam, K. Class, J. Fargnoli, J. B. Bolen, and R. C. Penhallow.** 1994. Ctk: a protein tyrosine kinase related to Csk that defines an enzyme family. Proc. Natl. Acad. Sci. USA **91**:2597–2601.
34. **Kmiecik, T. E., and D. Shalloway.** 1987. Activation and suppression of pp60$^{c\text{-}src}$ transforming ability by mutation of its primary sites of tyrosine phosphorylation. Cell **49**:65–83.
35. **Koch, C. A., D. Anderson, M. F. Moran, C. Ellis, and T. Pawson.** 1991. SH2 and SH3 domains: elements that control interactions of cytoplasmic signaling molecules. Science **252**:668–674.
36. **Krueger, J. G., E. A. Garber, S. S.-M. Chin, H. Hanafusa, and A. R. Goldberg.** 1984. Size-variant pp60^{src} proteins of recovered avian sarcoma viruses interact with adhesion plaques as peripheral membrane proteins: effects on cell transformation. Mol. Cell. Biol. **4**:454–467.
37. **Krueger, J. G., E. A. Garber, and A. R. Goldberg.** 1983. Subcellular localization of pp60^{src} in RSV-transformed cells. Curr. Top. Microbiol. Immunol. **107**:52–124.
38. **Kypta, R., Y. Goldberg, E. Ulug, and S. A. Courtneidge.** 1990. Association between the PDGF receptor and members of the src family of tyrosine kinases. Cell **62**:481–492.
39. **Liebel, E. C., and G. S. Martin.** 1992. Intracellular targeting of pp60^{src} expression: localization of v-Src to adhesion plaques is sufficient to transform chicken embryo fibroblasts. Oncogene **7**:2417–2428.
40. **Liu, X., S. R. Brodeur, G. Gish, Z. Songyang, L. C. Cantley, A. P. Laudano, and T. Pawson.** 1993. Regulation of c-Src tyrosine kinase activity by the Src SH2 domain. Oncogene **8**:1119–1126.
41. **Liu, X., L. E. M. Marengere, C. A. Koch, and T. Pawson.** 1993. The v-Src SH3 domain binds phosphatidylinositol 3′-kinase. Mol. Cell. Biol. **13**:5225–5232.
42. **MacAuley, A., and J. A. Cooper.** 1988. The carboxy-terminal sequence of p56^{lck} can regulate p60$^{c\text{-}src}$. Mol. Cell. Biol. **8**:3560–3564.
43. **MacAuley, A., M. Okada, S. Nada, H. Nakagawa, and J. A. Cooper.** 1993. Phosphorylation of Src mutants at Tyr 527 in fibroblasts does not correlate with in vitro phosphorylation by CSK. Oncogene **8**:117–124.
44. **Mayer, B. J., P. K. Jackson, R. A. Van Etten, and D. Baltimore.** 1992. Point mutations in the *abl* SH2 domain coordinately impair phosphotyrosine binding in vitro and transforming activity in vivo. Mol. Cell. Biol. **12**:609–618.
45. **Merilainen, J., R. Palovuori, R. Sormunen, V. M. Wasenius, and V. P. Lehto.** 1993. Binding of the alpha-fodrin SH3 domain to the leading lamellae of locomoting chicken fibroblasts. J. Cell Sci. **105**:647–654.
46. **Miller, A. D., D. G. Miller, J. V. Garcia, and C. M. Lynch.** 1993. Use of retroviral vectors for gene transfer and expression. Methods Enzymol. **217**:581–599.
47. **Miller, A. D., and G. J. Rosman.** 1989. Improved retroviral vectors for gene transfer and expression. BioTechniques **7**:980–988.
48. **Miller, A. D., D. R. Trauber, and C. Buttimore.** 1986. Factors involved in production of helper virus-free retrovirus vectors. Somatic Cell Genet. **12**:175–183.
49. **Murphy, S. M., M. Bergman, and D. O. Morgan.** 1993. Suppression of c-Src activity by C-terminal Src kinase involves the c-Src SH2 and SH3 domains: analysis with *Saccharomyces cerevisiae*. Mol. Cell. Biol. **13**:5290–5300.
50. **Mustelin, T.** 1994. Role of *src*-family PTKs in leukocyte physiology. RG Landes Co., Austin, Tex.
51. **Nada, S., M. Okada, A. MacAuley, J. A. Cooper, and H. Nakagawa.** 1991. Cloning of a complementary DNA for a protein-tyrosine kinase that specifically phosphorylates a negative regulatory site of p60$^{c\text{-}src}$. Nature (London) **351**:69–72.
52. **Nada, S., T. Yagi, H. Takeda, T. Tokunaga, H. Nakagawa, Y. Ikawa, M. Okada, and S. Aizawa.** 1993. Constitutive activation of Src family kinases in mouse embryos that lack CSK. Cell **73**:1125–1136.
53. **Nigg, E. A., B. M. Sefton, T. Hunter, G. Walter, and S. J. Singer.** 1982. Immunofluorescent localization of the transforming protein of Rous sarcoma virus with antibodies against a synthetic Src peptide. Proc. Natl. Acad. Sci. USA **79**:5322–5326.
54. **O'Brien, M. C., Y. Fukui, and H. Hanafusa.** 1990. Activation of the proto-oncogene p60$^{c\text{-}src}$ by point mutations in the SH2 domain. Mol. Cell. Biol. **10**:2855–2862.
55. **Okada, M., B. W. Howell, M. A. Broome, and J. A. Cooper.** 1993. Deletion of the SH3 domain of Src interferes with regulation by the phosphorylated carboxyl-terminal tyrosine. J. Biol. Chem. **268**:18070–18075.
56. **Okada, M., S. Nada, Y. Yamanishi, T. Yamamoto, and H. Nakagawa.** 1991. CSK: a protein-tyrosine kinase involved in regulation of *src* family kinases. J. Biol. Chem. **266**:24249–24252.
57. **Okada, M., and H. Nakagawa.** 1989. A protein tyrosine kinase involved in pp60$^{c\text{-}src}$ function. J. Biol. Chem. **264**:20886–20893.
58. **Paige, L. A., M. J. Nadler, M. L. Harrison, J. M. Cassady, and R. L. Geahlen.** 1993. Reversible palmitoylation of the protein-tyrosine kinase p56^{lck}. J. Biol. Chem. **268**:8669–8674.
59. **Parsons, J. T., and M. J. Weber.** 1989. Genetics of src: structure and functional organization of a protein tyrosine kinase. Curr. Top. Microbiol. Immunol. **147**:79–127.
60. **Pawson, T., and G. D. Gish.** 1992. SH2 and SH3 domains: from structure to function. Cell **71**:359–362.
61. **Piwnica-Worms, H., K. B. Saunders, T. M. Roberts, A. E. Smith, and S. H. Cheng.** 1987. Tyrosine phosphorylation regulates the biochemical and biological properties of pp60$^{c\text{-}src}$. Cell **49**:75–82.
62. **Resh, M. D.** 1994. Myristylation and palmitylation of Src family members: the fats of the matter. Cell **76**:411–414.
63. **Reynolds, A. B., J. Vila, T. J. Lansing, W. M. Potts, M. J. Weber, and J. T. Parsons.** 1987. Activation of the oncogenic potential of the avian cellular src protein by specific structural alteration of the carboxy terminus. EMBO J. **6**:2359–2364.
64. **Rohrschneider, L. R.** 1980. Adhesion plaques of Rous sarcoma virus-transformed cells contain the *src* gene product. Proc. Natl. Acad. Sci. USA **77**:3514–3518.
65. **Roussel, R. R., S. R. Brodeur, D. Shalloway, and A. P. Laudano.** 1991. Selective binding of activated pp60$^{c\text{-}src}$ by an immobilized synthetic peptide modeled on the carboxyl terminus of pp60$^{c\text{-}src}$. Proc. Natl. Acad. Sci. USA **88**:10696–10700.

65a. **Sabe, H., A. Hata, M. Okada, H. Nakagawa, and H. Hanafusa.** 1994. Analysis of the binding of the Src homology 2 domain of Csk to tyrosine phosphorylated proteins in the suppression and mitotic activation of c-Src. Proc. Natl. Acad. Sci. USA **91**:3984–3988.

66. **Sabe, H., B. Knudsen, M. Okada, S. Nada, H. Nakagawa, and H. Hanafusa.** 1992. Molecular cloning and expression of chicken

C-terminal Src kinase: lack of stable association with c-Src protein. Proc. Natl. Acad. Sci. USA 89:2190–2194.
67. **Sabe, H., M. Okada, B. Knudsen, S. Nada, H. Nakagawa, and H. Hanafusa.** 1992. CSK induced reversion of rat 3Y1 cells transformed by coexpression of c-*src* and v-*crk*. J. Cell. Biochem. Suppl. 16B:H345.
68. **Sadowski, I., J. C. Stone, and T. Pawson.** 1986. A noncatalytic domain conserved among cytoplasmic protein-tyrosine kinases modifies the kinase function and transforming activity of Fujinami sarcoma virus $P130^{gag\text{-}fps}$. Mol. Cell. Biol. 6:4396–4408.
69. **Seidel-Dugan, C., B. E. Meyer, S. M. Thomas, and J. S. Brugge.** 1992. Effects of SH2 and SH3 deletions on the functional activities of wild-type and transforming variants of c-Src. Mol. Cell. Biol. 12:1835–1845.
70. **Shenoy-Scaria, A. M., L. K. T. Gauen, J. Kwong, A. S. Shaw, and D. M. Lublin.** 1993. Palmitylation of an amino-terminal cysteine motif of protein tyrosine kinases $p56^{lck}$ and $p59^{fyn}$ mediates interaction with glycosyl-phosphatidylinositol-anchored proteins. Mol. Cell. Biol. 13:6385–6392.
71. **Songyang, Z., S. E. Shoelson, J. McGlade, P. Olivier, T. Pawson, X. R. Bustelo, M. Barbacid, H. Sabe, H. Hanafusa, T. Yi, R. Ren, D. Baltimore, S. Ratnofsky, R. A. Feldman, and L. C. Cantley.** 1994. Specific motifs recognized by the SH2 domains of Csk, 3BP2, fps/fes, GRB-2, HCP, SHC, Syk, and Vav. Mol. Cell. Biol. 14:2777–2785.
72. **Stockschlaeder, M. A., R. Storb, W. R. Osborne, and A. D. Miller.** 1991. L-histidinol provides effective selection of retrovirus-vector-transduced keratinocytes without impairing their proliferative potential. Hum. Gene Ther. 2:33–39.
73. **Supertifurga, G., S. Fumagalli, M. Koegl, S. A. Courtneidge, and G. Draetta.** 1993. Csk inhibition of c-Src activity requires both the SH2 and SH3 domains of src. EMBO J. 12:2625–2634.
74. **Takeuchi, M., S. Kuramochi, N. Fusaki, S. Nada, J. Kawamuratsuzuku, S. Matsuda, K. Semba, K. Toyoshima, M. Okada, and T. Yamamoto.** 1993. Functional and physical interaction of protein-tyrosine kinases Fyn and Csk in the T-cell signaling system. J. Biol. Chem. 268:27413–27419.
75. **Thomas, S. M.** 1994. Personal communication.
76. **Twamley-Stein, G. M., R. Pepperkok, W. Ansorge, and S. A. Courtneidge.** 1993. The Src family tyrosine kinases are required for platelet-derived growth factor-mediated signal transduction in NIH 3T3 cells. Proc. Natl. Acad. Sci. USA 90:7696–7700.
77. **Verderame, M. F., J. M. Kaplan, and H. E. Varmus.** 1989. A mutation in v-*src* removing a single conserved residue in the SH2 domain of pp60 restricts transformation in a host-dependent manner. J. Virol. 63:338–348.
78. **Wages, D. S., J. Keefer, T. B. Rall, and M. J. Weber.** 1992. Mutations in the SH3 domain of the *src* oncogene which decrease association of phosphatidylinositol 3′-kinase activity with $pp60^{v\text{-}src}$ and alter cellular morphology. J. Virol. 66:1866–1874.
79. **Weng, Z., J. A. Taylor, C. E. Turner, J. S. Brugge, and C. Seidel-Dugan.** 1993. Detection of Src homology 3-binding proteins, including paxillin, in normal and v-Src-transformed Balb/c 3T3 cells. J. Biol. Chem. 268:14956–14963.
80. **Wu, H., and J. T. Parsons.** 1993. Cortactin, an 80/85-kilodalton $pp60^{src}$ substrate, is a filamentous actin-binding protein enriched in the cell cortex. J. Cell Biol. 120:1417–1426.
81. **Wu, H., A. B. Reynolds, S. B. Kanner, R. R. Vines, and J. T. Parsons.** 1991. Identification and characterization of a novel cytoskeleton-associated $pp60^{src}$ substrate. Mol. Cell. Biol. 11: 5113–5124.

The listing of the Claims begins on page 3.

The Remarks begin on page 6.

Applicants believe no fee is due in connection herewith. However, should the Patent and Trademark Office determine otherwise, please charge the required fee to Jones Day deposit account no. 50-3013; a duplicate of this sheet is enclosed.